

Department of Medicine III, LMU Klinikum

**Investigation of transcription factor alterations in core binding
factor leukemia: Implications in clonal expansion, cell
metabolism and lineage fate decisions**



Dissertation
for the awarding of a Doctor
of Philosophy (Ph.D.)
at the Medical Faculty of
Ludwig-Maximilians-Universität, Munich

**Enric Redondo Monte
Munich 2020**

Department of Medicine III, LMU Klinikum



Dissertation
for the awarding of a Doctor
of Philosophy (Ph.D.)
at the Medical Faculty of
Ludwig-Maximilians-Universität, Munich

**Investigation of transcription factor alterations in core binding
factor leukemia: Implications in clonal expansion, cell
metabolism and lineage fate decisions**

submitted by:

Enric Redondo Monte

born in:

Corbera de Llobregat, Barcelona, Spain

Year:
2020

First supervisor: PD. Dr. Philipp A. Greif

Second supervisor: Prof. Dr. Irmela Jeremias

Third supervisor: PD. Dr. Christian Wichmann

Dean: Prof. Dr. med. dent. Reinhard Hickel

Defense Date:

17.11.2020

To my grandparents

Table of contents

I. Abbreviations	1
II. Table and Figures	2
1. Introduction	3
1.1. Acute myeloid leukemia	3
1.2. Core Binding Factor AML	5
1.3. RUNX1-RUNX1T1	6
1.4. ZBTB7A	10
1.4.1. ZBTB7A and lineage commitment	11
1.4.2. ZBTB7A and cancer	13
2. Objectives	16
3. Summary and Contribution	17
3.1 Publication I	17
3.2 Publication II	18
4. Conclusion and outlook	19
5. References	21
6. Acknowledgments	28
7. Publication list	29
Affidavit	30
Confirmation of congruency	31
Appendix	32
Publication I	
Publication II	

I. Abbreviations

2DG	2-deoxy-D-glucose
AML	Acute myeloid leukemia
BCOR	BCL-6 corepressor
CBF	Core Binding Factor
CLP	Common lymphoid progenitor
CMP	Common myeloid progenitor
CR	Complete response/remission
GMP	Granulocyte-monocyte progenitor
HDAC	Histone deacetylase
HSC	Hematopoietic stem cell
KO	Knockout
MEP	Megakaryocyte-erythrocyte progenitor
MPP	Multi-potent progenitor.
MYND	Myeloid-Nervy-DEAF-1
NCOR1	Nuclear receptor corepressor 1
NHR	Nervy homology regions
NLS	Nuclear localization sequence
NMTS	Nuclear matrix targeting signal
OS	Overall survival
PDX	Patient derived xenograft
PKA RII α	Type 2 cyclic AMP-dependent protein kinase
POK	POZ/BTB and Krüppel
POZ/BTB	Poxvirus and zinc finger/BR-C, ttk and bab
RHD	Runt homology domain
SMRT	Silencing mediator of retinoid and thyroid receptors

II. Table and Figures

Table 1: European Leukemia Network 2017 stratification of AML by genetics

Figure 1: Mutations in patients with CBF AML

Figure 2: Schematic representation of the proteins RUNX1, RUNX1T1 and their fusion

Figure 3: Translocation t(8;21) disrupts the normal function of the core binding factor complex.

Figure 4: ZBTB7A interacts with transcriptional corepressors and it is expressed across a variety of tissues

Figure 5: ZBTB7A regulates hematopoietic differentiation

Figure 6: *ZBTB7A* mutations in AML with t(8;21)

Figure 7: Schematic representation of the objectives of this thesis.

1. Introduction

1.1. Acute myeloid leukemia

Acute myeloid leukemia (AML) is a hematological malignancy characterized by the presence of abnormal blasts in the bone marrow and often also in the peripheral blood. These blasts are immature hematopoietic cells with a block of differentiation and an uncontrolled proliferation. A patient is diagnosed with AML when his or her bone marrow contains >20% myeloid blasts, as determined by microscopical examination of a biopsy. According to the World Health Organization (WHO) classification of myeloid neoplasms and acute leukemia, patients that present with <20% blasts are diagnosed with AML if they are positive for one of the recurrent fusion genes: *PML-RARA*, *RUNX1-RUNX1T1* or *CBFB-MYH11*, representing disease defining lesions (1). The incidence of AML is 3.1 per 100.000 persons per year in Germany (2).

The current scheme for AML therapy consists of an induction therapy, aiming to achieve a complete remission (CR) of the disease, that is to say, it aims to eradicate all signs and symptoms of the disease (i.e. <5% blasts in the bone marrow and normal blood cell counts). The most commonly used induction therapy is known as the 3+7 regime. It consists of 3 days of anthracycline infusion, a DNA intercalating agent, combined with 7 days of cytarabine, a cytosine analog (3). This treatment leads to a CR in 70-80% of patients under 60 years of age (4). To prevent relapse, the induction is followed by a consolidation therapy which can consist of conventional chemotherapy as well as of allogeneic stem cell transplantation. The choice between these therapies depends on the assessment of individual risk factors and availability (5). Despite consolidation therapy, half of the patients will eventually relapse with a therapy-refractory disease. The overall survival (OS) after 5 years is around 25%, but this value varies highly depending on the type of AML, age of the patient and comorbidities, amongst others (6). The European Leukemia Network (ELN) classifies AML in three risk categories depending on the genetic characteristics of the leukemia cells (Table 1). Of note, Core Binding Factor (CBF) AML, characterized by the presence of either *RUNX1-RUNX1T1* or *CBFB-MYH11* fusion genes, is classified into the favorable risk category.

Table 1: European Leukemia Network 2017 stratification of AML by genetics

ELN risk category	Genetic characteristics
Favorable	<i>RUNX1-RUNX1T1</i> fusion <i>CBFB-MYH11</i> fusion Biallelic <i>CEBPA</i> mutation <i>NPM1</i> mutation without <i>FLT3</i> -ITD or low <i>FLT3</i> -ITD
Intermediate	<i>NPM1</i> mutation with high <i>FLT3</i> -ITD Wild-type <i>NPM1</i> without <i>FLT3</i> -ITD or low <i>FLT3</i> -ITD <i>MLL3-KMT2A</i> fusion Other abnormalities without classification
Adverse	<i>DEK-NUP214</i> fusion <i>KMT2A</i> rearranged <i>BCR-ABL1</i> fusion <i>GATA2, EVI1</i> rearranged Complex karyotype Monosomal karyotype -5 or del(5q); -7; -17/abn(17p) Wild-type <i>NPM1</i> with high <i>FLT3</i> -ITD Mutated <i>RUNX1</i> Mutated <i>ASXL1</i> Mutated <i>TP53</i>

Low indicates allelic frequency lower than 0.5; high indicates allelic frequency equal or higher than 0.5; del: deletion, abn: abnormality; complex refers to three or more unrelated chromosomal aberrations without presence of a recurring translocation; monosomal refers to one monosomy (except for loss of Y or X) in association with at least another additional monosomy or structural abnormality (except for t(8;21), t(16;16) and inv(16)). Adapted from Dohner et al., 2017 (7).

1.2. Core Binding Factor AML

CBF AML accounts for 12-15% of adult and 25% of pediatric cases of myeloid leukemia (8, 9). CBF AML has an overall better prognosis than other types of AML with the vast majority (87%) of patients achieving CR after induction therapy (10). Despite having better prognosis, the ten-year OS is still at 44%, with elderly patients performing particularly poorly (11).

Molecularly, this leukemia is characterized by chromosomal aberrations affecting genes encoding subunits of the CBF - a heterodimeric protein complex that acts as a key transcription factor for normal hematopoiesis (12, 13). The heterodimers are formed by an alpha and a beta unit. The genes encoding the alpha unit are *RUNX1*, *RUNX2* and *RUNX3* and their protein products have DNA-binding properties. The beta unit is encoded by *CBFB* which does not bind DNA but protects the alpha units from degradation (13). Cytogenetically, CBF AML is characterized by the presence of translocation $t(8;21)(q22;q22)$, inversion $inv(16)(p13q22)$ or translocation $t(16;16)(p13;q22)$. These genomic rearrangements lead to the fusion genes *RUNX1-RUNX1T1* (also known as *AML1-ETO*, *AML1-MTG8* and *RUNX1-ETO*) and *CBFB-MYH11*, respectively.

The main oncogenic mechanism for *RUNX1-RUNX1T1* and *CBFB-MYH11* seems to rely on the disruption of CBF-dependent transcription (14, 15). Still, mouse models demonstrated that these fusion genes lead to a block of myeloid differentiation, but are not enough to cause leukemia (16, 17). The current understanding is that additional genetic and/or epigenetic lesions are needed for CBF AML to arise. The most common mutations occurring in combination with *RUNX1-RUNX1T1* and *CBFB-MYH11* are depicted in Figure 1, with obvious differences in the mutation distribution between the two aberrations. Concurrent mutations are not the only difference between $t(8;21)$ and $inv(16)/t(16;16)$ leukemia. On a cytomorphological level *CBFB-MYH11* leukemia is classified as M4 (myelomonocytic with abnormal eosinophils) according to the French-American-British classification, while *RUNX1-RUNX1T1* leukemia is considered M2, (myeloblastic, with granulocytic maturation) (18). Other characteristics such as prognostic factors, outcome and concurrent chromosomal aberrations also vary between the two CBF subgroups (10, 19, 20).

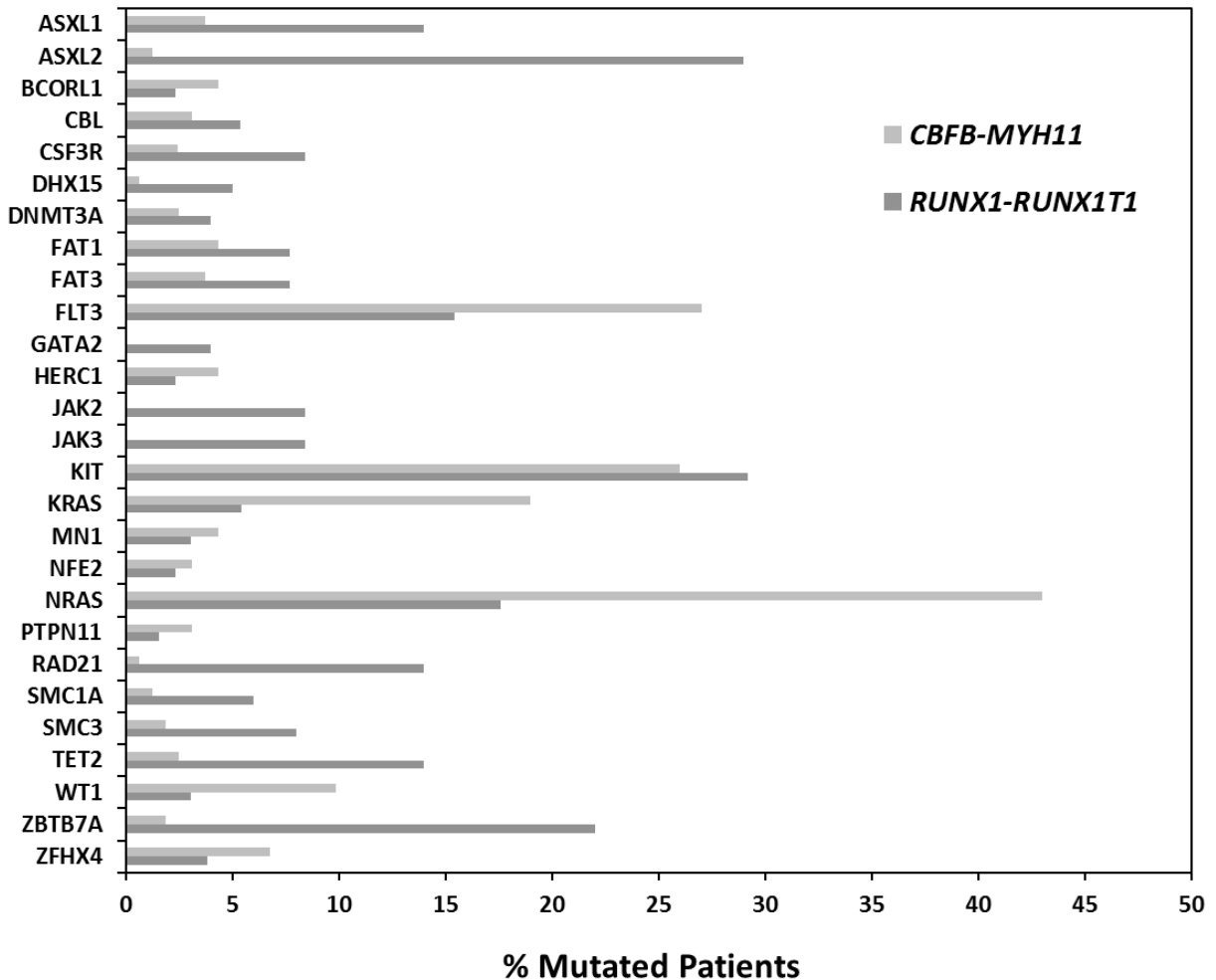


Figure 1: Mutations in patients with CBF AML. Mutational data from 130 AML patients with *RUNX1-RUNX1T1* and 162 patients with *CBFB-MYH11* obtained via targeted amplicon sequencing. FLT3 represents both point mutations and internal tandem duplications. Adapted from Opatz et al., 2020 (21).

1.3. RUNX1-RUNX1T1

As introduced above, translocation t(8;21) results in the formation of the fusion gene *RUNX1-RUNX1T1*. The N-terminal part of the fusion gene is derived from the transcription factor *RUNX1*, a gene from the *RUNX* transcription factor family, which plays key roles in the regulation of lineage fate decisions (22). *RUNX1* is involved in other recurrent chromosomal translocations, such as t(3;21) and t(12;21) (23, 24). In addition, somatic mutations are frequently found in this gene in patients with AML, myelodysplastic syndrome and secondary

AML (25-27). Moreover, germline point mutations in *RUNX1* are associated with thrombocytopenia and increased risk of AML (28-30). Mouse models demonstrate that *RUNX1* plays a key role in embryonic hematopoiesis, where it is essential for the development of hematopoietic stem cells (HSC) (31, 32). On the other hand, the role of *RUNX1* in adult hematopoiesis is not as clear. Conditional *RUNX1* knockout (KO) mice show defects on platelet maturation and lymphocytic differentiation but not in HSC establishment (33-35). Structurally, *RUNX1* contains a runt homology domain (RHD) which has DNA binding characteristics and can interact with C/EBP β (36), a transactivation domain, a nuclear matrix attachment signal (37), and two transcription inhibition domains (38) (Figure 2a). The breakpoint in *RUNX1* underlying translocation t(8;21) localizes to the intronic region between exon 5 and 6, colocalizing with DNase I and topoisomerase II cleavage hypersensitive sites (39). As a consequence, it brings the N-terminal part of *RUNX1* into the *RUNX1*-*RUNX1T1* fusion protein, which contains its RHD domain (Figure 2c).

The C-terminal part of the fusion gene stems from *RUNX1T1*, a transcriptional repressor from the *ETO* family. Gene disruption in a mouse model showed that *RUNX1T1* plays an essential role in the development of the gastrointestinal track (40). What is more, gene expression studies and functional validation in mutant mice revealed that *RUNX1T1* plays a key role in pancreas development (41). On a structural level, *RUNX1T1* contains four Nrvy Homology Regions (NHR) with distinct functions, directing protein-protein interactions but not DNA binding (Figure 2b). The breakpoint in *RUNX1T1* related to translocation t(8;21) localizes to the intronic region between exon 1 and 2, bringing the four NHR domains into the fusion (Figure 2c). NHR1 mediates the interaction with the histone acetyltransferase p300 (42). NHR2 allows for dimerization with other transcription factors from the *ETO* family (43). Furthermore, NHR2 is essential for homo-tetramer formation, which is critical for *RUNX1*-*RUNX1T1* oncogenicity (44, 45). NHR3 mediates the interaction with the regulatory subunit of type 2 cyclic AMP-dependent protein kinase (PKA RII α) (46). Mutation of key amino acid residues for this interaction showed that NHR3-PKA RII α interaction does not seem to be critical for *RUNX1*-*RUNX1T1* oncogenicity (47). Finally, NHR4, sometimes referred as myeloid-Nrvy-DEAF-1 (MYND), mediates the interaction with the co-repressors nuclear receptor corepressor/silencing mediator of retinoid and thyroid receptors (N-COR/SMRT) (48). On the other hand,

NHR4 mediates the interaction with the splicing co-factor SON, which may mediate anti-proliferative signals (49).

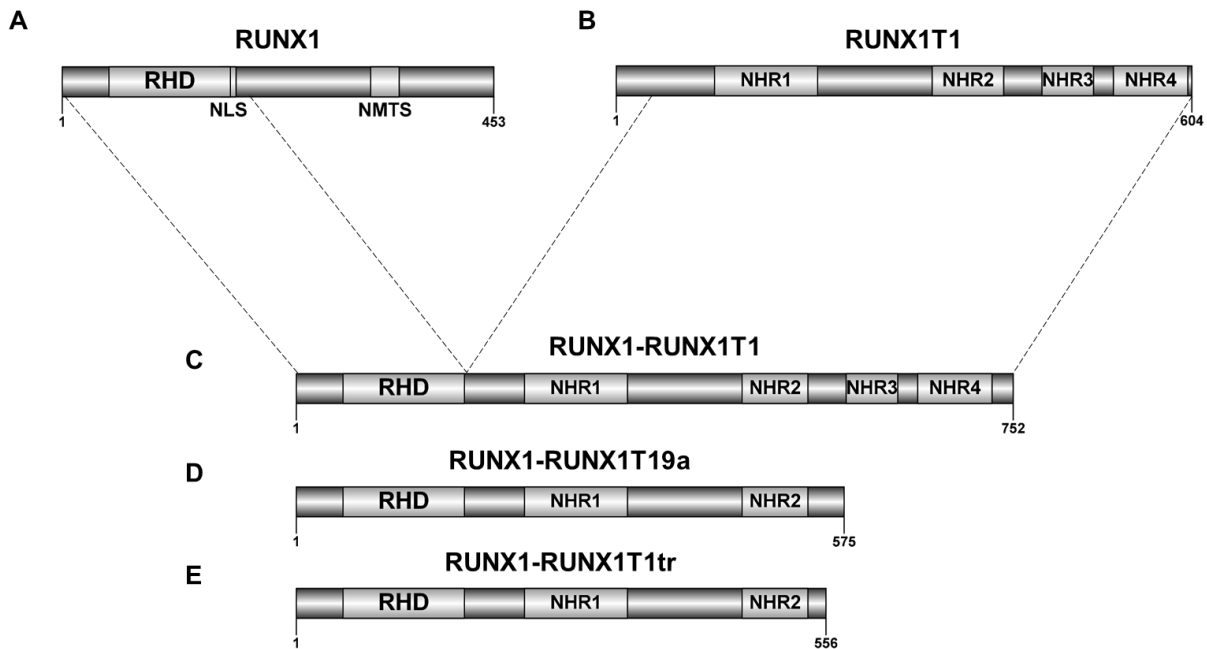


Figure 2: Schematic representation of the proteins RUNX1, RUNX1T1 and their fusion. A RUNX1. **B** RUNX1T1. **C** RUNX1-RUNX1T1 full-length fusion. **D** RUNX1-RUNX1T1 alternatively spliced isoform 9a. **E** RUNX1-RUNX1T1 truncated version. RHD: runt homology domain; NLS: Nuclear localization sequence; NMTS: nuclear matrix targeting signal; NHR: Nerve homology region. Illustrated using IBS 1.0.3 software. Adapted from Yan et al., 2004; Yan et al., 2006; Lam et al., 2012 and El-Gebali et al., 2019 (50-53).

In the fusion, the RHD domain allows RUNX1-RUNX1T1 to bind RUNX1 targets genes, while the NHR domains allow for dimerization and protein-protein interaction, recruiting co-repressors such as histone deacetylases (HDACs) and N-COR/SMRT (Figure 3).

Overexpression of RUNX1-RUNX1T1 in mouse HSC causes stem cell expansion and aberrant granulocytic differentiation (54), while overexpression in embryonic zebrafish reprograms erythroid cells into the granulocytic lineage (55). The full-length fusion gene can only induce leukemia in mouse models with a concurrent alteration (ie. FLT3 internal tandem duplication,

WT-1 overexpression...) (56, 57). A shorter alternatively spliced version of the fusion protein, known as RUNX1-RUNX1T19a, was also identified in patients with t(8;21) (51). Interestingly, RUNX1-RUNX1T19a lacks NHR3 and NHR4 (Figure 2d). This shorter fusion gene has an increased leukemia induction potential compared to the full-length fusion. Nevertheless, disease progression can be accelerated by the introduction of further mutations (i.e. *Nras*^{G12D} or *p53*^{-/-}) (58). Further work using a truncated version of RUNX1-RUNX1T1 lacking NHR3 and NHR4 (Figure 2e) demonstrated that NHR1 is not critical for leukemogenesis, while NHR2 seems to play a key function (59). Taking these data into account, the question arises which domains of RUNX1-RUNX1T1 are critical for the development of t(8;21) AML and to which extent they can be substituted by other functional domains.

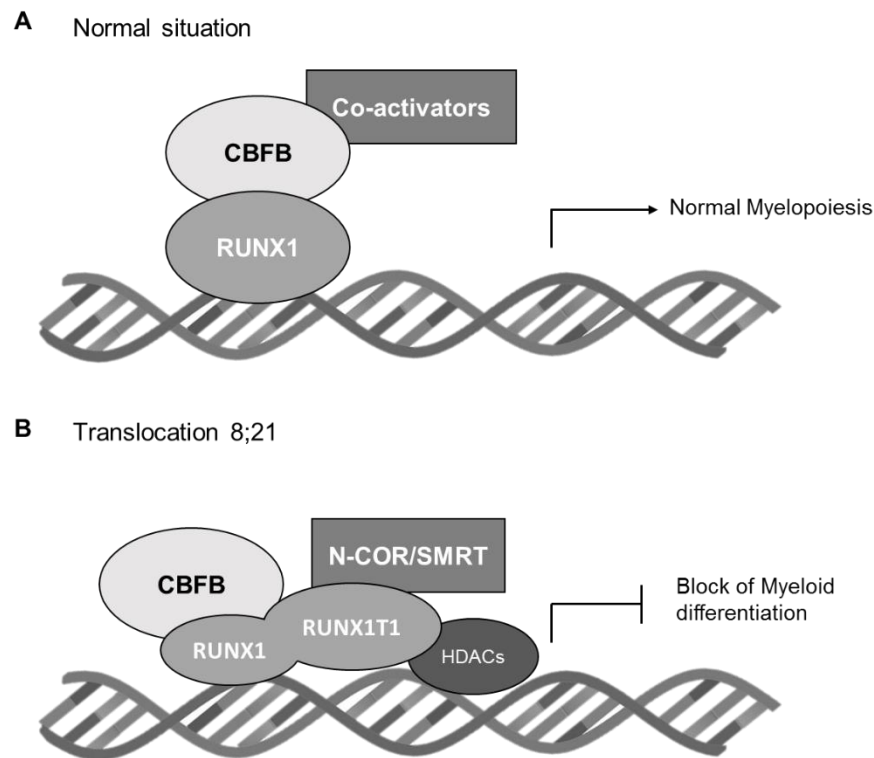


Figure 3: Translocation t(8;21) disrupts the normal function of the core binding factor complex. A RUNX1 binds DNA while CBFB recruits histone acetylases and other co-activators, allowing for transcription and normal myelopoiesis. **B** In the context of translocation t(8;21), RUNX1 binds DNA while RUNX1T1 recruits co-repressors such as histone deacetylases (HDACs) and nuclear receptor corepressor / silencing mediator of retinoid and thyroid receptors (N-COR/SMRT), leading to a block of myeloid differentiation. Adapted from Solh et al., 2014 (9).

1.4. ZBTB7A

ZBTB7A (also known as *LRF*, *FBI-1*, *Pokemon* and *OCZF*) is a transcription factor and member of the Poxvirus and Zinc finger/BR-C, ttk and bab (POZ/BTB) and Krüppel (POK) family located on chromosome 19p13.3 (60). This gene family is characterized by an N-terminal POZ/BTB domain that permits protein-protein interaction, dimerization with other POK proteins and recruitment of a co-repressor complex (61). Additionally, they present N-terminal Krüppel type zinc-finger domains for DNA interaction and possibly protein-protein interactions. The POK gene family has up to 43 members (62) that have key roles in developmental processes and cellular differentiation (63), several of them being linked to cancer (64-66).

ZBTB7A is capable of recruiting both the BCL-6 corepressor (BCOR) and the nuclear receptor corepressor 1 (NCOR1) (Figure 4a). It can bind multiple promoters throughout the genome where it regulates the accessibility of other transcription factors (67). Due to these characteristics, *ZBTB7A* has multiple and sometimes conflicting roles depending on the epigenetic and cellular context. *ZBTB7A* is not only expressed across a variety of tissues but also during different stages of development (Figure 4b) (68).

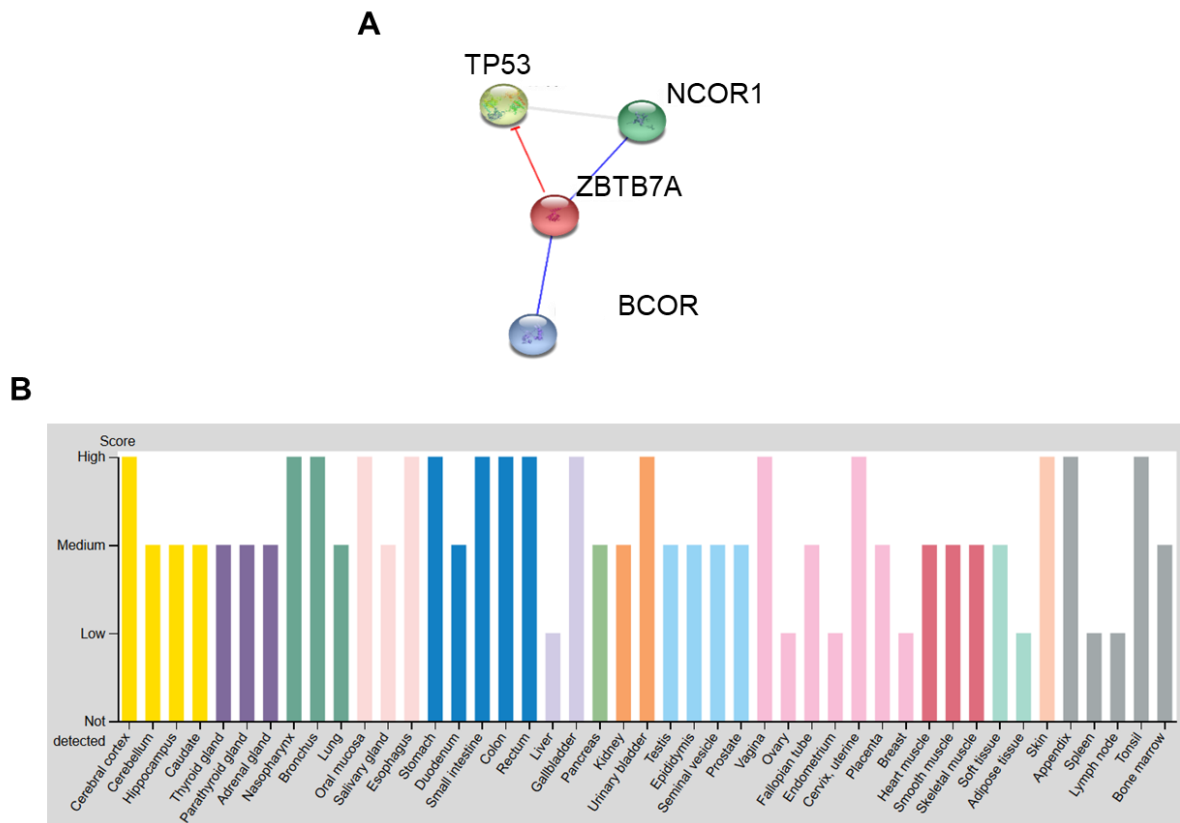


Figure 4: ZBTB7A interacts with transcriptional corepressors and it is expressed across a variety of tissues. **A** ZBTB7A protein interaction partners from String Database v11.0. Only interactions with a confidence score higher than 0.7 were considered. Blue lines represent interactions between ZBTB7A and a partner. Red lines represent inhibition by ZBTB7A. Grey lines represent interactions independent of ZBTB7A. BCOR: BCL-6 corepressor, NCOR: Nuclear receptor corepressor 1, TP53: Tumor Protein P53. **B** ZBTB7A expression across different human tissues. Score indicates protein levels based on immunohistochemistry staining and validated with either an independent antibody or RNA-Sequencing. Colors indicate type of tissue. Data from the Human Protein Atlas available at <https://www.proteinatlas.org/ENSG00000178951-ZBTB7A/tissue>, version 19.1 (68).

1.4.1. ZBTB7A and lineage commitment

ZBTB7A is implicated in different developmental processes and lineage commitment decisions (reviewed in Lunardi et al., 2013) (69). The role of ZBTB7A in hematopoietic lineage fate decisions was mostly determined using *ZBTB7A* complete KO mice as well as mice with a *ZBTB7A* hematopoietic tissue specific conditional KO (*ZBTB7A^{Flox/Flox};Mx1-Cre*). *ZBTB7A* null mouse embryos die at day 16.5 *postcoitum* due to severe anemia, demonstrating the need of functional ZBTB7A for normal erythropoiesis (70, 71) (Figure 5). Interestingly, these embryos presented a deficiency of mature myeloid cells as well as a reduction in number of granulocytic-monocytic progenitors in fetal liver, suggesting a role of ZBTB7A in the development of myeloid cells. *ZBTB7A* hematopoietic conditional KO mice are viable although this model showed that ZBTB7A is important to maintain a stemness phenotype of immature HSC (72). Mice with a hematopoietic tissue specific *ZBTB7A* KO also showed a reduction of myeloid progenitors in the bone marrow, further supporting the idea that ZBTB7A is involved in the granulocytic-monocytic differentiation pathway (72). The most dramatic effect though was observed in the lymphoid lineage, where *ZBTB7A* inactivation leads to an accumulation of CD4+CD8+ T cells in detriment of B cells due to NOTCH deregulation (70). What is more, ZBTB7A was also necessary for CD4+ T cell differentiation (73). Finally, ZBTB7A promoted follicular B cell differentiation in detriment of marginal zone B cells (74).

ZBTB7A also plays a key role during osteoclast formation (75), another cell type with a hematopoietic origin. Specifically, ZBTB7A blocks differentiation in early-stage osteoclasts, while being essential for the normal function of differentiated osteoclasts (76).

Outside the hematopoietic system, ZBTB7A has been described to regulate oligodendrocyte lineage commitment, adipogenesis and neuron re-myelination (77-79).

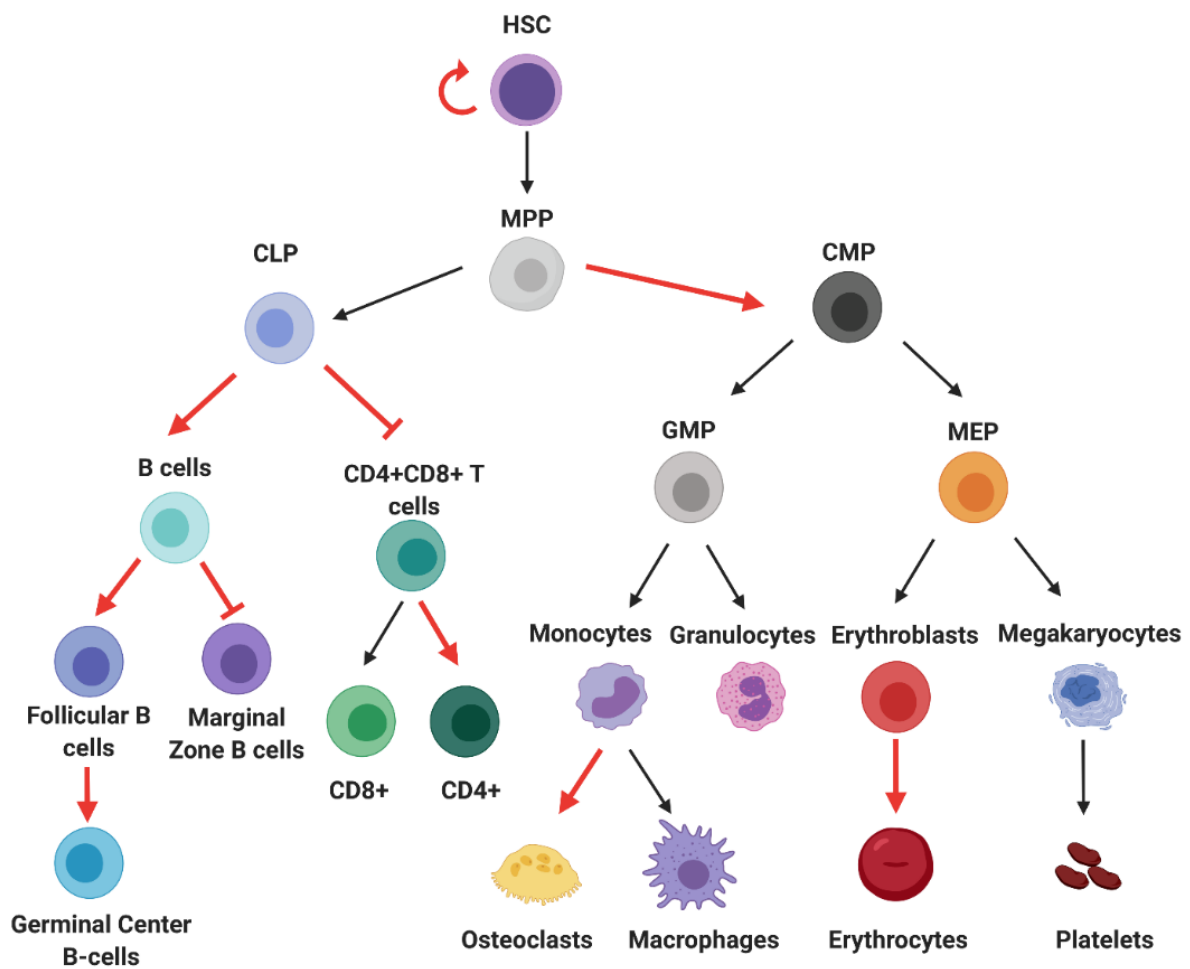


Figure 5: ZBTB7A regulates hematopoietic differentiation. Red arrows depict a role of ZBTB7A in differentiation while red blunt arrows depict an inhibitory effect of ZBTB7A in differentiation. CLP: common lymphoid progenitor, CMP: common myeloid progenitor, GMP: granulocyte-monocyte progenitor, HSC: hematopoietic stem cell, MEP: megakaryocyte-erythrocyte progenitor, MPP: multi-potent progenitor. Created with BioRender. Adapted from Lunardi et al., 2013 and Lee et al., 2013 (69, 72).

1.4.2. ZBTB7A and cancer

ZBTB7A has been described to act both as an oncogene and as a tumor suppressor depending on the cellular context. These discrepancies may arise due to the fact that *ZBTB7A* can block or promote differentiation depending on the tissue where it is expressed. Besides, *ZBTB7A* participates in other cellular processes such as cell cycle regulation, growth, apoptosis and invasion, amongst others, which adds a new layer of complexity to determine its role as an oncogene or tumor suppressor (80).

Role as an oncogene

ZBTB7A can act as an oncogene in a variety of ways. It is overexpressed in approximately 30% of diffuse large B-cell lymphoma cases where it directly represses the expression of the tumor suppressor *ARF* (65). Another example of *ZBTB7A* overexpression is the presence of *ZBTB7A* gene amplification in 27.7% of cases of non-small cell lung carcinoma (81). Overexpression also occurs in hepatocellular carcinoma where knockdown of *ZBTB7A* inhibits cell growth through suppression of *AKT* (82). This mechanism is also relevant in glioma where *ZBTB7A* knockdown not only reduces proliferation, but also invasion capacity through inactivation of the *AKT* pathway (83, 84). A role in cell migration and invasion was also described in ovarian cancer, where *ZBTB7A* promotes the expression of the membrane type 1 matrix metalloproteinase (85). In addition, *ZBTB7A* also plays a role in breast cancer, where it controls the expression of the estrogen receptor alpha and drives proliferation (86, 87). Further studies using cancer cell lines also implicated *ZBTB7A* in sarcoma, renal carcinoma, liver cancer and bladder cancer (88-91).

Role as a tumor suppressor

The role of *ZBTB7A* as a tumor suppressor is equally heterogeneous as its role as an oncogene. Loss of *ZBTB7A* in *PTEN* negative prostate cancer leads to tumor invasion due to de-repression of *Sox9* expression (92). Moreover, it can repress cell migration and promote apoptosis in gastric cancer (93). Additionally, loss of 19p13.3 is related to *ZBTB7A* down-regulation and

increased metastasis in melanoma due to increased *MCAM* expression (94). Surprisingly, *ZBTB7A* also takes the role of a tumor suppressor by maintaining the genome integrity in a transcription-independent manner, being directly involved in the non-homologous end joining pathway, in charge of repairing DNA double-strand breaks (95).

Mutation is another process by which *ZBTB7A* can be inactivated: 4.2% of colorectal adenocarcinomas show mutations in this gene, as well as 2.1% of esophageal adenocarcinoma cases and lower proportions of other solid tumors (96). Liu and colleagues described that *ZBTB7A* directly represses the transcription of genes involved in the glycolytic pathway such as the glucose transporter *SLC2A3*, the phosphofructokinase *PFKP* and the pyruvate kinase *PKM* (96). This repression takes places independently from other well-known glycolysis control pathways such as *MYC* and *HIF1* (97). Furthermore, downregulation of *ZBTB7A* correlates with overexpression of the lactate membrane transporter *SLC16A3* (98). In this context, *ZBTB7A* mutation leads to an increased aerobic glycolysis (known as Warburg Effect) and an increased proliferation of colon cancer cell lines *in vitro* and *in vivo* (97).

Previously, our group and others reported mutations in *ZBTB7A* in 9.4-23% of AML patients with translocation t(8;21) as well as in 1.8-4.5% of patients with inv(16) (Figure 6) (21, 99-102), both genomic rearrangements defining CBF AML. These mutations showed a loss-of-function phenotype in luciferase reporter assays, DNA binding capacity and proliferation assays (99). Interestingly, no mutations have been described in other AML subtypes. Nevertheless, our group showed that *ZBTB7A* expression is a prognostic factor in cytogenetically normal (CN) AML patients. Patients with a high *ZBTB7A* expression lived longer than patients with a low expression (99). This data suggests that the role of *ZBTB7A* as a tumor suppressor is not limited to AML t(8;21) but may also be important in other AML subtypes. Overall, the roles of both *ZBTB7A* and *RUNX1-RUNX1T1*, as well as their interplay in the development of AML are not fully understood.

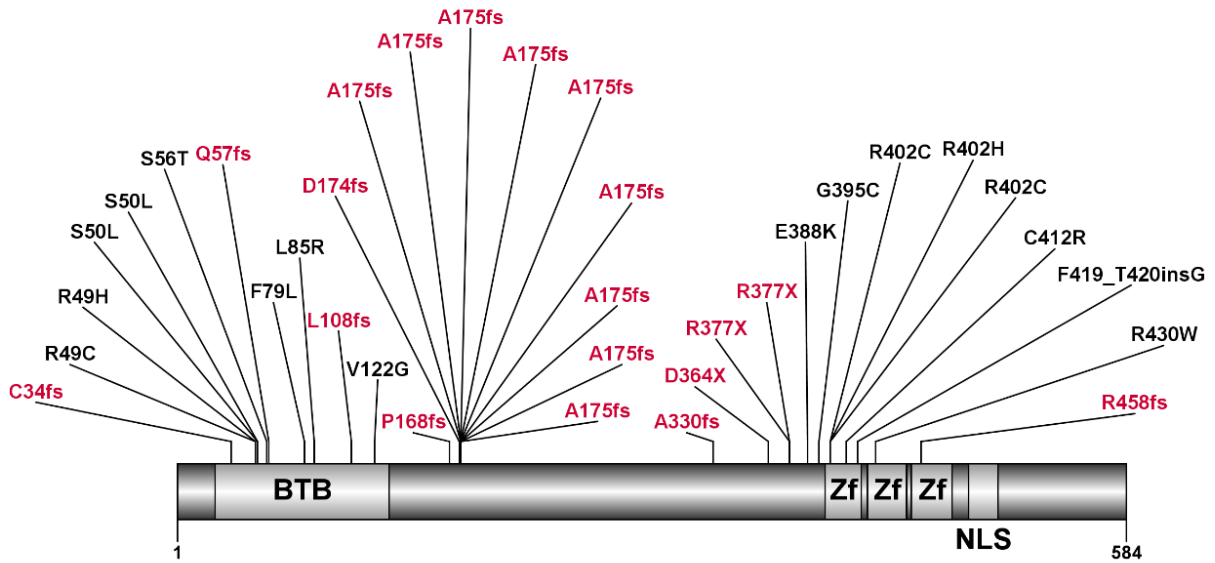


Figure 6: ZBTB7A mutations in AML with t(8;21). ZBTB7A protein and domains representation using the annotation NP_056982.1. Red indicates truncating mutations. Black indicates in-frame insertions and missense mutations. BTB: BR-C ttk and bab, Zf: zinc finger, NLS: nuclear localization sequence. Compiled from Hartmann et al., 2016; Lavalley et al., 2016; Faber et al., 2016 and Kawashima et al., 2019 (99-102) and first published in Redondo Monte et al., 2020 (103). Illustrated using IBS 1.0.3 software.

2. Objectives

The process by which *RUNX1-RUNX1T1* and other mutations lead to the development of AML is still poorly understood. Although patients with t(8;21) have a rather favorable prognosis, they are still treated with very toxic and aggressive chemotherapy regimens and about half of them will eventually relapse (7). In this context, patients could benefit from targeted therapies that focus on exploiting vulnerabilities present in this leukemia.

The publications presented in this thesis aimed to study the development of AML t(8;21), with a focus on alterations affecting transcription factors. Understanding the molecular mechanisms by which the *RUNX1-RUNX1T1* fusion gene and mutations in the transcription factor *ZBTB7A* lead to the development of leukemia is the first step towards the identification of specific targetable vulnerabilities (Figure 7).

The specific aims of this study were:

- To study the functional role of the domains of *RUNX1-RUNX1T1*
- To evaluate the effect of *ZBTB7A* mutations in myeloid leukemia
- To clarify the role of *ZBTB7A* in normal hematopoiesis
- To investigate the specific interplay between *ZBTB7A* mutations and t(8;21) and the resulting therapeutic implications.

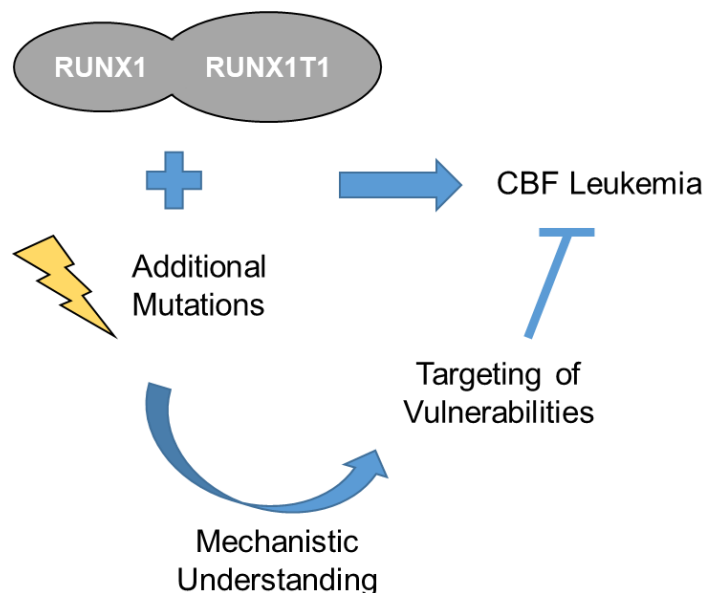


Figure 7: Schematic representation of the objectives of this thesis. *RUNX1-RUNX1T1* needs additional mutations to cause core binding factor (CBF) leukemia. Understanding the mechanism by which leukemia arises, enables us to target specific vulnerabilities present in the malignant cells.

3. Summary and Contribution

Publication I

Chen-Wichmann L, Shvartsman M, Preiss C, Hockings C, Windisch R, Redondo Monte E, Leubolt G, Spiekermann K, Lausen J, Brendel C, Grez M, Greif PA and Wichmann C. Compatibility of RUNX1/ETO Fusion Protein Modules Driving CD34+ Human Progenitor Cell Expansion. *Oncogene*, 38 (2), 261-272 (2019)

Previous work demonstrated that the domains NHR3 and NHR4 of RUNX1-RUNX1T1 are not essential for its leukemic effect (50). In addition, the homo-oligomerization properties of NHR2 were hinted to be crucial for the oncogenicity of the fusion gene (104). In this publication, we studied the RUNX1-RUNX1T1 domains, with focus on their capacity to induce human stem cell expansion. Finally, we evaluated if the domains can be substituted by homologous sequences and retain their functions.

Working with human hematopoietic stem and progenitor cells from healthy donors, we could demonstrate that substitution of the tetramer domain NHR2 for the structurally related BCR domain in a truncated form of the protein (lacking NHR3 and NHR4) retains stability and localization, but not stem cell expansion potential. Moreover, using HEK 293T cells and a luciferase reporter assay, we could show that the truncated, NHR2 substituted protein loses its transcriptional repression ability. Re-introduction of the NHR4 repressor domain restored repression ability and thus expansion of progenitor cells, highlighting the importance of a functional repressor domain for RUNX1-RUNX1T1-directed cell transformation. Using an inducible system for modular protein assembly, we could also show that NHR4 is crucial for the initial expansion of CD34+ progenitor cells in the NHR2 substituted truncated protein. Interestingly, repression and cell expansion could be restored solely by the introduction of the repression domain 3 of the co-repressor NCOR. Therefore, we concluded that the NHR2 domain can only be substituted in RUNX1-RUNX1T1 fusions containing a functional repression domain. This demonstrates that NHR4 is important due to its repression activity and that the RUNX1T1-NCOR axis could represent an important target as a therapy for AML with t(8;21). The need for a tetramerization domain and a repressor domain also suggest a mechanistic explanation for recurrent RUNX1 fusions with other members of the ETO family, which contain both mentioned domains (105).

In this study, I performed the luciferase reporter assay (Figure 4f) and participated in the assessment of stem cell outgrowth through flow cytometry of fluorochromes (Figures 2f, 3bd, 5b, 6e). Finally, I assisted in the manuscript preparation and proofreading.

Publication II

Redondo Monte E, Wilding A, Leubolt L, Kerbs P, Bagnoli JW, Hartmann L, Hiddemann W, Chen-Wichmann L, Krebs S, Blum H, Cusan M, Vick B, Jeremias I, Enard W, Theurich S, Wichmann C and Greif PA. ZBTB7A prevents RUNX1-RUNX1T1-dependent clonal expansion of human hematopoietic stem and progenitor cells. *Oncogene* 39, 3195–3205 (2020).

Previous work from our group and others demonstrated that the transcription factor *ZBTB7A* is frequently and specifically mutated in AML t(8;21), which harbors the *RUNX1-RUNX1T1* fusion gene (21, 99-102). In this study, we investigated the function of *ZBTB7A* in myeloid differentiation as well as the relationship between *ZBTB7A* mutations and the fusion gene *RUNX1-RUNX1T1*.

Working with myeloid cell lines, we demonstrated that *ZBTB7A* promotes granulopoiesis and erythropoiesis, while blocking monocytic differentiation. On the other hand, using hematopoietic stem and progenitor cells, we corroborated the previously described role of *ZBTB7A* in stem cell maintenance (72). We also showed that *ZBTB7A* loss increases the expression of glycolytic genes such as *SLC2A1*, *SLC2A3*, *ENO2*, *PGM2* and *PGM3*. This results in an increased glycolysis and therefore sensitizes to glycolysis inhibition by 2-deoxy-D-glucose (2DG). Furthermore, we demonstrated that 2DG can inhibit the growth of AML patient derived xenografts (PDX) *in vitro*. What is more, *ZBTB7A* KO led to an increased oxygen consumption, hinting towards a role of *ZBTB7A* in metabolism regulation beyond glycolysis. Finally, in human stem and progenitor cells, we observed that ectopic *ZBTB7A* expression prevents the expansion of progenitors directed by the fusion gene *RUNX1-RUNX1T1*. On the other hand, *ZBTB7A* mutations enable the outgrowth of progenitors. Moreover, we could explain the *ZBTB7A*-mediated block of expansion by the fact that *ZBTB7A* overexpression stops cell cycle progression and proliferation, in line with a phenotype of decreased glycolysis. Taken together, our results suggest that patients with translocation t(8;21) and additional *ZBTB7A* mutation might benefit from treatment with glycolytic inhibitors as a potential strategy to restore *ZBTB7A* function.

In this study, I established the KO and overexpression cell lines and stem cell models. Using these models, I performed all the functional assays such as cell differentiation, metabolic flow assays, growth inhibition, stem cell clonal expansion and cell cycle analysis, amongst others. I analyzed the data, performed statistics and prepared the figures (except for the RNA-sequencing data). Finally, I wrote the manuscript.

4. Conclusion and outlook

Although the translocation between chromosomes 8 and 21 was discovered as early as 1973 (106), the resulting mechanism of leukemogenesis is not fully understood. Exome sequencing of patient cohorts (21, 101) as well as extensive work using mouse and zebra fish models (54, 55, 107) have demonstrated that the *RUNX1-RUNX1T1* fusion requires additional genetic lesions for leukemogenesis. *RUNX1-RUNX1T1* comprises different domains related to protein and DNA interaction. The presence in some patients of a shorter isoform lacking NHR3 and NHR4 and *in vitro* and *in vivo* studies showed that these domains are not crucial for the oncogenic function of the fusion protein (51, 59). We could show that NHR2 can be substituted by a tetramerization domain in the presence of a repressor domain and that NHR4 can be replaced with an NCOR repressor domain and still promote stem cell expansion. However, transcriptome studies should be performed in the modularly substituted proteins in order to clarify if the oncogenic mechanism remains the same. Our results highlight the need for a tetramerization domain, which is present in other ETO proteins (105), providing an explanation why *RUNX1* is often fused with different members of this protein family.

ZBTB7A is involved in several cancers (80) and is specifically mutated in AML t(8;21) (21, 99-102). Here, we could demonstrate that *ZBTB7A* acts as a tumor suppressor in the context of myeloid leukemia. Although we could show that *ZBTB7A* loss-of-function mutations affect both metabolism and cell differentiation, these two processes are interconnected and depend on each other (108). Therefore, further mechanistic studies need to be conducted in order to fully understand the role of *ZBTB7A* at the interphase of metabolism and lineage fate decisions.

Finally, not all patients with AML t(8;21) have detectable *ZBTB7A* mutations (21, 99-102). Further mechanisms may affect the metabolism in this type of leukemia, which is especially dependent on glycolysis for its survival (109). Further studies need to be pursued to completely elucidate the biology of *RUNX1-RUNX1T1* rearranged AML, as well as its propensity to present *ZBTB7A* mutations. In particular, a mouse model combining *RUNX1-RUNX1T1* or the spliced isoform 9a with genetic inactivation of *ZBTB7A* (e.g. knockdown or knockout) would be of particular interest. Understanding the biology of the disease is the first

step for the development of novel therapies for AML. Glycolysis inhibitors seem to provide an interesting treatment option for AML with t(8;21) that could complement chemotherapy regimens without increasing toxicity.

5. References

1. Arber DA, Orazi A, Hasserjian R, Thiele J, Borowitz MJ, Le Beau MM, et al. The 2016 revision to the World Health Organization classification of myeloid neoplasms and acute leukemia. *Blood*. 2016;127(20):2391-405.
2. Nennecke A, Wienecke A, Kraywinkel K. [Leukemia incidence and survival in Germany according to current standardized categories]. *Bundesgesundheitsblatt Gesundheitsforschung Gesundheitsschutz*. 2014;57(1):93-102.
3. Dohner H, Estey EH, Amadori S, Appelbaum FR, Buchner T, Burnett AK, et al. Diagnosis and management of acute myeloid leukemia in adults: recommendations from an international expert panel, on behalf of the European LeukemiaNet. *Blood*. 2010;115(3):453-74.
4. Burnett A, Wetzler M, Lowenberg B. Therapeutic advances in acute myeloid leukemia. *J Clin Oncol*. 2011;29(5):487-94.
5. Armand P, Kim HT, Logan BR, Wang Z, Alyea EP, Kalaycio ME, et al. Validation and refinement of the Disease Risk Index for allogeneic stem cell transplantation. *Blood*. 2014;123(23):3664-71.
6. Dohner H, Weisdorf DJ, Bloomfield CD. Acute Myeloid Leukemia. *N Engl J Med*. 2015;373(12):1136-52.
7. Dohner H, Estey E, Grimwade D, Amadori S, Appelbaum FR, Buchner T, et al. Diagnosis and management of AML in adults: 2017 ELN recommendations from an international expert panel. *Blood*. 2017;129(4):424-47.
8. Schoch C, Kern W, Schnittger S, Buchner T, Hiddemann W, Haferlach T. The influence of age on prognosis of de novo acute myeloid leukemia differs according to cytogenetic subgroups. *Haematologica*. 2004;89(9):1082-90.
9. Solh M, Yohe S, Weisdorf D, Ustun C. Core-binding factor acute myeloid leukemia: Heterogeneity, monitoring, and therapy. *Am J Hematol*. 2014;89(12):1121-31.
10. Appelbaum FR, Kopecky KJ, Tallman MS, Slovak ML, Gundacker HM, Kim HT, et al. The clinical spectrum of adult acute myeloid leukaemia associated with core binding factor translocations. *Br J Haematol*. 2006;135(2):165-73.
11. Brunner AM, Blonquist TM, Sadrzadeh H, Perry AM, Attar EC, Amrein PC, et al. Population-based disparities in survival among patients with core-binding factor acute myeloid leukemia: a SEER database analysis. *Leuk Res*. 2014;38(7):773-80.
12. Wang Q, Stacy T, Binder M, Marin-Padilla M, Sharpe AH, Speck NA. Disruption of the Cbfa2 gene causes necrosis and hemorrhaging in the central nervous system and blocks definitive hematopoiesis. *Proc Natl Acad Sci U S A*. 1996;93(8):3444-9.
13. Wang Q, Stacy T, Miller JD, Lewis AF, Gu TL, Huang X, et al. The CBFbeta subunit is essential for CBFalpha2 (AML1) function in vivo. *Cell*. 1996;87(4):697-708.
14. Meyers S, Lenny N, Hiebert SW. The t(8;21) fusion protein interferes with AML-1B-dependent transcriptional activation. *Mol Cell Biol*. 1995;15(4):1974-82.
15. Lutterbach B, Hou Y, Durst KL, Hiebert SW. The inv(16) encodes an acute myeloid leukemia 1 transcriptional corepressor. *Proc Natl Acad Sci U S A*. 1999;96(22):12822-7.
16. Rhoades KL, Hetherington CJ, Harakawa N, Yergeau DA, Zhou L, Liu LQ, et al. Analysis of the role of AML1-ETO in leukemogenesis, using an inducible transgenic mouse model. *Blood*. 2000;96(6):2108-15.

17. Yuan Y, Zhou L, Miyamoto T, Iwasaki H, Harakawa N, Hetherington CJ, et al. AML1-ETO expression is directly involved in the development of acute myeloid leukemia in the presence of additional mutations. *Proc Natl Acad Sci U S A*. 2001;98(18):10398-403.
18. Bennett JM, Catovsky D, Daniel MT, Flandrin G, Galton DA, Gralnick HR, et al. Proposed revised criteria for the classification of acute myeloid leukemia. A report of the French-American-British Cooperative Group. *Ann Intern Med*. 1985;103(4):620-5.
19. Schlenk RF, Benner A, Krauter J, Buchner T, Sauerland C, Ehninger G, et al. Individual patient data-based meta-analysis of patients aged 16 to 60 years with core binding factor acute myeloid leukemia: a survey of the German Acute Myeloid Leukemia Intergroup. *J Clin Oncol*. 2004;22(18):3741-50.
20. Marcucci G, Mrozek K, Ruppert AS, Maharry K, Kolitz JE, Moore JO, et al. Prognostic factors and outcome of core binding factor acute myeloid leukemia patients with t(8;21) differ from those of patients with inv(16): a Cancer and Leukemia Group B study. *J Clin Oncol*. 2005;23(24):5705-17.
21. Opatz S, Bamopoulos SA, Metzeler KH, Herold T, Ksienzyk B, Braundl K, et al. The clinical mutafome of core binding factor leukemia. *Leukemia*. 2020; <https://doi.org/10.1038/s41375-019-0697-0> [Online ahead of print].
22. Ito Y, Bae SC, Chuang LS. The RUNX family: developmental regulators in cancer. *Nat Rev Cancer*. 2015;15(2):81-95.
23. Romana SP, Poirel H, Leconiat M, Flexor MA, Mauchauffe M, Jonveaux P, et al. High frequency of t(12;21) in childhood B-lineage acute lymphoblastic leukemia. *Blood*. 1995;86(11):4263-9.
24. Rubin CM, Larson RA, Anastasi J, Winter JN, Thangavelu M, Vardiman JW, et al. t(3;21)(q26;q22): a recurring chromosomal abnormality in therapy-related myelodysplastic syndrome and acute myeloid leukemia. *Blood*. 1990;76(12):2594-8.
25. Preudhomme C, Warot-Loze D, Roumier C, Gardel-Duflos N, Garand R, Lai JL, et al. High incidence of biallelic point mutations in the Runt domain of the AML1/PEBP2 alpha B gene in Mo acute myeloid leukemia and in myeloid malignancies with acquired trisomy 21. *Blood*. 2000;96(8):2862-9.
26. Harada H, Harada Y, Niimi H, Kyo T, Kimura A, Inaba T. High incidence of somatic mutations in the AML1/RUNX1 gene in myelodysplastic syndrome and low blast percentage myeloid leukemia with myelodysplasia. *Blood*. 2004;103(6):2316-24.
27. Harada H, Harada Y, Tanaka H, Kimura A, Inaba T. Implications of somatic mutations in the AML1 gene in radiation-associated and therapy-related myelodysplastic syndrome/acute myeloid leukemia. *Blood*. 2003;101(2):673-80.
28. Song WJ, Sullivan MG, Legare RD, Hutchings S, Tan X, Kufryn D, et al. Haploinsufficiency of CBFA2 causes familial thrombocytopenia with propensity to develop acute myelogenous leukaemia. *Nat Genet*. 1999;23(2):166-75.
29. Walker LC, Stevens J, Campbell H, Corbett R, Spearing R, Heaton D, et al. A novel inherited mutation of the transcription factor RUNX1 causes thrombocytopenia and may predispose to acute myeloid leukaemia. *Br J Haematol*. 2002;117(4):878-81.
30. Michaud J, Wu F, Osato M, Cottles GM, Yanagida M, Asou N, et al. In vitro analyses of known and novel RUNX1/AML1 mutations in dominant familial platelet disorder with predisposition to acute myelogenous leukemia: implications for mechanisms of pathogenesis. *Blood*. 2002;99(4):1364-72.
31. Lancrin C, Sroczynska P, Stephenson C, Allen T, Kouskoff V, Lacaud G. The haemangioblast generates haematopoietic cells through a haemogenic endothelium stage. *Nature*. 2009;457(7231):892-5.

32. Okuda T, van Deursen J, Hiebert SW, Grosveld G, Downing JR. AML1, the target of multiple chromosomal translocations in human leukemia, is essential for normal fetal liver hematopoiesis. *Cell*. 1996;84(2):321-30.
33. Gowney JD, Shigematsu H, Li Z, Lee BH, Adelsperger J, Rowan R, et al. Loss of Runx1 perturbs adult hematopoiesis and is associated with a myeloproliferative phenotype. *Blood*. 2005;106(2):494-504.
34. Chen MJ, Yokomizo T, Zeigler BM, Dzierzak E, Speck NA. Runx1 is required for the endothelial to haematopoietic cell transition but not thereafter. *Nature*. 2009;457(7231):887-91.
35. Ichikawa M, Asai T, Saito T, Seo S, Yamazaki I, Yamagata T, et al. AML-1 is required for megakaryocytic maturation and lymphocytic differentiation, but not for maintenance of hematopoietic stem cells in adult hematopoiesis. *Nat Med*. 2004;10(3):299-304.
36. Ogawa E, Inuzuka M, Maruyama M, Satake M, Naito-Fujimoto M, Ito Y, et al. Molecular cloning and characterization of PEBP2 beta, the heterodimeric partner of a novel *Drosophila* runt-related DNA binding protein PEBP2 alpha. *Virology*. 1993;194(1):314-31.
37. Zeng C, McNeil S, Pockwinse S, Nickerson J, Shopland L, Lawrence JB, et al. Intranuclear targeting of AML/CBFalpha regulatory factors to nuclear matrix-associated transcriptional domains. *Proc Natl Acad Sci U S A*. 1998;95(4):1585-9.
38. Kanno T, Kanno Y, Chen LF, Ogawa E, Kim WY, Ito Y. Intrinsic transcriptional activation-inhibition domains of the polyomavirus enhancer binding protein 2/core binding factor alpha subunit revealed in the presence of the beta subunit. *Mol Cell Biol*. 1998;18(5):2444-54.
39. Zhang Y, Strissel P, Strick R, Chen J, Nucifora G, Le Beau MM, et al. Genomic DNA breakpoints in AML1/RUNX1 and ETO cluster with topoisomerase II DNA cleavage and DNase I hypersensitive sites in t(8;21) leukemia. *Proc Natl Acad Sci U S A*. 2002;99(5):3070-5.
40. Calabi F, Pannell R, Pavloska G. Gene targeting reveals a crucial role for MTG8 in the gut. *Mol Cell Biol*. 2001;21(16):5658-66.
41. Benitez CM, Qu K, Sugiyama T, Pauerstein PT, Liu Y, Tsai J, et al. An integrated cell purification and genomics strategy reveals multiple regulators of pancreas development. *PLoS Genet*. 2014;10(10):e1004645.
42. Wang L, Gural A, Sun XJ, Zhao X, Perna F, Huang G, et al. The leukemogenicity of AML1-ETO is dependent on site-specific lysine acetylation. *Science*. 2011;333(6043):765-9.
43. Lindberg SR, Olsson A, Persson AM, Olsson I. Interactions between the leukaemia-associated ETO homologues of nuclear repressor proteins. *Eur J Haematol*. 2003;71(6):439-47.
44. Liu Y, Cheney MD, Gaudet JJ, Chruszcz M, Lukasik SM, Sugiyama D, et al. The tetramer structure of the Nrvy homology two domain, NHR2, is critical for AML1/ETO's activity. *Cancer Cell*. 2006;9(4):249-60.
45. Wichmann C, Becker Y, Chen-Wichmann L, Vogel V, Vojtkova A, Herglotz J, et al. Dimer-tetramer transition controls RUNX1/ETO leukemogenic activity. *Blood*. 2010;116(4):603-13.
46. Fukuyama T, Sueoka E, Sugio Y, Otsuka T, Niho Y, Akagi K, et al. MTG8 proto-oncoprotein interacts with the regulatory subunit of type II cyclic AMP-dependent protein kinase in lymphocytes. *Oncogene*. 2001;20(43):6225-32.
47. Corpora T, Roudaia L, Oo ZM, Chen W, Manuylova E, Cai X, et al. Structure of the AML1-ETO NHR3-PKA(RIIalpha) complex and its contribution to AML1-ETO activity. *J Mol Biol*. 2010;402(3):560-77.

48. Liu Y, Chen W, Gaudet J, Cheney MD, Roudaia L, Cierpicki T, et al. Structural basis for recognition of SMRT/N-CoR by the MYND domain and its contribution to AML1/ETO's activity. *Cancer Cell*. 2007;11(6):483-97.
49. Ahn EY, Yan M, Malakhova OA, Lo MC, Boyapati A, Ommen HB, et al. Disruption of the NHR4 domain structure in AML1-ETO abrogates SON binding and promotes leukemogenesis. *Proc Natl Acad Sci U S A*. 2008;105(44):17103-8.
50. Yan M, Burel SA, Peterson LF, Kanbe E, Iwasaki H, Boyapati A, et al. Deletion of an AML1-ETO C-terminal NcoR/SMRT-interacting region strongly induces leukemia development. *Proc Natl Acad Sci U S A*. 2004;101(49):17186-91.
51. Yan M, Kanbe E, Peterson LF, Boyapati A, Miao Y, Wang Y, et al. A previously unidentified alternatively spliced isoform of t(8;21) transcript promotes leukemogenesis. *Nat Med*. 2006;12(8):945-9.
52. Lam K, Zhang DE. RUNX1 and RUNX1-ETO: roles in hematopoiesis and leukemogenesis. *Front Biosci (Landmark Ed)*. 2012;17:1120-39.
53. El-Gebali S, Mistry J, Bateman A, Eddy SR, Luciani A, Potter SC, et al. The Pfam protein families database in 2019. *Nucleic Acids Res*. 2019;47(D1):D427-D32.
54. de Guzman CG, Warren AJ, Zhang Z, Gartland L, Erickson P, Drabkin H, et al. Hematopoietic stem cell expansion and distinct myeloid developmental abnormalities in a murine model of the AML1-ETO translocation. *Mol Cell Biol*. 2002;22(15):5506-17.
55. Yeh JR, Munson KM, Chao YL, Peterson QP, Macrae CA, Peterson RT. AML1-ETO reprograms hematopoietic cell fate by downregulating scl expression. *Development*. 2008;135(2):401-10.
56. Schessl C, Rawat VP, Cusan M, Deshpande A, Kohl TM, Rosten PM, et al. The AML1-ETO fusion gene and the FLT3 length mutation collaborate in inducing acute leukemia in mice. *J Clin Invest*. 2005;115(8):2159-68.
57. Nishida S, Hosen N, Shirakata T, Kanato K, Yanagihara M, Nakatsuka S, et al. AML1-ETO rapidly induces acute myeloblastic leukemia in cooperation with the Wilms tumor gene, WT1. *Blood*. 2006;107(8):3303-12.
58. Zuber J, Radtke I, Pardee TS, Zhao Z, Rappaport AR, Luo W, et al. Mouse models of human AML accurately predict chemotherapy response. *Genes Dev*. 2009;23(7):877-89.
59. Yan M, Ahn EY, Hiebert SW, Zhang DE. RUNX1/AML1 DNA-binding domain and ETO/MTG8 NHR2-dimerization domain are critical to AML1-ETO9a leukemogenesis. *Blood*. 2009;113(4):883-6.
60. Lee SU, Maeda T. POK/ZBTB proteins: an emerging family of proteins that regulate lymphoid development and function. *Immunol Rev*. 2012;247(1):107-19.
61. Melnick A, Carlile G, Ahmad KF, Kiang CL, Corcoran C, Bardwell V, et al. Critical residues within the BTB domain of PLZF and Bcl-6 modulate interaction with corepressors. *Mol Cell Biol*. 2002;22(6):1804-18.
62. Stogios PJ, Downs GS, Jauhal JJ, Nandra SK, Prive GG. Sequence and structural analysis of BTB domain proteins. *Genome Biol*. 2005;6(10):R82.
63. Maeda T. Regulation of hematopoietic development by ZBTB transcription factors. *Int J Hematol*. 2016;104(3):310-23.
64. Polo JM, Dell'Oso T, Ranuncolo SM, Cerchietti L, Beck D, Da Silva GF, et al. Specific peptide interference reveals BCL6 transcriptional and oncogenic mechanisms in B-cell lymphoma cells. *Nat Med*. 2004;10(12):1329-35.

65. Maeda T, Hobbs RM, Merghoub T, Guernah I, Zelent A, Cordon-Cardo C, et al. Role of the proto-oncogene *Pokemon* in cellular transformation and ARF repression. *Nature*. 2005;433(7023):278-85.
66. Suliman BA, Xu D, Williams BR. The promyelocytic leukemia zinc finger protein: two decades of molecular oncology. *Front Oncol*. 2012;2:74.
67. Ramos Pittol JM, Oruba A, Mittler G, Sacconi S, van Essen D. *Zbtb7a* is a transducer for the control of promoter accessibility by NF-kappa B and multiple other transcription factors. *PLoS Biol*. 2018;16(5):e2004526.
68. Uhlen M, Fagerberg L, Hallstrom BM, Lindskog C, Oksvold P, Mardinoglu A, et al. Proteomics. Tissue-based map of the human proteome. *Science*. 2015;347(6220):1260419.
69. Lunardi A, Guarnerio J, Wang G, Maeda T, Pandolfi PP. Role of LRF/*Pokemon* in lineage fate decisions. *Blood*. 2013;121(15):2845-53.
70. Maeda T, Merghoub T, Hobbs RM, Dong L, Maeda M, Zakrzewski J, et al. Regulation of B versus T lymphoid lineage fate decision by the proto-oncogene LRF. *Science*. 2007;316(5826):860-6.
71. Maeda T, Ito K, Merghoub T, Polisenio L, Hobbs RM, Wang G, et al. LRF is an essential downstream target of GATA1 in erythroid development and regulates BIM-dependent apoptosis. *Dev Cell*. 2009;17(4):527-40.
72. Lee SU, Maeda M, Ishikawa Y, Li SM, Wilson A, Jubb AM, et al. LRF-mediated *Dll4* repression in erythroblasts is necessary for hematopoietic stem cell maintenance. *Blood*. 2013;121(6):918-29.
73. Carpenter AC, Grainger JR, Xiong Y, Kanno Y, Chu HH, Wang L, et al. The transcription factors *Thpok* and LRF are necessary and partly redundant for T helper cell differentiation. *Immunity*. 2012;37(4):622-33.
74. Sakurai N, Maeda M, Lee SU, Ishikawa Y, Li M, Williams JC, et al. The LRF transcription factor regulates mature B cell development and the germinal center response in mice. *J Clin Invest*. 2011;121(7):2583-98.
75. Kukita A, Kukita T, Nagata K, Teramachi J, Li YJ, Yoshida H, et al. The transcription factor FBI-1/OCZF/LRF is expressed in osteoclasts and regulates RANKL-induced osteoclast formation in vitro and in vivo. *Arthritis Rheum*. 2011;63(9):2744-54.
76. Tsuji-Takechi K, Negishi-Koga T, Sumiya E, Kukita A, Kato S, Maeda T, et al. Stage-specific functions of leukemia/lymphoma-related factor (LRF) in the transcriptional control of osteoclast development. *Proc Natl Acad Sci U S A*. 2012;109(7):2561-6.
77. Davidson NL, Yu F, Kijpaisalratana N, Le TQ, Beer LA, Radomski KL, et al. Leukemia/lymphoma-related factor (LRF) exhibits stage- and context-dependent transcriptional controls in the oligodendrocyte lineage and modulates remyelination. *J Neurosci Res*. 2017;95(12):2391-408.
78. Laudes M, Christodoulides C, Sewter C, Rochford JJ, Considine RV, Sethi JK, et al. Role of the POZ zinc finger transcription factor FBI-1 in human and murine adipogenesis. *J Biol Chem*. 2004;279(12):11711-8.
79. Dobson NR, Moore RT, Tobin JE, Armstrong RC. Leukemia/lymphoma-related factor regulates oligodendrocyte lineage cell differentiation in developing white matter. *Glia*. 2012;60(9):1378-90.
80. Constantinou C, Spella M, Chondrou V, Patrinos GP, Papachatzopoulou A, Sgourou A. The multi-faceted functioning portrait of LRF/ZBTB7A. *Hum Genomics*. 2019;13(1):66.
81. Apostolopoulou K, Pateras IS, Evangelou K, Tsantoulis PK, Lontos M, Kittas C, et al. Gene amplification is a relatively frequent event leading to ZBTB7A (*Pokemon*) overexpression in non-small cell lung cancer. *J Pathol*. 2007;213(3):294-302.

82. Zhu X, Dai Y, Chen Z, Xie J, Zeng W, Lin Y. Knockdown of Pokemon protein expression inhibits hepatocellular carcinoma cell proliferation by suppression of AKT activity. *Oncol Res.* 2013;20(8):377-81.
83. Huang R, Xie T, Zhao Y, Yao CS. Attenuation of Leukemia/Lymphoma-Related Factor Protein Expression Inhibits Glioma Cell Proliferation and Invasion. *J Environ Pathol Toxicol Oncol.* 2015;34(2):125-31.
84. Lin CC, Zhou JP, Liu YP, Liu JJ, Yang XN, Jazag A, et al. The silencing of Pokemon attenuates the proliferation of hepatocellular carcinoma cells in vitro and in vivo by inhibiting the PI3K/Akt pathway. *PLoS One.* 2012;7(12):e51916.
85. Jiang L, Siu MK, Wong OG, Tam KF, Lam EW, Ngan HY, et al. Overexpression of proto-oncogene FBI-1 activates membrane type 1-matrix metalloproteinase in association with adverse outcome in ovarian cancers. *Mol Cancer.* 2010;9:318.
86. Molloy ME, Lewinska M, Williamson AK, Nguyen TT, Kuser-Abali G, Gong L, et al. ZBTB7A governs estrogen receptor alpha expression in breast cancer. *J Mol Cell Biol.* 2018;10(4):273-84.
87. Chen L, Zhong J, Liu JH, Liao DF, Shen YY, Zhong XL, et al. Pokemon Inhibits Transforming Growth Factor beta-Smad4-Related Cell Proliferation Arrest in Breast Cancer through Specificity Protein 1. *J Breast Cancer.* 2019;22(1):15-28.
88. Kumari R, Li H, Haudenschild DR, Fierro F, Carlson CS, Overn P, et al. The oncogene LRF is a survival factor in chondrosarcoma and contributes to tumor malignancy and drug resistance. *Carcinogenesis.* 2012;33(11):2076-83.
89. Wang L, Li Q, Ye Z, Qiao B. ZBTB7/miR-137 Autoregulatory Circuit Promotes the Progression of Renal Carcinoma. *Oncol Res.* 2019;27(9):1007-14.
90. Jin XL, Sun QS, Liu F, Yang HW, Liu M, Liu HX, et al. microRNA 21-mediated suppression of Sprouty1 by Pokemon affects liver cancer cell growth and proliferation. *J Cell Biochem.* 2013;114(7):1625-33.
91. Guo C, Zhu K, Sun W, Yang B, Gu W, Luo J, et al. The effect of Pokemon on bladder cancer epithelial-mesenchymal transition. *Biochem Biophys Res Commun.* 2014;443(4):1226-31.
92. Wang G, Lunardi A, Zhang J, Chen Z, Ala U, Webster KA, et al. Zbtb7a suppresses prostate cancer through repression of a Sox9-dependent pathway for cellular senescence bypass and tumor invasion. *Nat Genet.* 2013;45(7):739-46.
93. Sun G, Peng B, Xie Q, Ruan J, Liang X. Upregulation of ZBTB7A exhibits a tumor suppressive role in gastric cancer cells. *Mol Med Rep.* 2018;17(2):2635-41.
94. Liu XS, Genet MD, Haines JE, Mehanna EK, Wu S, Chen HI, et al. ZBTB7A Suppresses Melanoma Metastasis by Transcriptionally Repressing MCAM. *Mol Cancer Res.* 2015;13(8):1206-17.
95. Liu XS, Chandramouly G, Rass E, Guan Y, Wang G, Hobbs RM, et al. LRF maintains genome integrity by regulating the non-homologous end joining pathway of DNA repair. *Nat Commun.* 2015;6:8325.
96. Liu XS, Liu Z, Gerarduzzi C, Choi DE, Ganapathy S, Pandolfi PP, et al. Somatic human ZBTB7A zinc finger mutations promote cancer progression. *Oncogene.* 2016;35(23):3071-8.
97. Liu XS, Haines JE, Mehanna EK, Genet MD, Ben-Sahra I, Asara JM, et al. ZBTB7A acts as a tumor suppressor through the transcriptional repression of glycolysis. *Genes Dev.* 2014;28(17):1917-28.
98. Choi SH, Kim MY, Yoon YS, Koh DI, Kim MK, Cho SY, et al. Hypoxia-induced RelA/p65 derepresses SLC16A3 (MCT4) by downregulating ZBTB7A. *Biochim Biophys Acta Gene Regul Mech.* 2019;1862(8):771-85.

99. Hartmann L, Dutta S, Opatz S, Vosberg S, Reiter K, Leubolt G, et al. ZBTB7A mutations in acute myeloid leukaemia with t(8;21) translocation. *Nat Commun.* 2016;7:11733.
100. Lavallee VP, Lemieux S, Boucher G, Gendron P, Boivin I, Armstrong RN, et al. RNA-sequencing analysis of core binding factor AML identifies recurrent ZBTB7A mutations and defines RUNX1-CBFA2T3 fusion signature. *Blood.* 2016;127(20):2498-501.
101. Faber ZJ, Chen X, Gedman AL, Boggs K, Cheng J, Ma J, et al. The genomic landscape of core-binding factor acute myeloid leukemias. *Nat Genet.* 2016;48(12):1551-6.
102. Kawashima N, Akashi A, Nagata Y, Kihara R, Ishikawa Y, Asou N, et al. Clinical significance of ASXL2 and ZBTB7A mutations and C-terminally truncated RUNX1-RUNX1T1 expression in AML patients with t(8;21) enrolled in the JALSG AML201 study. *Ann Hematol.* 2019;98(1):83-91.
103. Redondo Monte E, Kerbs P, Greif PA. ZBTB7A links tumor metabolism to myeloid differentiation. *Exp Hematol.* 2020;87:20-4 e1.
104. Kwok C, Zeisig BB, Qiu J, Dong S, So CW. Transforming activity of AML1-ETO is independent of CBFbeta and ETO interaction but requires formation of homo-oligomeric complexes. *Proc Natl Acad Sci U S A.* 2009;106(8):2853-8.
105. Hug BA, Lazar MA. ETO interacting proteins. *Oncogene.* 2004;23(24):4270-4.
106. Rowley JD. Identification of a translocation with quinacrine fluorescence in a patient with acute leukemia. *Ann Genet.* 1973;16(2):109-12.
107. Schwieger M, Lohler J, Friel J, Scheller M, Horak I, Stocking C. AML1-ETO inhibits maturation of multiple lymphohematopoietic lineages and induces myeloblast transformation in synergy with ICSBP deficiency. *J Exp Med.* 2002;196(9):1227-40.
108. Oburoglu L, Tardito S, Fritz V, de Barros SC, Merida P, Craveiro M, et al. Glucose and glutamine metabolism regulate human hematopoietic stem cell lineage specification. *Cell Stem Cell.* 2014;15(2):169-84.
109. Isa A, Martinez-Soria N, McKenzie L, Blair H, Issa H, Luli S, et al. Identification of glycolytic pathway as RUNX1/ETO-dependent for propagation and survival. *Klin Padiatr.* 2018;230(03):165.

6. Acknowledgments

I would like to express my gratitude to my supervisor PD. Dr. Philipp A. Greif for the opportunity to work as part of his team in the Department for Experimental Leukemia and Lymphoma Research and for his open-door policy. I would also like to thank Prof. Dr. Irmela Jeremias and PD. Dr. Christian Wichmann for being an indispensable part of my thesis advisory committee and for their support and suggestions. I am also grateful to Prof. Dr. Sebastian Theurich for his advice regarding cell metabolism. Many thanks to the people from my Department, with special mention to Georg Leubolt, Paul Kerbs, Dr. Sebastian Vosberg, Anja Wilding, Dr. Monica Cusan and Alessandra Caroleo for their assistance. Additionally, I must mention all the members of the Experimental Hematology and Cell Therapies Laboratory for always welcoming me and for their help, with special mention to Linping Chen-Wichmann and Roland Windisch. I am thankful to the SFB 1243 Cancer Evolution for its financial support as well as the IRTG 1243 for all the training opportunities I could benefit from. Last but not least, I would like to thank my family and my girlfriend Viktoria for their unconditional support.

7. Publication list

Peer-reviewed Publications:

1. **Redondo Monte E**, Kerbs P, and Greif PA. ZBTB7A links tumor metabolism to myeloid differentiation. *Experimental Hematology*, 87, 20-24E.1 (2020).
2. **Redondo Monte E**, Wilding A, Leubolt L, Kerbs P, Bagnoli JW, Hartmann L, Hiddemann W, Chen-Wichmann L, Krebs S, Blum H, Cusan M, Vick B, Jeremias I, Enard W, Theurich S, Wichmann C and Greif PA. ZBTB7A prevents RUNX1-RUNX1T1-dependent clonal expansion of human hematopoietic stem and progenitor cells. *Oncogene*, 39, 3195–3205 (2020).
3. Leubolt G, **Redondo Monte E** and Greif PA. GATA2 mutations in myeloid malignancies: Two zinc fingers in many pies. *IUBMB Life*, 72 (1), 151-158 (2019).
4. Chen-Wichmann L, Shvartsman M, Preiss C, Hockings C, Windisch R, **Redondo Monte E**, Leubolt G, Spiekermann K, Lausen J, Brendel C, Grez M, Greif PA and Wichmann C. Compatibility of RUNX1/ETO Fusion Protein Modules Driving CD34+ Human Progenitor Cell Expansion. *Oncogene*, 38 (2), 261-272 (2019).
5. Cánovas V, Puñal Y, Maggio V, **Redondo E**, Marín M, Mellado B, Oliván M, Lleonart M, Planas J, Morote J and Paciucci R. Prostate Tumor Overexpressed-1 (PTOV1) promotes docetaxel-resistance and survival of castration resistant prostate cancer cells. *Oncotarget*, 8:59165-59180 (2017).

Peer-reviewed International Conference Abstracts:

1. **Redondo Monte E**, Wilding A, Leubolt G, Kerbs P, Bagnoli J, Hiddemann W, Enard W, Theurich S and Greif PA. Loss of ZBTB7A Enhances Glycolysis and Beta Oxidation in Myeloid Leukemia. *Blood* 134 (Supplement_1): 1453 (2019). 62nd Annual Meeting and Exposition of the American Society of Hematology.
2. **Redondo Monte E**, Wilding A, Leubolt G, Hartmann L, Hiddemann W, Chen-Wichmann L, Wichmann C and Greif PA. ZBTB7A Mutations in Acute Leukemia Deregulate Lineage Commitment. *Ann Hematol* 98, 1–75 (2019). ACUTE LEUKEMIAS XVII Biology and Treatment Strategies.
3. **Redondo Monte E**, Wilding A, Leubolt G, Hartmann L, Dutta S, Hiddemann W, Chen-Wichmann L, Wichmann C and Greif PA. Loss of ZBTB7A Facilitates RUNX1/RUNX1T1-Dependent Clonal Expansion and Sensitizes for Metabolic Inhibition. *Blood* 132 (Supplement 1): 1499 (2018). 61st Annual Meeting and Exposition of the American Society of Hematology.



LUDWIG-
MAXIMILIANS-
UNIVERSITÄT
MÜNCHEN

Dekanat Medizinische Fakultät
Promotionsbüro



Affidavit

Redondo Monte, Enric

Surname, first name

Max-Lebsche-Platz 30, 81377 Munich, Germany

Address

I hereby declare, that the submitted thesis entitled

Investigation of transcription factor alterations in core binding factor leukemia: Implications in clonal expansion, cell metabolism and lineage fate decisions

is my own work. I have only used the sources indicated and have not made unauthorised use of services of a third party. Where the work of others has been quoted or reproduced, the source is always given.

I further declare that the submitted thesis or parts thereof have not been presented as part of an examination degree to any other university.

Munich, 04.05.2020

Place, Date

Enric Redondo Monte

Signature doctoral candidate



LUDWIG-
MAXIMILIANS-
UNIVERSITÄT
MÜNCHEN

Dekanat Medizinische Fakultät
Promotionsbüro



Confirmation of congruency between printed and electronic version of the doctoral thesis

Doctoral Candidate: Enric Redondo Monte

Address: Max-Lebsche-Platz 30, 81377 Munich, Germany

I hereby declare that the electronic version of the submitted thesis, entitled

**Investigation of transcription factor alterations in core binding factor leukemia: Implications
in clonal expansion, cell metabolism and lineage fate decisions**

is congruent with the printed version both in content and format.

Munich, 04.05.2020

Place, Date

Enric Redondo Monte

Signature doctoral candidate

Appendix

Publication I

Publication II



Compatibility of RUNX1/ETO fusion protein modules driving CD34⁺ human progenitor cell expansion

Linping Chen-Wichmann¹ · Marina Shvartsman¹ · Caro Preiss¹ · Colin Hockings² · Roland Windisch¹ · Enric Redondo Monte³ · Georg Leubolt³ · Karsten Spiekermann^{3,4,5} · Jörn Lausen⁶ · Christian Brendel⁷ · Manuel Grez⁸ · Philipp A. Greif^{3,4,5} · Christian Wichmann¹

Received: 16 December 2017 / Revised: 14 June 2018 / Accepted: 24 July 2018 / Published online: 9 August 2018
© Springer Nature Limited 2018

Abstract

Chromosomal translocations represent frequent events in leukemia. In t(8;21)⁺ acute myeloid leukemia, RUNX1 is fused to nearly the entire ETO protein, which contains four conserved *nervy homology regions*, NHR1-4. Furthermore RUNX1/ETO interacts with ETO-homologous proteins via NHR2, thereby multiplying NHR domain contacts. As shown recently, RUNX1/ETO retains oncogenic activity upon either deletion of the NHR3 + 4 N-CoR/SMRT interaction domain or substitution of the NHR2 tetramer domain. Thus, we aimed to clarify the specificities of the NHR domains. A C-terminally NHR3 + 4 truncated RUNX1/ETO containing a heterologous, structurally highly related non-NHR2 tetramer interface translocated into the nucleus and bound to RUNX1 consensus motifs. However, it failed to interact with ETO-homologues, repress RUNX1 targets, and transform progenitors. Surprisingly, transforming capacity was fully restored by C-terminal fusion with ETO's NHR4 zinc-finger or the repressor domain 3 of N-CoR, while other repression domains failed. With an inducible protein assembly system, we further demonstrated that NHR4 domain activity is critically required early in the establishment of progenitor cultures expressing the NHR2 exchanged truncated RUNX1/ETO. Together, we can show that NHR2 and NHR4 domains can be replaced by heterologous protein domains conferring tetramerization and repressor functions, thus showing that the NHR2 and NHR4 domain structures do not have irreplaceable functions concerning RUNX1/ETO activity for the establishment of human CD34⁺ cell expansion. We could resemble the function of RUNX1/ETO through modular recombination with protein domains from RUNX1, ETO, BCR and N-CoR without any NHR2 and NHR4 sequences. As most transcriptional repressor proteins do not comprise tetramerization domains, our results provide a possible explanation as to the reason that RUNX1 is recurrently found translocated to ETO family members, which all contain tetramer together with transcriptional repressor moieties.

These authors contributed equally: Linping Chen-Wichmann, Marina Shvartsman, Caro Preiss.

Electronic supplementary material The online version of this article (<https://doi.org/10.1038/s41388-018-0441-7>) contains supplementary material, which is available to authorized users.

✉ Christian Wichmann
christian.wichmann@med.uni-muenchen.de

¹ Department of Transfusion Medicine, Cell Therapeutics and Hemostaseology, Ludwig-Maximilians University Hospital Munich, Munich, Germany

² Department of Chemical Engineering and Biotechnology, University of Cambridge, Cambridge, UK

³ Department of Internal Medicine 3, Ludwig-Maximilians University Hospital Munich, Munich, Germany

⁴ German Cancer Consortium (DKTK), Heidelberg, Germany

Introduction

In t(8;21) acute myeloid leukemia, RUNX1 is fused to nearly the entire *ETO* gene resulting in the fusion protein RUNX1/ETO (RE). Albeit less frequently, RUNX1 has also

⁵ German Cancer Research Center (DKFZ), Heidelberg, Germany

⁶ Institute for Transfusion Medicine and Immunohematology, Johann-Wolfgang-Goethe University and German Red Cross Blood Service, Frankfurt am Main, Germany

⁷ Division of Pediatric Hematology/Oncology, Boston Children's Hospital, Dana-Farber Cancer Institute, Harvard Medical School, Boston, Massachusetts, USA

⁸ Institute for Tumor Biology and Experimental Therapy, Georg-Speyer-Haus, Frankfurt, Germany

been found to fuse to the genes *MTGR1* and *ETO2*, which results in comparable translocation products [1, 2]. It is generally believed that the ETO family members ETO, ETO2 and MTGR1 act as transcriptional repressor proteins via multiple binding to corepressors, such as nuclear receptor corepressor (N-CoR), silencing-mediator for retinoid/thyroid hormone receptor (SMRT), mSin3a, and various members of the histone deacetylase (HDAC) family [3–5]. These interactions are conferred by ETO's four evolutionarily conserved *nerve homology regions* (NHR), which are all retained in the different RUNX1 fusion proteins. NHR-mediated interactions further include the E-protein HEB [6, 7] and the apoptosis-related protein SON [8]. A recent report has also shown binding of p300/CBP followed by acetylation of the fusion protein RUNX1/ETO [9]. Furthermore, ETO family members are able to form mixed complexes via the NHR2 domain, thereby multiplying the NHR domain contacts of the RUNX1/ETO fusion protein [10, 11]. Moreover, the NHR2 domain mediates homo-tetramer formation through hydrophobic and ionic/polar interactions critical for its leukemogenic potential [12, 13]. Interestingly, replacement of the NHR2 domain with a self-oligomerization FKBP domain has been shown to fully maintain the transforming capacity of full-length RE [14].

We have previously shown that truncated RUNX1/ETO (REtr) strongly cooperates with activated c-KIT to transform human CD34+ hematopoietic stem and progenitor cells (HSPCs) similarly to full-length RUNX1/ETO, thus rendering this cellular model highly attractive for studies involving the molecular determinants of RE-induced oncogenesis [15]. It has been recently demonstrated that the C-terminal NHR3 + 4-lacking splice variant of RUNX1/ETO, RUNX1/ETO9a, triggers CD34+ cell expansion similar to full-length RE. However, compared to full-length RE, RUNX1/ETO9a expanded cells express higher oncogene amounts [16]. Interestingly, these short RUNX1/ETO forms, truncated RUNX1/ETO and RUNX1/ETO9a, were shown to rapidly induce leukemia in a mouse bone marrow transplantation model [17, 18]. As truncated forms of RE have diminished N-CoR and SMRT interaction activity and a less potent transcriptional repressor function compared with full-length RE [16, 19], reduced repressive function may trigger RUNX1/ETO leukemia in this particular mouse model. These observations challenge the general understanding regarding the contribution of transcriptional repression in RUNX1/ETO leukemogenic function.

On the basis of previous studies, it remains uncertain whether the NHR2 and NHR4 domains have a specific function or can be replaced or deleted to retain RE oncogenic function. In this study, we investigated the relevance and specificity of NHR2 and NHR4/MYND domain activity for RE-triggered human CD34+ progenitor cell

transformation. Our data reveal that the NHR2 domain can be replaced by a non-ETO homologous tetramer interface. However, the resulting fusion protein then fully depends on a functional repressor domain to induce CD34+ cell expansion.

Results

NHR2 and amino acids 1–72 of BCR are highly structurally related homotetrameric interfaces

A recent study has shown that the C-terminal truncated RUNX1/ETO variant, RUNX1/ETO9a, holds equal CD34+ cell expansion capacity in ex vivo cultures compared with the full-length protein [16]. To clarify the function of the C-terminal ETO sequences, we generated a truncated RE version by replacing the NHR2 interface with a structurally similar non-ETO tetramer domain to circumvent interaction with the ETO-homologous proteins ETO, ETO2 and MTGR1. A PISA (Protein Interfaces, Surfaces and Assemblies; EMBL; [20]) database query for structurally related tetramer domains of 55–75 amino acids in length and an accessible surface area ranging between 13,000 and 15,000 Å² revealed 14 candidate domains of human origin (Fig. 1a). We selected the BCR tetramer domain because of its high structural similarity and comparable biochemical properties (Fig. 1b) without involvement in transcription and cellular localization processes. Furthermore, ETO- and BCR-interacting proteins do not show overlap (Supplementary Figure 1). Despite the low amino acid sequence homology, both tetrameric structures are composed of four similar alpha helices (Fig. 1c) forming antiparallel dimers. Two dimers then yield a tetramer in a sandwich-like fashion with high quaternary structure similarity (Fig. 1d; [12, 21]).

Substitution of the NHR2 interface via the structurally related BCR tetramer domain retains nuclear translocation and DNA-binding of truncated RUNX1/ETO but loses CD34+ ex vivo expansion capacity

The BCR tetramer interface was cloned, separated by a glycine–serine linker, to the C-terminus of the truncated RE to replace the NHR2 tetramer domain (Fig. 2a). As predicted, the chimeric RE-BCRtr had the same molecular weight as REtr (~70 kDa) (Fig. 2b). The chimeric protein translocated equally to the nucleus and bound to RUNX1 DNA-binding motifs (Fig. 2c–e; Supplementary Figure 2). Binding to PU.1 and RUNX3 tandem RUNX1 motifs was established preferentially in the oligomeric state, as previously shown [15, 22]. Deletion of the tetramer domain or substitution of amino acid L148 within the RHD domain,

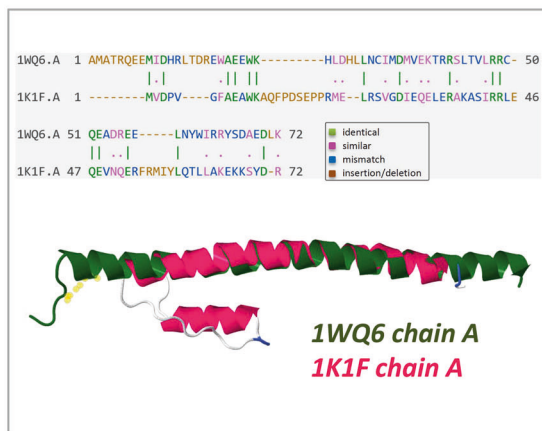
A)

##	entry	mm size	sym. num.	space group	ASA, Å ²	BSA, Å ²	ΔG ^{fold} kcal/mol	title
1	4mhe	4	2	P 1 21 1	14860.0	4605.6	4.7	STRUCTURE OF CC-CHEMOKINE 18
2	2xk5	4	2	P 43 3 2	14734.1	3916.2	2.3	STRUCTURE OF K6-LINKED DIUBIQUITIN
3	1k1f	4	2	P 1 21 1	14648.6	11261.2	15.7	STRUCTURE OF THE BCR-ABL ONCOPROTEIN OLIGOMERIZATION DOMAIN
4	2xtc	4	2	P 61 2 2	14431.5	7805.2	15.5	STRUCTURE OF THE TBL1 TETRAMERISATION DOMAIN
5	3eb5	4	4	C 2 2 2	14358.2	5196.5	0.1	STRUCTURE OF THE CIAP2 RING DOMAIN
6	1wq6	4	4	P 21 21 2	14078.5	10930.8	62.0	NHR2 TETRAMER STRUCTURE OF THE NERVY HOMOLGY TWO (NHR2) DOMAIN OF AML1-ETO
7	3ree	4	4	141 2 2	14009.0	14844.9	14.2	STRUCTURE OF MITONEET
8	4ppe	4	4	P 21 21 2	13957.7	7580.0	21.6	HUMAN RNF4 RING DOMAIN
9	2esw	4	2	P 32 2 1	13660.6	4696.8	3.3	STRUCTURE OF THE N-TERMINAL SH3 DOMAIN OF β PIX.P21-ACTIVATED KINASE (PAN)-INTERACTING EXCHANGE FACTOR
10	4e6r	4	4	P 65 2 2	13646.7	5159.0	44.0	STRUCTURE OF A CYTOPLASMIC PROTEIN NCK2 (NCK2)
11	3n52	4	2	P 21 21 21	13522.3	6830.5	12.3	STRUCTURE ANALYSIS OF MIP2
12	1ndd	4	2	P 1 21 1	13410.1	5990.6	13.6	STRUCTURE OF NEDD8
13	3hls	4	4	C 12 1	13297.7	11654.7	46.3	STRUCTURE OF THE SIGNALING HELIX COILED-COIL DOMAIN OF THE β-1 SUBUNIT OF THE SOLUBLE GUANYLYL CYCLASE
14	1f9q	4	2	P 21 21 21	13178.5	6256.4	11.7	STRUCTURE OF PLATELET FACTOR 4

B)

characteristics	NHR2	BCR
PDB	1WQ6	1K1F
method	x-ray diffraction	x-ray diffraction
resolution, Å	2.0	2.2
AA	59	72
ASA, Å ²	14078.5	14648.6
MW, kDa	29.6	34.4
stoichiometry	homo 4-mer - A4	homo 4-mer - A4
2nd structure	alpha-helical	alpha-helical
helical	73%	66%
3rd structure	4 alpha-helical tetramer	4 alpha-helical tetramer
dimer	anti-parallel (head-to-tail)	anti-parallel (head-to-tail)
tetramer	two dimer sandwich	two dimer sandwich
T _m	>90°C	84°C
citation	Liu et al., 2006	Zhao et al., 2002

C)



D)

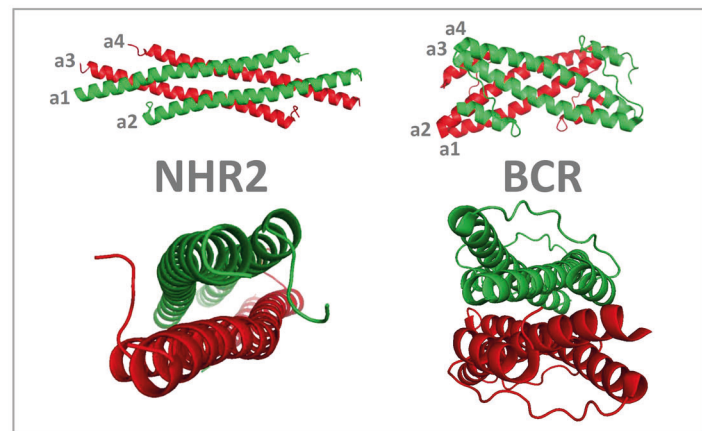


Fig. 1 Identification of the structurally related BCR tetramer domain. **a** PISA query results of tetramer domains of human origin with 55–75 amino acids in length and an accessible surface area ranging between 13,000 and 15,000 Å². **b** Structural and biochemical characteristics of NHR2 and BCR tetramer domains. **c** NHR2 and BCR amino acid

Needleman-Wunsch sequence alignment and alpha-helical structure overlay (RCSB PDB Protein Comparison Tool). **d** Quaternary structure presentation of NHR2 and BCR tetrameric composition using PyMOL software

the DNA-binding region of RUNX1, resulted in complete loss of DNA-binding (Fig. 2d). Both REtr and RE-BCRtr bound with similar strength and outperformed DNA binding of wild-type RUNX1 (Fig. 2e). Further substitution of single base pairs within the RUNX1-binding motifs of a double-stranded RUNX3 DNA sequence abolished DNA binding, thus indicating the specificity of the chimeric RE-BCRtr fusion protein to RUNX1-binding motifs. We observed binding to endogenous BCR (Supplementary Figure 1A), nevertheless expression of RE-BCRtr did not induce apoptosis as analyzed in stably expressing U937 cells (Supplementary Figure 3). However, retroviral expression of chimeric RE-BCRtr in human primary CD34+ progenitor cells from healthy donors entirely failed to induce CD34+ cell expansion in long-term ex vivo cultures. The cells were depleted from the cultures and underwent terminal monocytic differentiation (Fig. 2f, g), while REtr-expressing cells grew out and continued to

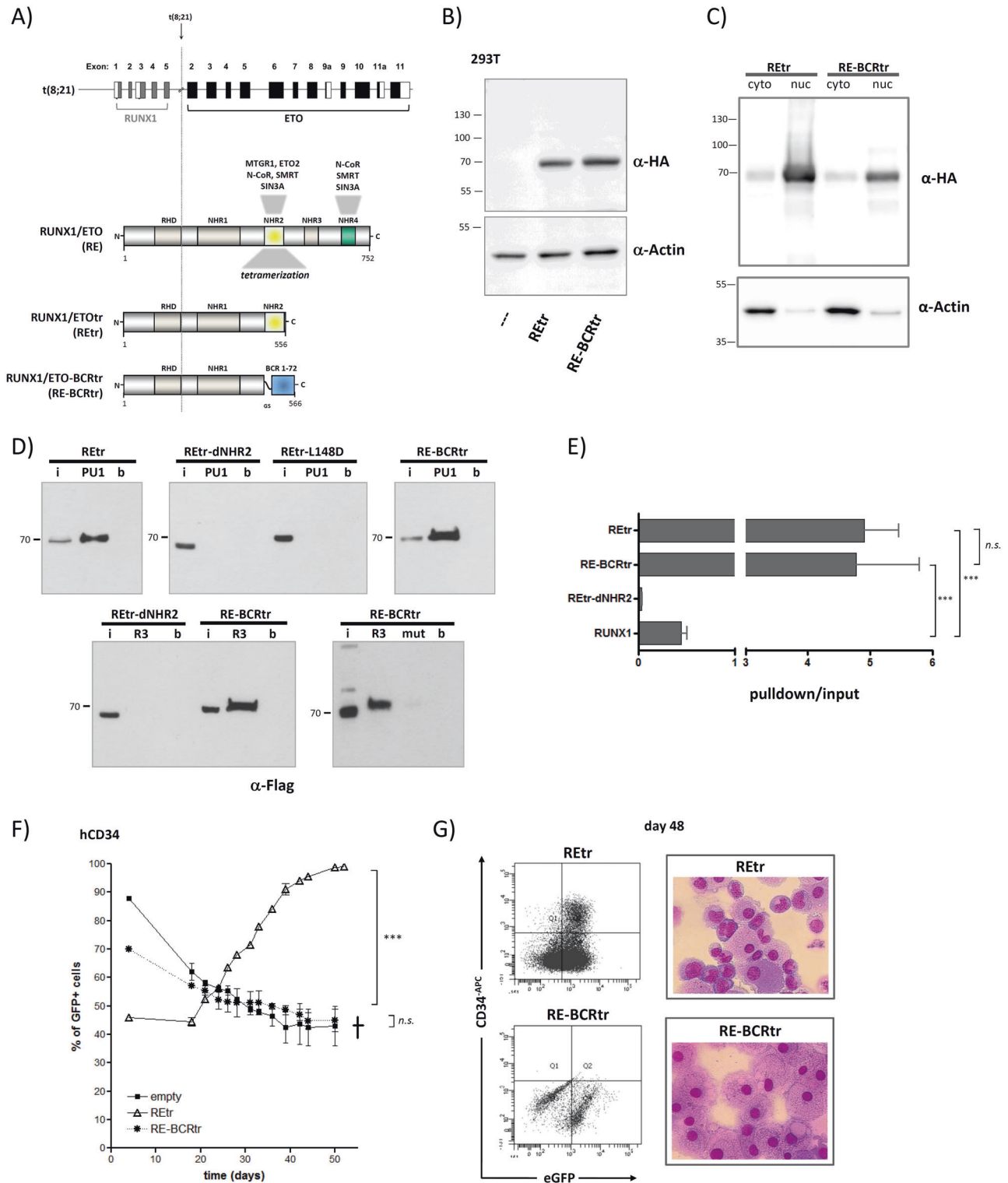
express the CD34+ antigen as previously described [15, 16]. Similar results were obtained in murine primary hematopoietic progenitor cells (Supplementary Figure 4). Self-oligomerization induced by FKBP (F36M) [14] or by an AP20187 inducible oligomerization domain [23] containing truncated RE also triggered DNA binding, although CD34+ progenitor cell expansion remained defective (Supplementary Figure 5).

C-terminal fusion of the functional NHR4/MYND zinc-finger domain rescued RE-BCRtr capacity to expand human CD34+ progenitor cells

Surprisingly, substitution of NHR2 with the BCR tetramer domain within the full-length RUNX1/ETO (RE-BCR) completely preserved the functional capacity to expand CD34+ human progenitor cells ex vivo (Fig. 3a–c). We observed similar positive selection rates of eGFP+ cells in

RE- and RE-BCR-expressing CD34⁺ cells during 55 days of ex vivo culture. Restoration of NHR2 tetramer domain-dependent functions was further validated in several myeloid cell line assays, thus demonstrating that RE and RE-BCR exert comparable effects on myeloid differentiation

block, growth arrest and apoptosis induction (Supplementary Figure 6). Furthermore, RE-BCR deletion constructs revealed that the intact NHR4/MYND domain was the critical driver that rescued the chimeric RE-BCRtr construct function in human CD34⁺ progenitors, as only constructs



◀ **Fig. 2** Functional analysis of truncated RUNX1/ETO tetramer domain switch constructs in human CD34⁺ progenitor cells. **a** Diagram of chimeric truncated RUNX1/ETO fusion proteins. **b** Western blot showing expression of truncated RUNX1/ETO forms, REtr and RE-BCRtr, upon transfection of 293T cells. **c** Cellular fractionation of REtr and RE-BCRtr transfected 293T cells analyzed via western blot. **d** ABCD-assay of flag-tagged RUNX1/ETO binding to RUNX3 and PU.1 promoter-derived RUNX1-binding motifs. **e** Quantitative analysis of DNA-binding capacity. **f** Time course of eGFP⁺ cells in human CD34⁺ ex vivo cell cultures expressing the indicated RUNX1/ETO variants. **g** FACS analysis of CD34 surface marker expression and cytopins of REtr and RE-BCRtr expressing cells at day 48 of ex vivo culture. I, input; PU1, PU1 promoter oligonucleotide; R3, RUNX3 promoter oligonucleotide; b, beads; mut, mutated RUNX3 promoter oligonucleotide. Empty, empty vector. Statistical significance determined by unpaired two-tailed *t* test unless otherwise stated in the text. *n* = 3. Bar diagrams show mean ± SD. ****P* < 0.001. n.s. not significant

encompassing a functional NHR4 zinc-finger domain induced expansion. By contrast, cells transduced with constructs lacking NHR4 did not expand due to differentiation (Fig. 3d, e). Introducing a single amino acid substitution within the NHR4 zinc-finger chelating amino acids (H695A) abolished CD34⁺ cell expansion capacity, thus indicating that only a properly folded NHR4 zinc-finger moiety can rescue the expansion defect of the chimeric RE-BCRtr (Fig. 3d). Compared to RE-BCRtr, the sole fusion of the NHR4 domain and adjacent C-terminal amino acids (647cT) protected RE-BCRtr-647cT-expressing cells from differentiation (Fig. 3f, g) and conferred colony-forming capacity in long-term cultures (Fig. 3h). Expression levels of both, functional and non-functional fusion genes, did not show significant differences (Supplementary Figure 7).

The BCR tetramer interface prevents binding of truncated RUNX1/ETO to ETO-homologous proteins and transcriptional repression of RUNX1 target genes

ETO-homologous proteins are generally involved in transcriptional repression. Therefore, we analyzed the binding properties of HA-tagged RE-BCRtr to co-expressed ETO2 and ETO. As expected, only the NHR2 domain containing REtr was able to co-immunoprecipitate with ETO2 and ETO (Fig. 4a, b). Immunoprecipitation of flag-tagged NHR2, but not flag-tagged BCR, co-purified with the ETO-homologue ETO2 (Fig. 4c). Of note, we detected wild-type ETO protein expression in human CD34⁺ cells expanded by REtr, thus indicating possible heterologous protein complex formation of RUNX1/ETOtr and wild-type ETO in primary CD34⁺ progenitor cells. We also detected MTGR1 expression in c-KIT(N822K) co-expressing CD34⁺ ex vivo cultures (Fig. 4d, e).

To compare the transcriptional properties of the chimeric RE-BCR constructs and truncated REtr, we examined the repressor activity of the recently identified RE target miR-144 via luciferase assay [24]. All constructs containing the NHR2 or NHR4 domain significantly repressed luciferase gene expression from a promoter sequence containing RUNX1 binding sites. Nonetheless, the RE-BCRtr construct failed to do so (Fig. 4f). Notably, the suppressor function of full-length RE was superior to that of the shorter REtr and RE-BCRtr-647cT forms. The repression levels of REtr and RE-BCRtr-647cT together were equivalent to those of full-length RE. Similar results were obtained when analyzing PSGL-1 cell surface expression on KG-1 cells (Fig. 4g). PSGL-1 has been recently shown to be epigenetically repressed by RUNX1/ETO [25]. Compared to empty vector-transduced cells, only REtr and RE-BCRtr-647cT were able to reduce PSGL-1 expression in transduced myeloid leukemia KG-1 cells, while RE-BCRtr-expressing cells slightly upregulated PSGL-1 expression. Altogether, the truncated form of RUNX1/ETO containing the BCR tetramer domain failed to recruit ETO-homologous proteins and did not repress the transcription of RUNX1 target genes.

The NHR4 zinc-finger domain of RE-BCR can be replaced by the repression domain 3 of N-CoR/SMRT to recapitulate the CD34⁺ expansion capacity of RUNX1/ETO

We next aimed to determine whether the NHR4 domain has a unique function or could be replaced by heterologous repressor domains. Therefore, we cloned various well-defined repressor domains to the C-terminus of truncated RE-BCRtr (Fig. 5a). The repressor domains included the mSIN3A-interacting domain of MAD1, the HDAC2 binding domain of YY1, the zinc-finger repression domain of GFI-1 and the repression domain 3 of N-CoR/SMRT. Of note, only the repression domain 3 of N-CoR (RD3), which has been described as the portion of the transcriptional corepressor N-CoR/SMRT that interacts with NHR4, was able to rescue the CD34⁺ expansion defect of RE-BCRtr (Fig. 5b). During ex vivo culture, RE-BCRtr-RD3-expressing cells were selected and continued to express the CD34 antigen (Fig. 5c). After selection of transduced cells, RE-BCRtr-RD3-expressing cells morphologically showed differentiated and blast-like cells (Fig. 5d). These cells were also able to generate colony-forming units at around day 50 of ex vivo culture (Fig. 5e). These findings indicate that the NHR4 domain does not have a unique function and can be replaced by the N-CoR repression domain 3.

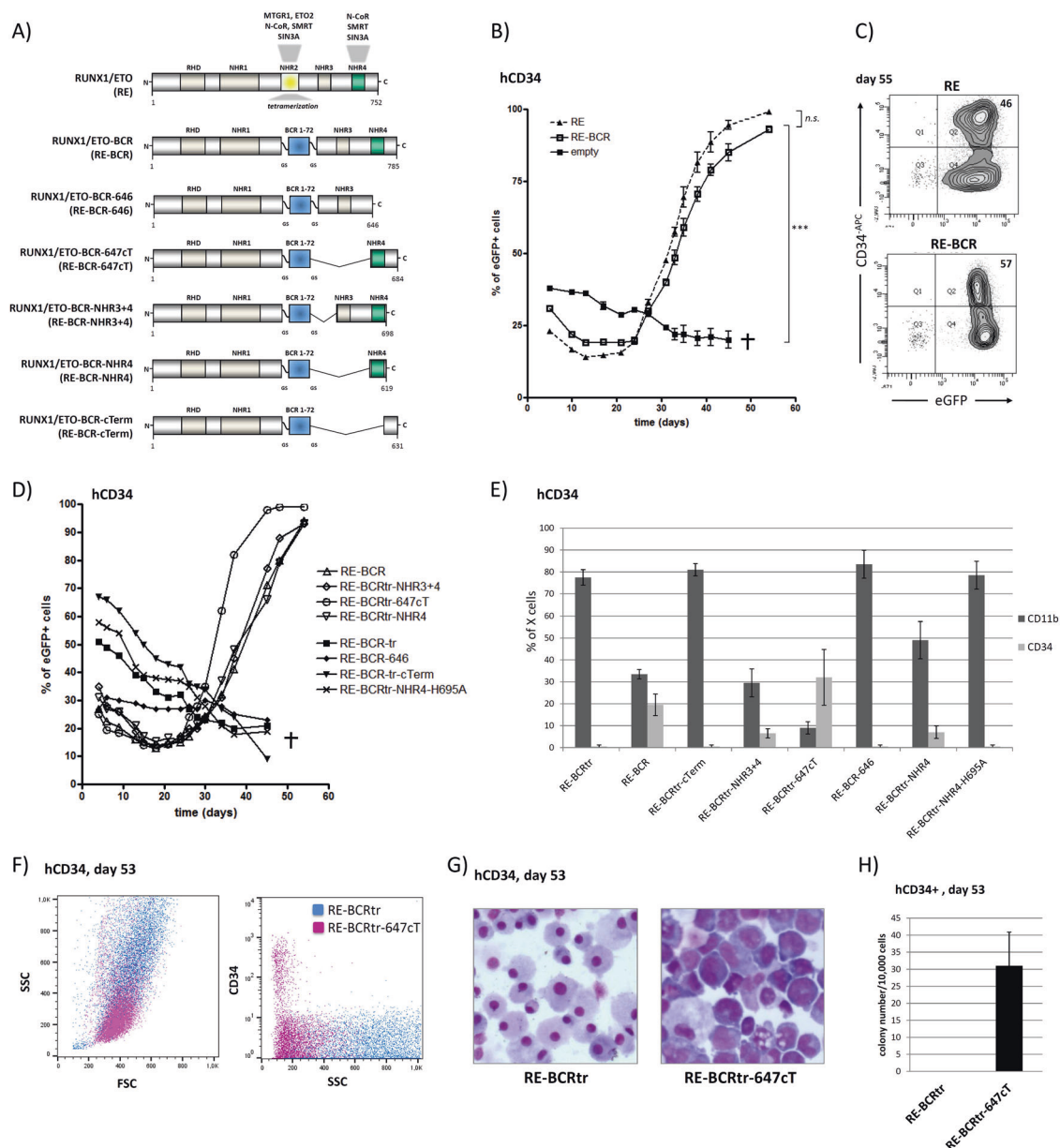


Fig. 3 Functional analysis of full-length RUNX1/ETO, RUNX1/ETO-BCR and deletion variants in human CD34⁺ progenitor cells. **a** Diagram of chimeric RUNX1/ETO fusion proteins. **b** Time course of eGFP⁺ cells expressing full-length RUNX1/ETO variants. **c** CD34 surface marker expression of RUNX1/ETO and RUNX1/ETO-BCR selected cells at day 55 of ex vivo culture. **d** Time course of eGFP⁺ cells expressing RUNX1/ETO-BCR deletion forms measured by flow cytometry. **e** CD34 and CD11b surface marker expression of

transduced cells at day 55 of ex vivo culture. One out of three experiments showing similar results. **f** FSC/SSC and SSC/CD34 overlay of hCD34⁺ cells expressing RE-BCRtr vs. RE-BCRtr-647cT at day 53 measured by flow cytometry. **g** Cytopins of hCD34⁺ cells expressing RE-BCRtr vs. RE-BCRtr-647cT at day 53. **h** CFU assays of RE-BCRtr vs. RE-BCRtr-647cT transduced CD34⁺ cells. Empty, empty vector. *** $P < 0.001$

NHR4/MYND zinc-finger domain activity is required during the early stages of ex vivo culture for the efficient expansion of colony-forming CD34⁺ progenitors

To define the temporal requirements of NHR4 domain activity for ex vivo expansion, we established a small molecule inducible heterodimerization system [26] to

induce complex formation, including the chimeric inert RE-BCRtr and the NHR4/MYND zinc-finger moiety plus a few C-terminal ETO sequences (647cT). We thus cloned one heterodimerization domain (DmrA, FKBP fragment) to the C-terminus of RE-BCRtr and the second heterodimerization domain (DmrC, FRB(T2098L)-domain of mTOR) to the N-terminus of NHR4 (647cT), separated by an internal ribosomal entry site (IRES) element into the retroviral MSCV

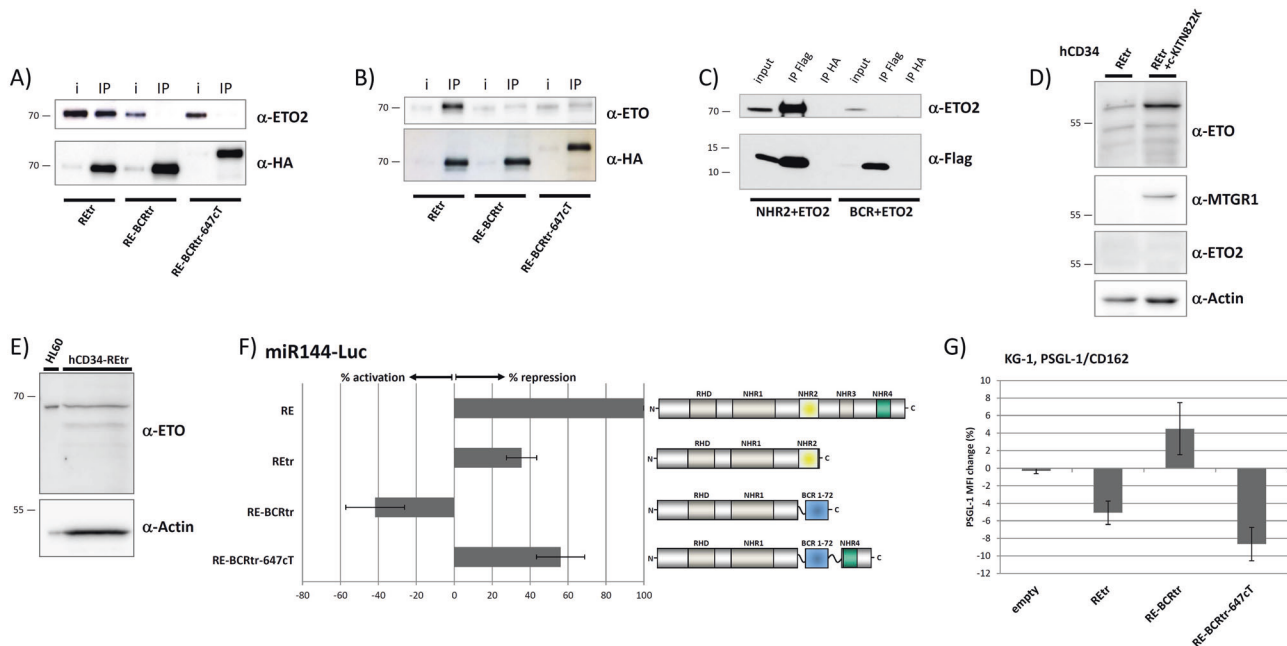


Fig. 4 The BCR-containing truncated RUNX1/ETO fails to interact with ETO-homologous proteins and does not repress RUNX1 target genes. **a** Immunoprecipitation experiments of HA-tagged RUNX1/ETO constructs and ETO2 in co-transfected 293T cells. **b** IP experiments of HA-tagged RUNX1/ETO constructs and ETO in co-transfected 293T cells. **c** IP experiments of flag-tagged NHR2 and flag-BCR tetramer domains with ETO2 in co-transfected 293T cells. **d**,

e Detection of wild-type ETO and wild-type MTGR1 in REtr- and REtr + c-KIT(N822K)-expanded CD34⁺ progenitor cells via western blot. **f** Luciferase assays with a RUNX1-dependent miR-144 luciferase construct in 293T cells 24 h after transfection (RE = 100%). **g** PSGL-1 cell surface expression of retrovirally transduced KG-1 cells. Empty, empty vector

backbone. The NHR4 domain was further equipped with a C-terminal eGFP tag (Fig. 6a). Protein association can be irreversibly induced by the rapamycin analog AP21967 (AP). Appropriate expression of the two independent constructs was verified via western blot analysis (Fig. 6b). Upon AP treatment of transfected 293T cells, we observed a shift of the eGFP-tagged NHR4 protein into the nucleus, thus suggesting complex formation with RE-BCRtr (Fig. 6c). To verify protein-protein interaction, we performed immunoprecipitation assays of transfected 293T cellular lysates. We observed interaction of RE-BCRtr and the NHR4-eGFP protein only upon AP treatment, thus indicating efficient AP-induced protein assembly (Fig. 6d). When tested in primary CD34⁺ progenitors, eGFP-positive selection was observed solely in AP-treated cells. The outgrowth resulted in undifferentiated cells, with the remaining CD34⁺ cells able to form CFUs even after 82 days ex vivo culture (Fig. 6e, f; Supplementary Fig. 8). Without AP, the cells underwent differentiation as assessed by FACS analysis. These observations confirm the RE-BCRtr and RE-BCRtr-647cT results (Fig. 3). As AP21967 does not enhance growth of untransduced human CD34⁺ cells as well as growth of RUNX1/ETO-expressing cells lacking the heterodimerizer domains DmrA and DmrC, we can exclude impact of AP21967 on the observed outgrowth of progenitor cells (Supplementary Fig. 8C). Via application

of the heterodimerization small molecule at different time points after transduction of the ex vivo cultures, we found that only treatment of early cultures resulted in sufficient CFU-inducing progenitor cells. Application at day 5 or later was associated with drastically reduced colony formation at around day 60, thus indicating that NHR4 zinc-finger activity is required in early CD34⁺ progenitor cells to maintain colony-forming capacity in ex vivo cultures (Fig. 6g, h; Supplementary Fig. 9).

Discussion

Recent reports have shown that C-terminal-deleted RUNX1/ETO variants, RUNX1/ETO9a and truncated RUNX1/ETO lacking NHR3 + 4 moieties, equally transform human CD3⁺ progenitor cells compared with full-length RE [15, 16].

In this study, we exchanged the NHR2 tetramer domain within the truncated RUNX1/ETO protein. We found that the structurally related tetramer interface of BCR retained protein stability and nuclear localization. It compensated for oligomerization-dependent DNA-binding, but lacked the ability to recruit ETO-homologous proteins and confer transcriptional repressor activity. This resulted in a transcriptional repression defective fusion protein unable to

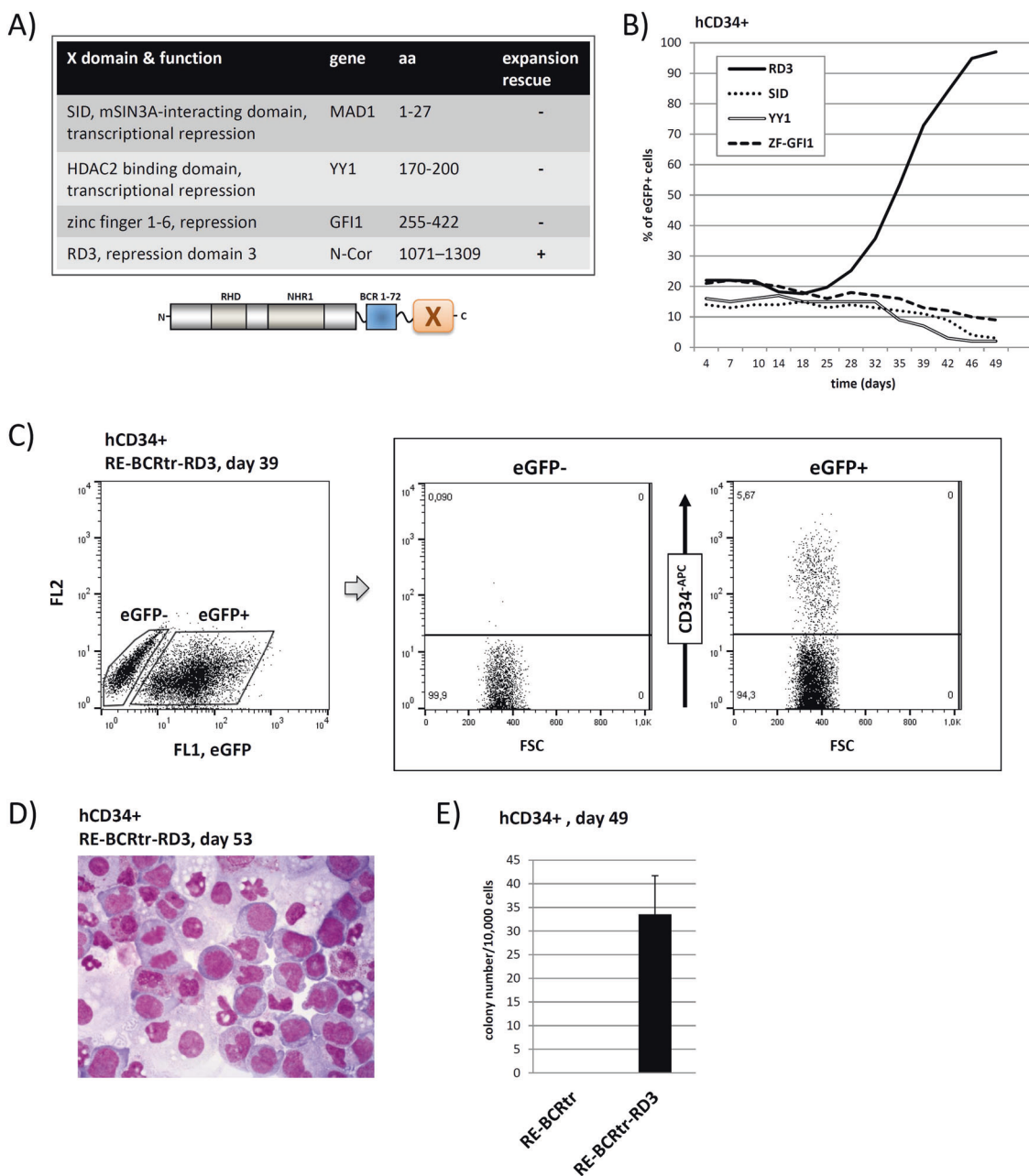


Fig. 5 The NHR4 zinc-finger domain can be replaced by the repression domain 3 of N-CoR to recapitulate the CD34⁺ expansion capacity of RUNX1/ETO. **a** List of repressor domains cloned to the C-terminus of RE-BCRtr. **b** Time course of eGFP⁺ RE-BCRtr-X-transduced CD34⁺ cells over time. **c** CD34 surface marker expression of transduced

cells at day 39 of ex vivo culture. One out of three experiments showing similar results. **d** Cytopins of hCD34⁺ cells expressing RE-BCRtr-RD3 at day 53. **e** CFU assays of RE-BCRtr vs. RE-BCRtr-RD3-transduced CD34⁺ cells

expand human CD34⁺ progenitor cells. However, the NHR4 repressor domain is preserved in the NHR2 substituted full-length RE-BCR protein, thus granting its capacity to repress transcription and transform human CD34⁺ progenitors, despite the heterologous tetramer domain (Fig. 7). These results indicate that minimal repressor activity is critically required for CD34⁺ ex vivo expansion of human CD34⁺ progenitor cells. It can be speculated that the strong repressor effect of full-length RE,

which does not hinder CD34⁺ cell expansion, might compromise murine progenitor cells to generate AML in bone marrow transplanted mice. Additionally, our results rule out critical contribution of the NHR3 domain, as deletion of the domain does not weaken RUNX1/ETO oncogenic activity in CD3⁺ cells. Furthermore, upon H695A mutation within the NHR4 zinc-finger, destroying its structure and thereby preventing N-CoR/SMRT interaction [8, 27], the chimeric RE-BCR construct failed to

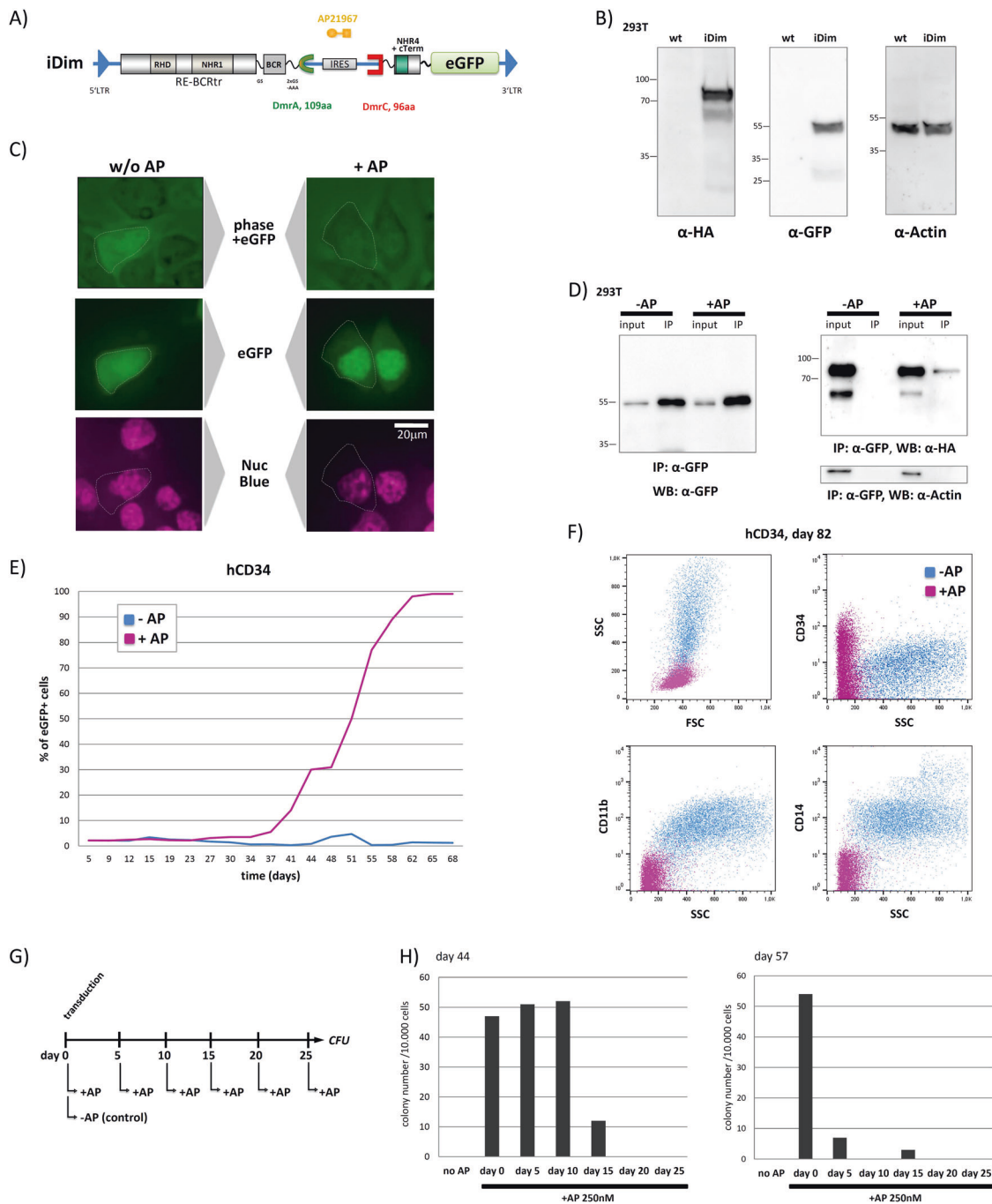


Fig. 6 NHR4 domain function is required for the ex vivo expansion of RUNX1/ETO-expressing CD34⁺ cells. **a** MSCV-based bicistronic retroviral vector construct (iDim) for simultaneous expression of a DmrA domain fused to the C-terminus of RUNX1/ETO-BCRtr and NHR4 domain sequences with an N-terminal DmrC domain, separated by an IRES element. **b** Validation of protein expression in transfected 293T cells. Proteins ran at predicted sizes. **c** Induced nuclear localization of the eGFP-tagged NHR4-DmrC protein upon AP21967 (AP) treatment. **d** Examination of heterodimerization in +/- AP-treated

lysates of iDim-transfected 293T cells via immunoprecipitation. **e** Percentage of eGFP⁺ iDim-transduced CD34⁺ cells +/- AP treatment over time. **f** SSC/FSC profile and cell surface marker expression of expanded CD34⁺ progenitor cells at day 82 of ex vivo culture. **g** Experimental timeline of AP triggered heterodimerization in transduced human CD34⁺ cells. **h** CFU assays of iDim transduced CD34⁺ cells treated with AP at different time points during ex vivo expansion. The data show representative results obtained from three experiments. IP immunoprecipitation

expand CD34⁺ cells. By contrast, the amino acid substitution C663S within NHR4 did not affect the oncogenic activity of RE-BCR (data not shown). Interestingly, this

mutation has been shown to preserve N-CoR/SMRT interaction with RUNX1/ETO [8]. Accordingly, N-CoR/SMRT might be an essential RE transmitter, which is lost in the

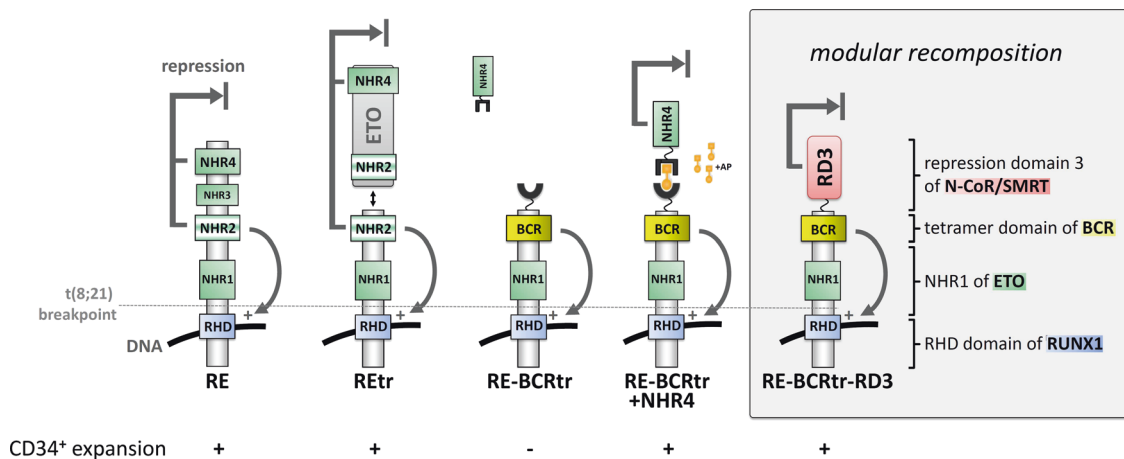


Fig. 7 Schematic model of RUNX1/ETO fusion protein compositions. Full-length and truncated RUNX1/ETO protein complexes, but not RUNX1/ETO-BCRtr, contain an intact NHR4 moiety and induce CD34⁺ cell expansion. Rescue of RE-BCRtr was observed upon C-

terminal linking of the functional NHR4 domain of ETO or the repression domain 3 of N-CoR (RD3). Minimal transcriptional repression capacity was required for efficient CD34⁺ progenitor cell expansion properties

chimeric truncated RUNX1/ETO-BCRtr protein but preserved within the truncated RUNX1/ETO protein comprising the NHR2 domain. The latter fusion protein is able to recruit N-CoR/SMRT directly via N-terminal regions of the NHR2 domain or indirectly via NHR2-mediated contacts to ETO-homologous proteins (Fig. 4). In fact, significant expression levels of different ETO-homologous proteins are evident in hematopoietic progenitor cells. However, expression of ETO homologues decreased during differentiation [28, 29]. A previous study has shown the preserved function of full-length RE with a self-oligomerizing FKBP moiety [14]. We also tested this FKBP domain, as a self-oligomerizing FKBP mutant as well as an AP21967-inducible variant. Both domains were cloned to replace the NHR2 domain within the truncated RE protein, but both failed to confer CD34⁺ cell expansion capacity, thus confirming the results obtained with chimeric RE-BCRtr. These data clearly show that the NHR2 tetramer domain can be substituted only within the full-length RE protein containing a functional NHR4 domain with repressor activity. Of note, we rescued the chimeric RE-BCRtr protein by coupling it to the repression domain 3 of N-CoR/SMRT. This domain directly recruits histone deacetylases and is able to bind to ETO [5, 30]. Additionally, from the here investigated repressor proteins, only N-CoR was mentioned to interact with HEB/E2A arguing for a potential critical role of E-proteins in functional RUNX1/ETO complexes (Supplementary Fig. 10). Our data cannot exclude that untested repressor domains can substitute for NHR4/RD3, but provide evidence that the ETO/NHR4 - N-CoR axis represents a worthwhile targeting structure within RUNX1/ETO. Overall, these findings indicate that the ETO portion of RE comprises tetramer formation and transcriptional repression activity, which can both be restored by heterologous protein

domains. However, we cannot rule out differences in RUNX1 transcriptomes between the respective RUNX1/ETO construct expressing primary cells. To our knowledge, most transcriptional repressor proteins do not comprise tetramer domains, thus providing potential insight into the reason for which RUNX1 is recurrently found translocated to ETO family members such as ETO, MTGR1 and ETO2, which all provide the NHR2 tetramer moiety together with the NHR4/MYND domain. Our results also show that the NHR2 domain is replaceable, although repressor domain function must be retained for efficient transcriptional repression and CD34⁺ cell expansion in ex vivo cultures.

Materials and methods

Cloning of MSCV vectors

All RUNX1/ETO deletions and domain-switch variants were cloned into the expression plasmid MSCV-REtr-IRES-eGFP, which includes an HA-tag for immunodetection [17]. DrmA and DrmC heterodimerization domain sequences were obtained from Clontech and cloned in frame to obtain the bicistronic iDim construct. All constructs were verified via sequence analysis.

Cell culture and retroviral transduction

293T, KG-1, K562 and U937 cells were cultured as previously described [13]. Bone marrow-derived CD34⁺ cells (LONZA, Walkersville, MD, USA) were cultured in Iscove's modified Dulbecco's medium (Life Technologies, Karlsruhe, Germany) supplemented with 20% FCS, 20 ng/mL Flt-3L, 20 ng/mL GM-CSF, 20 ng/mL SCF, 20 ng/mL

TPO, 20 ng/mL IL-6, 10 ng/mL IL-3 (all cytokines were obtained from Peprotech, Hamburg, Germany), 100 U/mL penicillin/streptomycin and 2 mM L-glutamine. Retroviral transduction and long-term cultivation were performed as previously described [31]. Bone marrow-derived human CD34+ cells (Lonza) were retrovirally transduced on retronectin coated 24-wells. 12 h after transduction, the cells were removed from retronectin and kept at high density (5×10^5 cells/ml) in tissue-coated wells. Thereafter the cells were divided every 1–2 days. Growing cultures were inspected daily and carefully pipetted up and down. Around day 28 RUNX1/ETO-expressing cells started growing out as measured by increase of eGFP+ expressing cells through FACS analysis.

FACS analysis, cell cycle and apoptosis assays

For the analysis of cell surface markers, we used FITC-, PE-, PE-Cy7 or APC-conjugated anti-human CD11b, CD14 and CD34 antibodies as well as mouse monoclonal IgG1 or mouse IgG1 isotype control antibodies (all obtained from BD Pharmingen, Heidelberg, Germany). For cell cycle analysis, cells were incubated for 15 min with 2 μ M DRAQ5 (Alexis Biochemicals, San Diego, CA, USA) at 37 °C followed by FACS analysis. AnnexinV-staining for detection of apoptotic cells was performed according to the manufacturer's instructions (BD Pharmingen).

Western blotting, immunoprecipitation, ABCD-assay and luciferase assay

The following antibodies were used to detect cellular proteins after SDS-PAGE: α -HA (HA.11; PRB-101P, Covance, Princeton, NJ, USA), α -Actin (I-19; sc-1616-R, Santa Cruz, CA, USA), α -eGFP (clone 7.1/13.1; 11814460001, Roche Life Science), α -Flag (M2; F1804, Sigma), α -ETO (C-20; sc-9737, Santa Cruz), α -ETO2/CBFA2T3 (ab33072; Abcam), α -MTGR1 (B-7; sc-390114, Santa Cruz), α -LaminB1 (ab65986, Abcam) and α -BCR (#3902, Cell Signaling). To observe protein expression in different cell compartments, 293T cells were fractionated with the Nuclear Complex Co-IP Kit (54001, Active Motif, CA, USA). The cytoplasmic and nuclear fractions were then loaded on SDS gels. Immunoprecipitation with magnetic-labeled monoclonal anti-HA antibodies (Cell Signaling, Leiden, Netherlands) and anti-GFP V_HH coupled magnetic microparticles (ChromoTek, Martinsried, Germany) was performed as described by the manufacturers. Forty-eight hours post-transfection, the 293T cells were lysed and incubated with the appropriate concentration of labeled magnetic beads. After extensive washing, the beads were magnetically collected, boiled and separated via SDS-PAGE for western blot analysis. ABCD-assay with PU.1-

and RUNX1- double-stranded oligos was performed as previously described [13]. Luciferase assays were performed as previously described [24]. Directly after seeding of 293T cells onto 96-well plates, the cells were transiently co-transfected with RUNX1/ETO-expression constructs, luciferase-reporter plasmids and renilla-reporter plasmids. A CMV-empty plasmid was co-transfected as a transfection control. At 24 h post-transfection, luciferase and renilla activity were measured using a GloMax Discover system (Promega) according to the manufacturer's instructions. ABCD-assays with PU.1- and RUNX1-double-stranded oligos was performed as previously described [13].

Acknowledgements We thank Simone Schwarz for expert technical assistance and Sandra Moore for critical comments on the manuscript. We are supported by research grants from the José Carreras Leukemia Foundation (DJCLS R 12/28, CW), the Wilhelm Sander-Foundation (2014.162.2, PG & CW) the Friedrich-Baur Foundation (CW) and the Deutsche Forschungsgemeinschaft (DFG LA 1389/6-1, JL).

Compliance with ethical standards

Conflict of interest The authors declare that they have no conflict of interest.

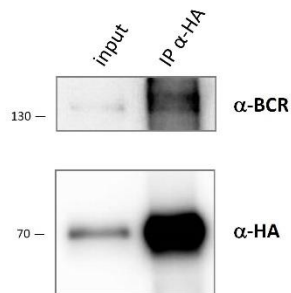
References

- Salomon-Nguyen F, Busson-Le Coniat M, Lafage Pochitaloff M, Mozziconacci J, Berger R, Bernard OA. AML1-MTG16 fusion gene in therapy-related acute leukemia with t(16;21)(q24; q22): two new cases. *Leukemia*. 2000;14:1704–5.
- Guastadisegni MC, Lonoce A, Impera L, Di Terlizzi F, Fugazza G, Aliano S, et al. CBFA2T2 and C20orf112: two novel fusion partners of RUNX1 in acute myeloid leukemia. *Leukemia*. 2010;24:1516–9.
- Wang J, Hoshino T, Redner RL, Kajigaya S, Liu JM. ETO, fusion partner in t(8;21) acute myeloid leukemia, represses transcription by interaction with the human N-CoR/mSin3/HDAC1 complex. *Proc Natl Acad Sci USA*. 1998;95:10860–5.
- Davis JN, McGhee L, Meyers S. The ETO (MTG8) gene family. *Gene*. 2003;303:1–10.
- Lausen J, Cho S, Liu S, Werner MH. The nuclear receptor corepressor (N-CoR) utilizes repression domains I and III for interaction and co-repression with ETO. *J Biol Chem*. 2004;279:49281–8.
- Park S, Chen W, Cierpicki T, Tonelli M, Cai X, Speck NA, et al. Structure of the AML1-ETO eTAFH domain-HEB peptide complex and its contribution to AML1-ETO activity. *Blood*. 2009;113:3558–67.
- Sun XJ, Wang Z, Wang L, Jiang Y, Kost N, Soong TD, et al. A stable transcription factor complex nucleated by oligomeric AML1-ETO controls leukaemogenesis. *Nature*. 2013;500:93–7.
- Ahn EY, Yan M, Malakhova OA, Lo MC, Boyapati A, Ommen HB, et al. Disruption of the NHR4 domain structure in AML1-ETO abrogates SON binding and promotes leukemogenesis. *Proc Natl Acad Sci USA*. 2008;105:17103–8.
- Wang L, Gural A, Sun XJ, Zhao X, Perna F, Huang G, et al. The leukemogenicity of AML1-ETO is dependent on site-specific lysine acetylation. *Science*. 2011;333:765–9.
- Kitabayashi I, Ida K, Morohoshi F, Yokoyama A, Mitsuhashi N, Shimizu K, et al. The AML1-MTG8 leukemic fusion protein

- forms a complex with a novel member of the MTG8(ETO/CDR) family, MTGR1. *Mol Cell Biol.* 1998;18:846–58.
11. Lindberg SR, Olsson A, Persson AM, Olsson I. Interactions between the leukaemia-associated ETO homologues of nuclear repressor proteins. *Eur J Haematol.* 2003;71:439–47.
 12. Liu Y, Cheney MD, Gaudet JJ, Chruszcz M, Lukasik SM, Sugiyama D, et al. The tetramer structure of the Neryv homology two domain, NHR2, is critical for AML1/ETO's activity. *Cancer Cell.* 2006;9:249–60.
 13. Wichmann C, Becker Y, Chen-Wichmann L, Vogel V, Vojtkova A, Herglotz J, et al. Dimer-tetramer transition controls RUNX1/ETO leukemogenic activity. *Blood.* 2010;116:603–13.
 14. Kwok C, Zeisig BB, Qiu J, Dong S, So CW. Transforming activity of AML1-ETO is independent of CBFbeta and ETO interaction but requires formation of homo-oligomeric complexes. *Proc Natl Acad Sci USA.* 2009;106:2853–8.
 15. Wichmann C, Quagliano-Lo Coco I, Yildiz O, Chen-Wichmann L, Weber H, Syzonenko T, et al. Activating c-KIT mutations confer oncogenic cooperativity and rescue RUNX1/ETO-induced DNA damage and apoptosis in human primary CD34+hematopoietic progenitors. *Leukemia.* 2015;29:279–89.
 16. Link KA, Lin S, Shrestha M, Bowman M, Wunderlich M, Bloomfield CD, et al. Supraphysiologic levels of the AML1-ETO isoform AE9a are essential for transformation. *Proc Natl Acad Sci USA.* 2016;113:9075–80.
 17. Yan M, Burel SA, Peterson LF, Kanbe E, Iwasaki H, Boyapati A, et al. Deletion of an AML1-ETO C-terminal NcoR/SMRT-interacting region strongly induces leukemia development. *Proc Natl Acad Sci USA.* 2004;101:17186–91.
 18. Yan M, Kanbe E, Peterson LF, Boyapati A, Miao Y, Wang Y, et al. A previously unidentified alternatively spliced isoform of t(8;21) transcript promotes leukemogenesis. *Nat Med.* 2006;12:945–9.
 19. DeKever RC, Yan M, Ahn EY, Shia WJ, Speck NA, Zhang DE. Attenuation of AML1-ETO cellular dysregulation correlates with increased leukemogenic potential. *Blood.* 2013;121:3714–7.
 20. Krissinel E, Henrick K. Inference of macromolecular assemblies from crystalline state. *J Mol Biol.* 2007;372:774–97.
 21. Zhao X, Ghaffari S, Lodish H, Malashkevich VN, Kim PS. Structure of the Bcr-Abl oncoprotein oligomerization domain. *Nat Struct Biol.* 2002;9:117–20.
 22. Okumura AJ, Peterson LF, Okumura F, Boyapati A, Zhang DE. t(8;21)(q22; q22) Fusion proteins preferentially bind to duplicated AML1/RUNX1 DNA-binding sequences to differentially regulate gene expression. *Blood.* 2008;112:1392–401.
 23. Pownall ME, Welm BE, Freeman KW, Spencer DM, Rosen JM, Isaacs HV. An inducible system for the study of FGF signalling in early amphibian development. *Dev Biol.* 2003;256:89–99.
 24. Kohrs N, Kolodziej S, Kuvardina ON, Herglotz J, Yillah J, Herkt S, et al. MiR144/451 expression is repressed by RUNX1 during megakaryopoiesis and disturbed by RUNX1/ETO. *PLoS Genet.* 2016;12:e1005946.
 25. Ponnusamy K, Kohrs N, Ptasinska A, Assi SA, Herold T, Hiddemann W, et al. RUNX1/ETO blocks selectin-mediated adhesion via epigenetic silencing of PSGL-1. *Oncogenesis.* 2015;4:e146.
 26. Graef IA, Holsinger LJ, Diver S, Schreiber SL, Crabtree GR. Proximity and orientation underlie signaling by the non-receptor tyrosine kinase ZAP70. *EMBO J.* 1997;16:5618–28.
 27. Liu Y, Chen W, Gaudet J, Cheney MD, Roudaia L, Cierpicki T, et al. Structural basis for recognition of SMRT/N-CoR by the MYND domain and its contribution to AML1/ETO's activity. *Cancer Cell.* 2007;11:483–97.
 28. Okumura AJ, Peterson LF, Lo MC, Zhang DE. Expression of AML/Runx and ETO/MTG family members during hematopoietic differentiation of embryonic stem cells. *Exp Hematol.* 2007;35:978–88.
 29. Lindberg SR, Olsson A, Persson AM, Olsson I. The Leukemia-associated ETO homologues are differently expressed during hematopoietic differentiation. *Exp Hematol.* 2005;33:189–98.
 30. Huang EY, Zhang J, Miska EA, Guenther MG, Kouzarides T, Lazar MA. Nuclear receptor corepressors partner with class II histone deacetylases in a Sin3-independent repression pathway. *Genes Dev.* 2000;14:45–54.
 31. Mulloy JC, Cammenga J, MacKenzie KL, Berguido FJ, Moore MA, Nimer SD. The AML1-ETO fusion protein promotes the expansion of human hematopoietic stem cells. *Blood.* 2002;99:15–23.

Suppl. Fig. 1

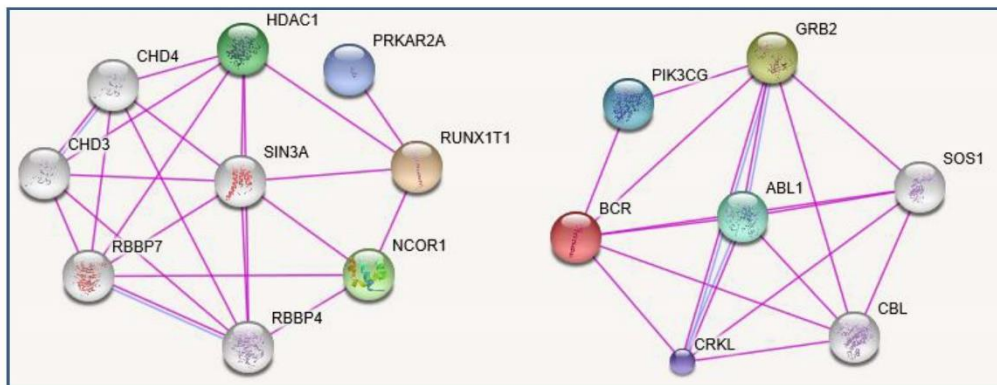
A)



B)

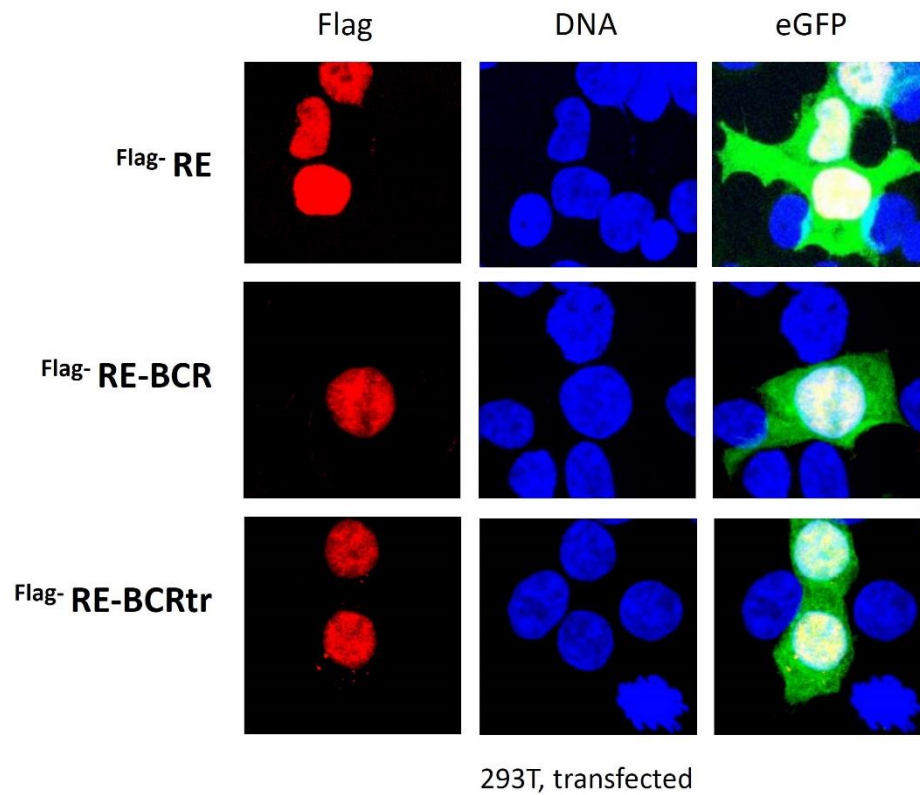
ETO		BCR	
GO:0000976	transcription regulatory region, sequence-specific DNA binding	GO:0005525	GTP binding
GO:0008134	transcription factor binding	GO:0032550	purine ribonucleoside binding
GO:0043425	bHLH transcription factor binding	GO:0032555	purine ribonucleotide binding
GO:0003700	transcription factor activity, sequence-specific DNA binding	GO:0035639	purine ribonucleoside triphosphate binding
GO:0000977	RNA polymerase II regulatory region sequence-specific DNA binding	GO:0046875	ephrin receptor binding

C)



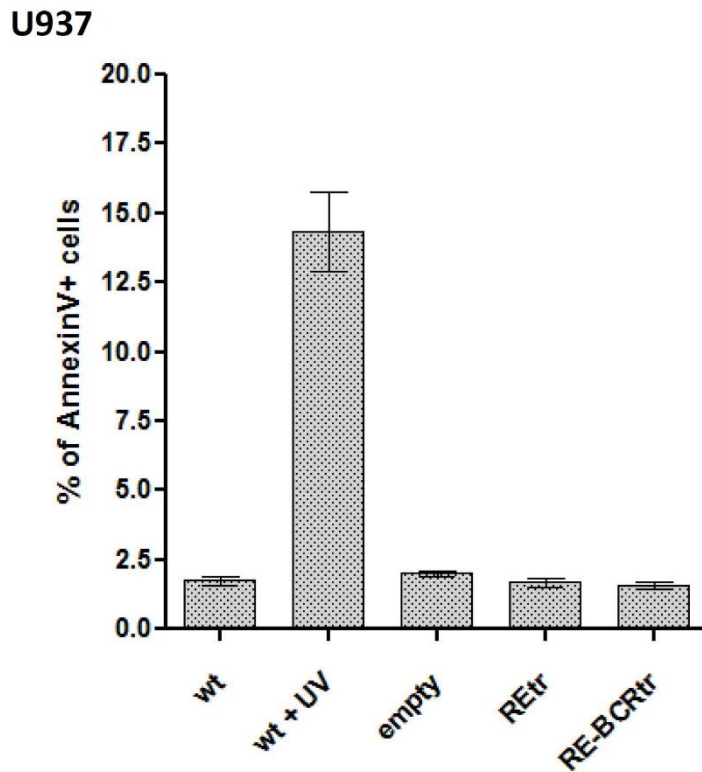
Supplementary Figure 1. A) Endogenous BCR co-immunoprecipitates with HA-tagged RE-BCRtr in transfected 293T cells. Western blot analysis of RE-BCRtr – BCR protein-protein interaction in whole cell extracts through immunoprecipitation experiments. B) Gene ontology: molecular function of ETO (RUNX1T1) versus BCR. Comparison of molecular functions using STRING database query. C) Comparison of ETO (RUNX1T1) and BCR interacting proteins (<https://string-db.org>). IP, immunoprecipitation.

Suppl. Fig. 2



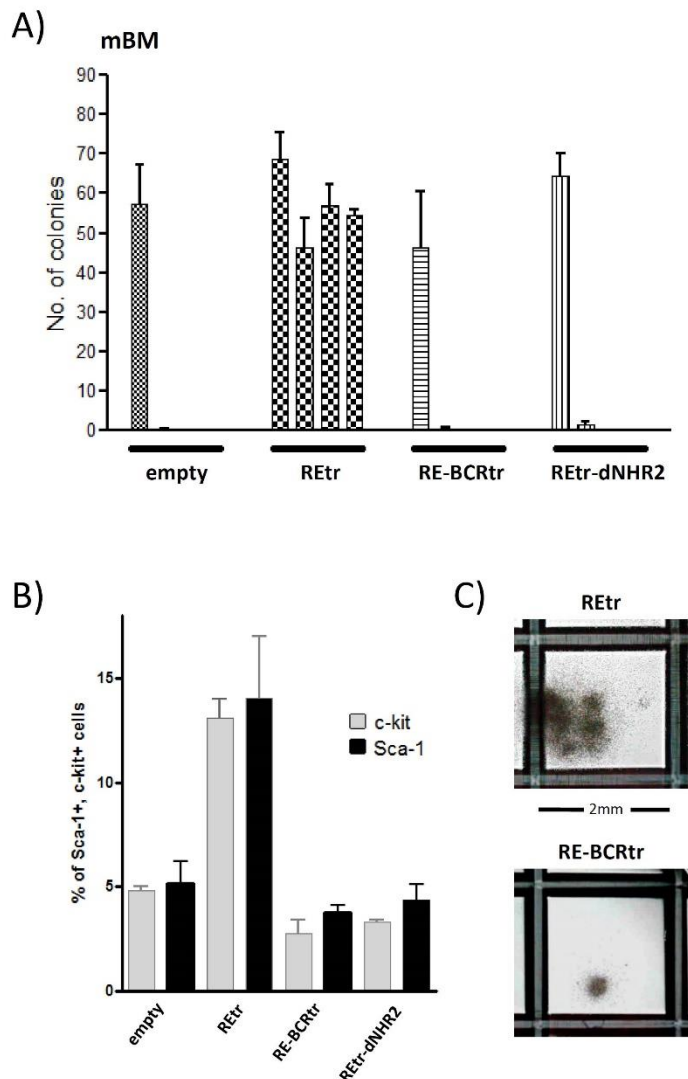
Supplementary Figure 2. RUNX1/ETO fusion proteins containing the BCR tetramer interface localize in the nucleus. Analysis of cellular localization of depicted RUNX1/ETO constructs in transfected 293T cells by fluorescence microscopy. RUNX1/ETO is stained with α -Flag antibodies. EGFP marks transfected 293T cells. Nuclear staining was performed using DAPI.

Suppl. Fig. 3



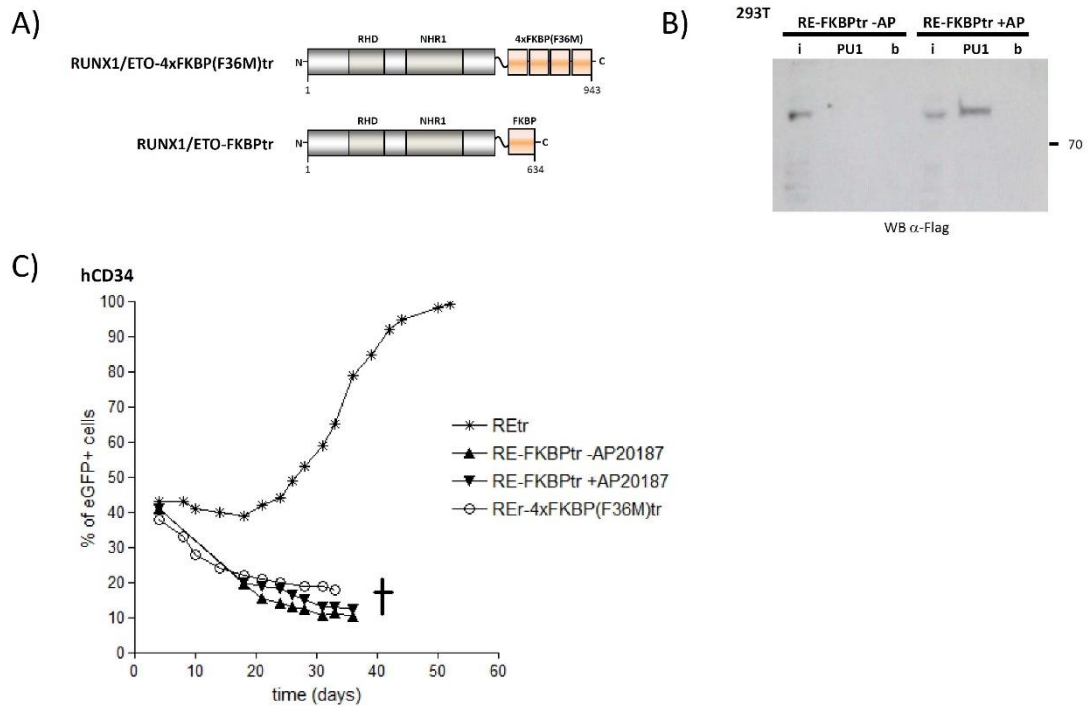
Supplementary Figure 3. The truncated RUNX1/ETO fusion protein containing the BCR tetramer interface does not induce apoptosis. Stably expressing U937 cells were analyzed for signs of apoptosis by AnnexinV-staining at day 4 after transduction. UV treated U937 wild type cells served as positive control cells. Empty, empty vector.

Suppl. Fig. 4



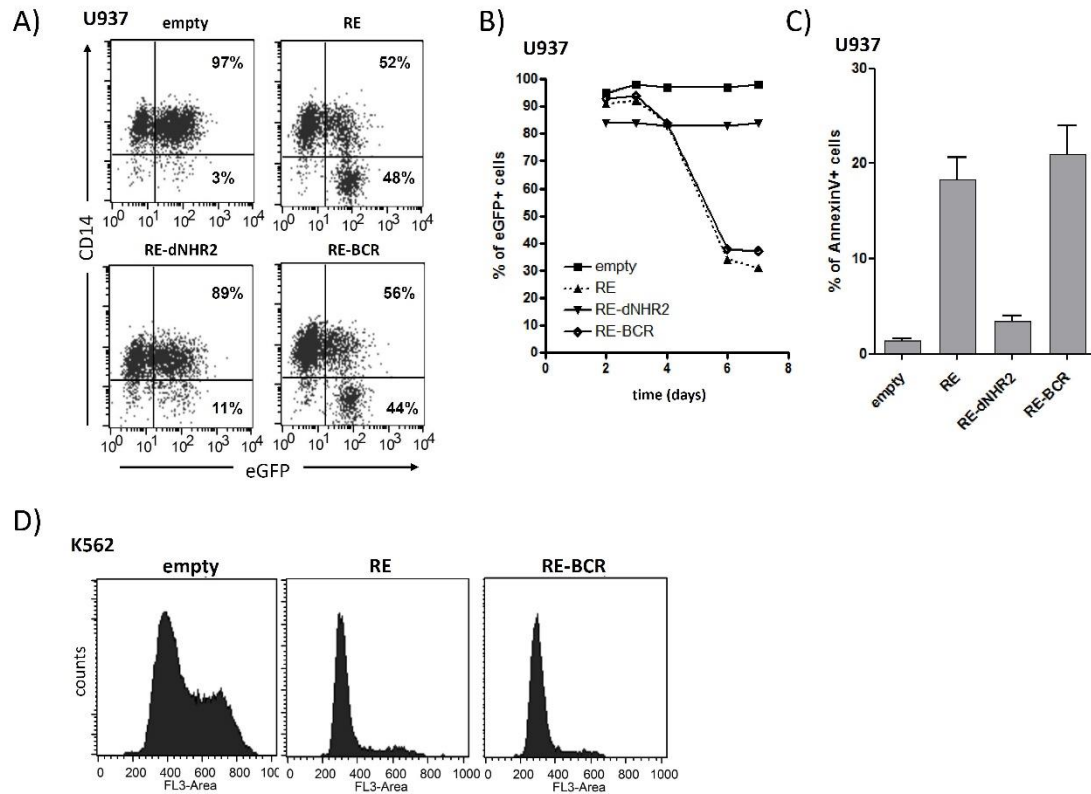
Supplementary Figure 4. The truncated RUNX1/ETO-BCR fusion protein (RE-BCRtr) fails to induce self-renewal in primary murine bone marrow cells. A) Lin-depleted murine bone marrow cells were retrovirally transduced with the indicated constructs. After transduction cells were subjected to serial methyl cellulose based colony-forming unit (CFU) assays to determine self-renewal capacity. (B) Analysis of progenitor cell surface marker expression after the first round of plating. (C) Microscopic colony formation documentation of REtr and RE-BCRtr expressing cells after the first round of plating. Depicted pictures represent typical colonies of REtr and RE-BCRtr transduced cells after the first round of plating. Empty, empty vector.

Suppl. Fig. 5



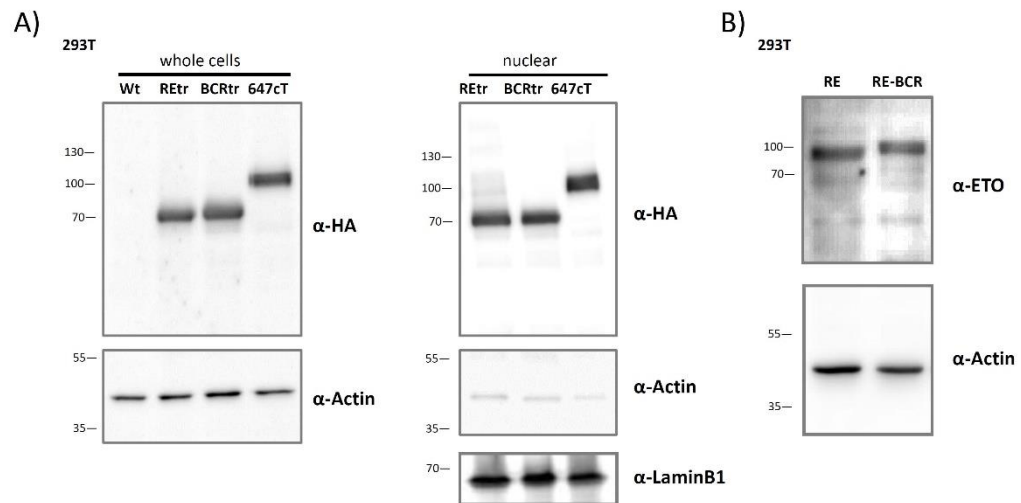
Supplementary Figure 5. NHR2 substitution through the FKBP oligomerization domain fails to expand human CD34+ progenitor cells ex vivo. A) Investigated truncated RUNX1/ETO constructs containing a self-oligomerizing FKBP variant (F36M) or an AP20187 inducible FKBP oligomerization domain (2xFKBP) separated via a glycine-serine linker. (B) AP20187 induced RUNX1/ETO-FKBPtr DNA-binding to a double-stranded PU.1 promoter element. (C) Percentage of eGFP+ cells over time measured by FACS.

Suppl. Fig. 6



Supplementary Figure 6. NHR2 domain exchange through the BCR tetramer interface rescues full length RUNX1/ETO functions in myeloid cell lines. A) FACS analysis of transduced U937 cells differentiated with vitaminD3/TGF β . 48 hours after vitaminD3/TGF β application cells were stained with CD14-PE and measured by FACS. (B) Fate of transduced eGFP-expressing U937 cells over time measured by FACS. (C) Analysis of apoptotic U937 cells 3 days after transduction as measured by eGFP/Annexin-V-APC staining. (D) Proliferative capacity of transduced K562 cells measured by Draq5-staining (FL3) followed by FACS measurement. Empty, empty vector.

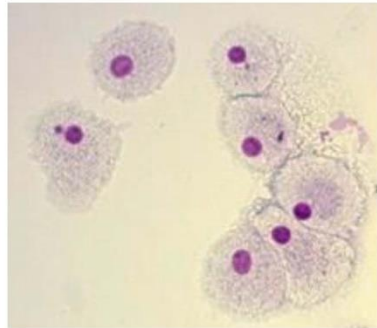
Suppl. Fig. 7



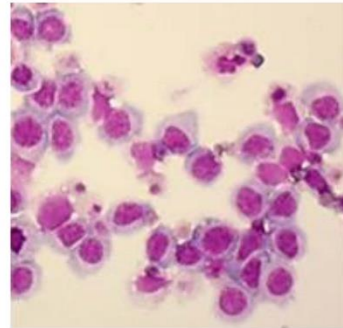
Supplementary Figure 7. Western blot expression analysis of functional and non-functional RUNX1/ETO-BCR variants. A) Whole cellular lysates and nuclear extracts of equally transfected 293T cells were analyzed for expression of HA-tagged truncated RUNX1/ETO fusion genes. (B) Comparison of full length RUNX1/ETO and RUNX1/ETO-BCR expression levels of equally transfected 293T cells.

Suppl. Fig. 8

A)
day 82



w/o AP21967



+AP21967 [250nM]

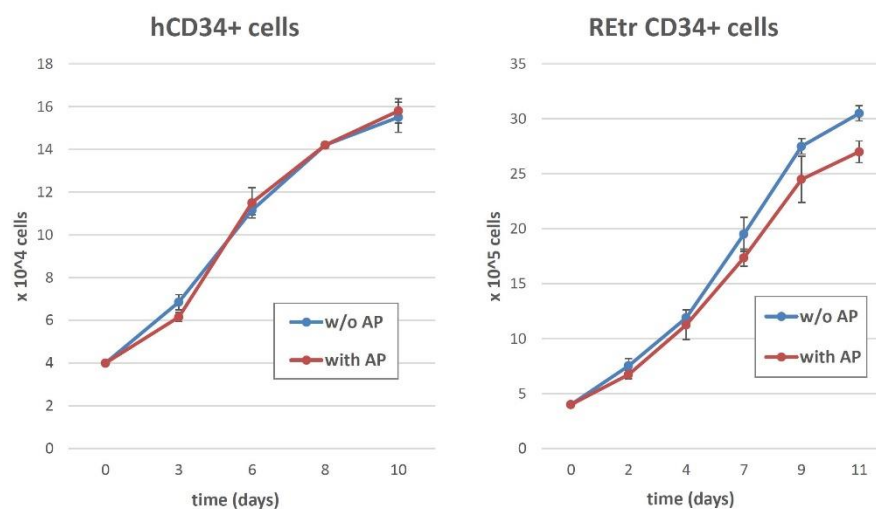
B)

CFU:

-AP21967	+AP21967
0	65 ± 9

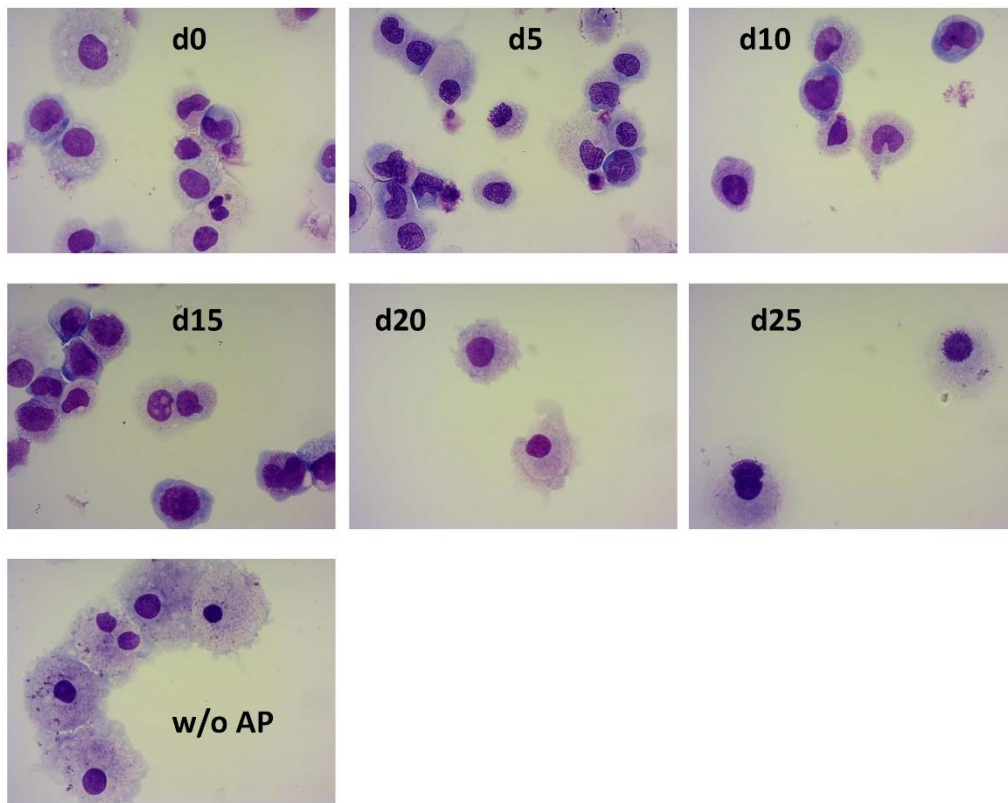
(colonies/10,000 cells)

C)



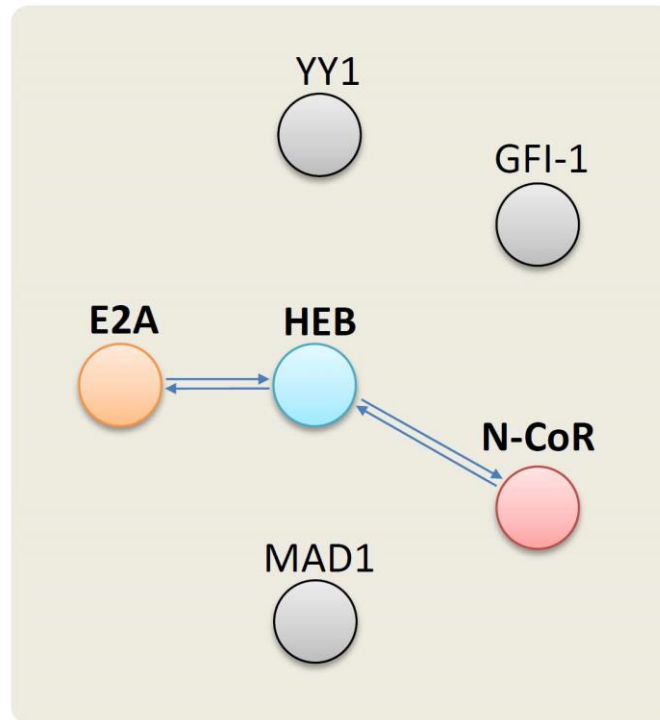
Supplementary Figure 8. Morphology, colony forming capacity and dimerizer specificity of untreated and AP21967 expanded human CD34+ progenitor cells. A) Cytospins of untreated and AP21967 selected CD34+ cells expressing the inducible heterodimerizer construct iDim at day 82 of ex vivo culture. (B) Colony forming capacity of iDim expressing CD34+ cells at day 82 of ex vivo culture. 10,000 cell were seeded into methylcellulose assay. Two weeks later colony formation was measured. (C) Cell counts of AP21967 (AP) treated untransduced CD34+ cells (left) and REtr expressing cultures (right) lacking heterodimerizer moieties over time.

Suppl. Fig. 9



Supplementary Figure 9. Morphology of untreated and AP21967 expanded human CD34+ progenitor cells expressing iDim. Cytospins of untreated and at days 0, 5, 10, 15, 20 and 25 AP21967 treated iDim transduced human CD34+ progenitor cells.




Suppl. Fig. 10



Supplementary Figure 10. HEB/E2A interactions to selected transcriptional repressor proteins. Illustration of HEB/E2A-interactions to YY1, GFI-1, MAD1 and N-CoR using STRING database (*string-db.org*).



ZBTB7A prevents RUNX1-RUNX1T1-dependent clonal expansion of human hematopoietic stem and progenitor cells

Enric Redondo Monte ^{1,2,3} · Anja Wilding ^{1,2,3} · Georg Leubolt ^{1,2,3} · Paul Kerbs ^{1,2,3} · Johannes W. Bagnoli ⁴ · Luise Hartmann ^{1,2,3} · Wolfgang Hiddemann ^{1,2,3} · Linping Chen-Wichmann ⁵ · Stefan Krebs ⁶ · Helmut Blum ⁶ · Monica Cusan ¹ · Binje Vick ⁷ · Irmela Jeremias ⁷ · Wolfgang Enard ⁴ · Sebastian Theurich ^{1,8} · Christian Wichmann ⁵ · Philipp A. Greif ^{1,2,3}

Received: 12 August 2019 / Revised: 30 January 2020 / Accepted: 4 February 2020 / Published online: 2 March 2020
© The Author(s) 2020. This article is published with open access

Abstract

ZBTB7A is frequently mutated in acute myeloid leukemia (AML) with t(8;21) translocation. However, the oncogenic collaboration between mutated ZBTB7A and the RUNX1–RUNX1T1 fusion gene in AML t(8;21) remains unclear. Here, we investigate the role of ZBTB7A and its mutations in the context of normal and malignant hematopoiesis. We demonstrate that clinically relevant ZBTB7A mutations in AML t(8;21) lead to loss of function and result in perturbed myeloid differentiation with block of the granulocytic lineage in favor of monocytic commitment. In addition, loss of ZBTB7A increases glycolysis and hence sensitizes leukemic blasts to metabolic inhibition with 2-deoxy-D-glucose. We observed that ectopic expression of wild-type ZBTB7A prevents RUNX1-RUNX1T1-mediated clonal expansion of human CD34+ cells, whereas the outgrowth of progenitors is enabled by ZBTB7A mutation. Finally, ZBTB7A expression in t(8;21) cells lead to a cell cycle arrest that could be mimicked by inhibition of glycolysis. Our findings suggest that loss of ZBTB7A may facilitate the onset of AML t(8;21), and that RUNX1-RUNX1T1-rearranged leukemia might be treated with glycolytic inhibitors.

Supplementary information The online version of this article (<https://doi.org/10.1038/s41388-020-1209-4>) contains supplementary material, which is available to authorized users.

✉ Philipp A. Greif
pgreif@med.lmu.de

- 1 Department of Medicine III, University Hospital, LMU Munich, 81377 Munich, Germany
- 2 German Cancer Consortium (DKTK), Partner Site Munich, 81377 Munich, Germany
- 3 German Cancer Research Center (DKFZ), 69121 Heidelberg, Germany
- 4 Anthropology & Human Genomics, Department of Biology II, LMU Munich, 82152 Martinsried, Germany
- 5 Department of Transfusion Medicine, Cell Therapeutics and Hemostasis, University Hospital, LMU Munich, 81377 Munich, Germany
- 6 Gene Center–Laboratory for Functional Genome Analysis, LMU Munich, 81377 Munich, Germany
- 7 Research Unit Apoptosis in Hematopoietic Stem Cells, Helmholtz Center Munich, 81377 Munich, Germany
- 8 Cancer & Immunometabolism Research Group, Gene Center, LMU Munich, 81377 Munich, Germany

Introduction

Recently, we and others found the transcription factor ZBTB7A mutated in acute myeloid leukemia (AML) with translocation t(8;21), at frequencies ranging from 9.4 to 23% [1–6]. Hotspot mutations result either in loss (A175fs) or alteration (R402) of the C-terminal zinc finger domain, which is critical for DNA-binding of ZBTB7A [1]. The specific association of ZBTB7A alterations with the t(8;21) subgroup of AML patients points toward a unique mechanism of leukemogenesis. While the RUNX1–RUNX1T1 fusion gene, which results from the t(8;21) translocation, has been studied extensively, it remains unclear how it may provide a fertile ground for the acquisition of genetic lesions in ZBTB7A.

This oncogenic collaboration may arise from a complementary action on perturbed hematopoietic development (i.e., block of specific arms of the myeloid lineage). Expression of full length RUNX1–RUNX1T1 in a murine model does not cause leukemia [7, 8], but causes a partial block of myeloid differentiation with suppression of erythropoiesis and accumulation of immature granulocytes [9]. Interestingly, *Zbtb7a* has been described as a key regulator

of hematopoietic differentiation with an essential role in erythropoiesis [10], lineage choice of B vs T lymphopoiesis [11] and long-term stem cell maintenance [12]. The involvement of *ZBTB7A* in myeloid differentiation has so far not been completely clarified, although *Zbtb7a* null mouse studies showed a deficiency of mature myeloid cells in fetal liver [12]. This suggests that *ZBTB7A* mutation could lead to a block of terminal myeloid differentiation, collaborating with *RUNX1–RUNX1T1* to produce a complete differentiation block.

Another way in which *ZBTB7A* mutation may collaborate with *RUNX1–RUNX1T1* is related to growth regulation and metabolism. While expression of *RUNX1–RUNX1T1* in stem cells causes increased proliferation [13], expression in myeloid cell lines results in growth arrest. This growth arrest is related to downregulation of *MYC* [14] and *PKM2* [15]—a master regulator of glycolysis and a key enzyme of the glycolytic pathway, respectively. Moreover, AML t(8;21) has been described to depend on glycolytic metabolism for its survival [16]. In turn, *ZBTB7A* can directly repress the transcription of several genes implicated in glycolysis (*SLC2A3*, *PFKP*, and *PKM*) in an *MYC*-independent manner, and *ZBTB7A* knockdown in a colon cancer cell line resulted in increased glycolysis and proliferation [17]. *ZBTB7A* function in glycolysis regulation has so far not been studied extensively in the hematopoietic system, but the observed upregulation of glycolytic genes upon *ZBTB7A* mutation in our patient cohort [1] may counteract the growth arrest caused by *RUNX1–RUNX1T1* in AML t(8;21).

Considering that *ZBTB7A* plays a critical role both in regulation of differentiation and cellular growth, alteration in either of the two functions may contribute to *RUNX1–RUNX1T1*-dependent leukemogenesis. In the present study, we investigate the effect of *ZBTB7A* mutation on cellular differentiation, glycolysis regulation, and *RUNX1–RUNX1T1* directed cell expansion.

Results

***ZBTB7A* promotes granulopoiesis while blocking monocytic differentiation**

Since *ZBTB7A* is a key regulator of hematopoietic lineage fate decisions, we set out to compare the effect of *ZBTB7A* wild type (WT) and mutants in the context of myeloid differentiation. The cell line HL60 is a well-established model for granulocytic and monocytic differentiation [18, 19]. Therefore, we generated HL60 cells stably expressing *ZBTB7A* WT or mutants. Granulocytic differentiation induced by all-trans retinoic acid (ATRA) was increased by *ZBTB7A* WT, while this effect was

significantly reduced for the mutants, with R402C showing residual activity (Fig. 1a, Supplementary Fig. 1a). In contrast, monocytic differentiation induced by phorbol 12-myristate 13-acetate (PMA) was reduced by *ZBTB7A* WT but not by the mutants (Fig. 1b, Supplementary Fig. 1b). In order to validate this effect, we generated an HL60 *ZBTB7A* knockout cell line. Interestingly, these cells presented a 5.5-fold increase in CD14 even without induction of differentiation (Fig. 1c, Supplementary Fig. 1c). Ectopic expression of *ZBTB7A* WT in the knockout cells restored CD14 to the native levels, while expression of the mutants had no effect (Fig. 1c, Supplementary Fig. 1d). With regard to potential therapeutic applications, we tested the PMA sensitivity of HL60 cells and found a significantly lower IC50 in absence of *ZBTB7A* (mean (pM): 256.6 in KO vs 619 in control; p value = 0.0002) (Supplementary Fig. 1e). We also observed that *ZBTB7A* WT expression lead to a loss of transduced cells in HL60 without cell sorting (Fig. 1d).

Since *ZBTB7A* was previously described to promote erythroid differentiation [10], we generated a K562 *ZBTB7A* knockout cell line (Fig. 1e). K562 cells can be used as a model for erythroid differentiation [20]. As expected, *ZBTB7A* knockout K562 cells presented a lower erythroid differentiation ($13.89 \pm 2.8\%$ reduction, p value = 0.0238) when compared with control cells (Fig. 1f, Supplementary Fig. 1f). This impaired differentiation could be rescued by ectopic expression of *ZBTB7A* WT but not by the mutants (Fig. 1f, Supplementary Fig. 1g). These findings confirm the observation that R402C and A175fs result in loss of the regulatory function of *ZBTB7A* in myeloid differentiation.

***ZBTB7A* blocks the differentiation of hematopoietic stem and progenitor cells (HSPCs)**

Considering that *ZBTB7A* was described to have a context-dependent effect on cell differentiation (i.e., block or promotion of differentiation) [21], we assessed the effect of *ZBTB7A* mutations on the HSPC compartment. To this aim, we generated human CD34+ cells stably expressing *ZBTB7A* WT or mutants. Upon differentiation, we observed a significant reduction of mature erythrocytes (CD71+ CD235a+) in WT expressing cells, consistent with previous reports [12]. In contrast, *ZBTB7A* mutant expressing cells differentiated to a similar extent as the control cells (Fig. 2a, b). When cells were differentiated to granulocytes and monocytes, we observed that WT transduced cells presented a reduction of CD15+ cells (corresponding to decreased granulopoiesis). Again, cells expressing the mutants did not exhibit this differentiation block (Fig. 2c, d). A schematic representation of the effects of *ZBTB7A* in differentiation is shown in Fig. 2e.

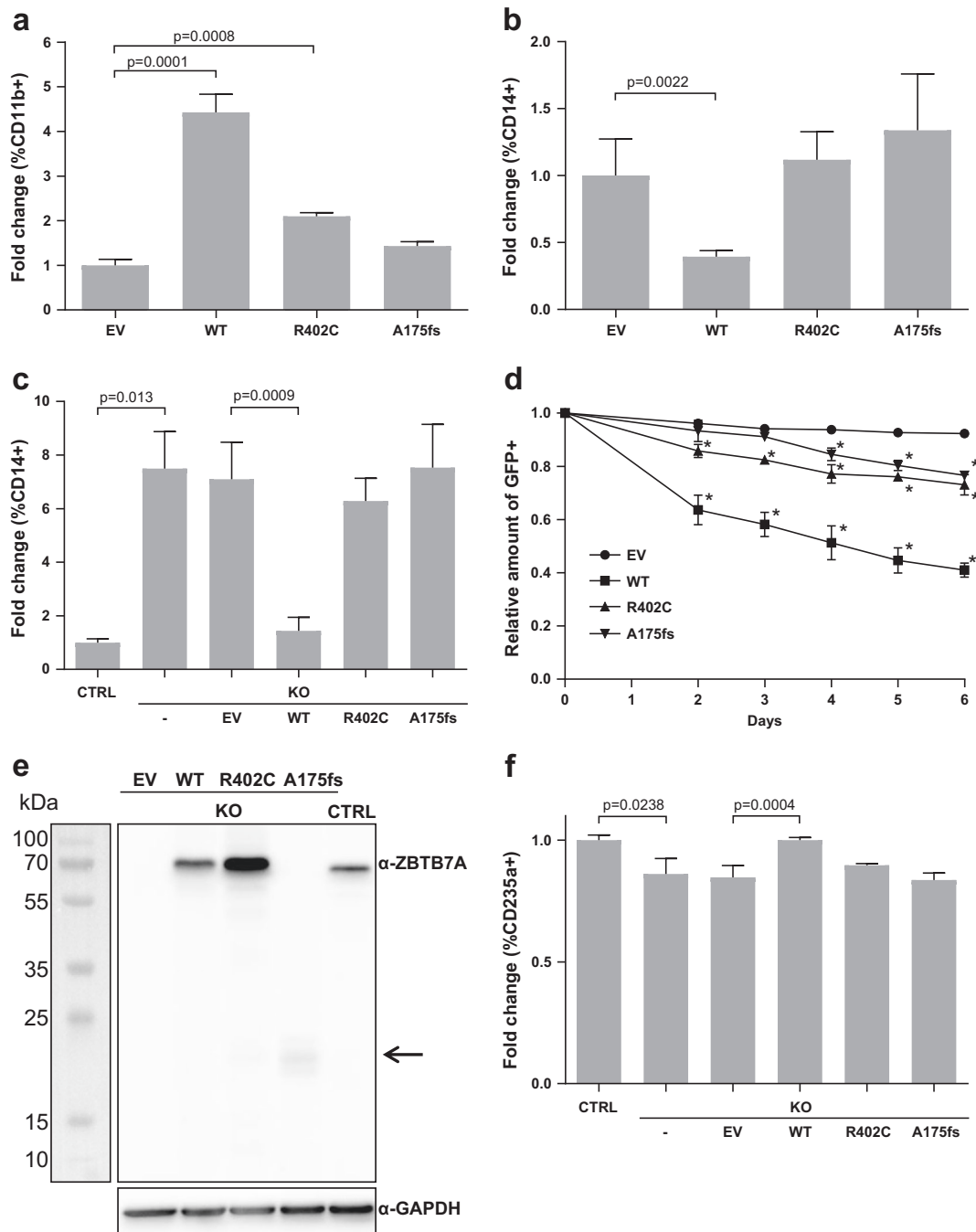


Fig. 1 ZBTB7A promotes granulopoiesis while blocking monocytic differentiation. **a** HL60 cells stably expressing an empty vector (EV), ZBTB7A WT or mutants were differentiated by ATRA treatment. CD11b expression was assessed by flow cytometry. **b** HL60 cells stably expressing ZBTB7A WT or mutants were differentiated by PMA treatment. CD14 expression was assessed by flow cytometry. **c** HL60 ZBTB7A KO and HL60 ZBTB7A KO stably expressing

ZBTB7A WT or mutants without induction of differentiation. CD14 expression was assessed by flow cytometry. **d** Competitive growth of HL60 cells stably expressing ZBTB7A WT or mutants. **e** Western blot from K562 cells, arrow indicates low levels of the ZBTB7A A175fs mutant. **f** K562 ZBTB7A KO without induction of differentiation. CD235a expression was assessed by flow cytometry. **p* value < 0.05 compared with control cells.

Loss of ZBTB7A sensitizes to glycolysis inhibition

In order to study the effects of ZBTB7A on metabolism described in other tissues [17], we analyzed transcriptomes by RNA-Seq in K562 ZBTB7A knockout and control

clones (GSE140472). Differential expression analysis revealed 1089 genes deregulated between the two settings (adjusted *p* value < 0.05 and log-fold-change > 0.5) (Supplementary Fig. 2a). Gene set enrichment analysis revealed NOTCH3 transcriptional regulation as well as nutrient

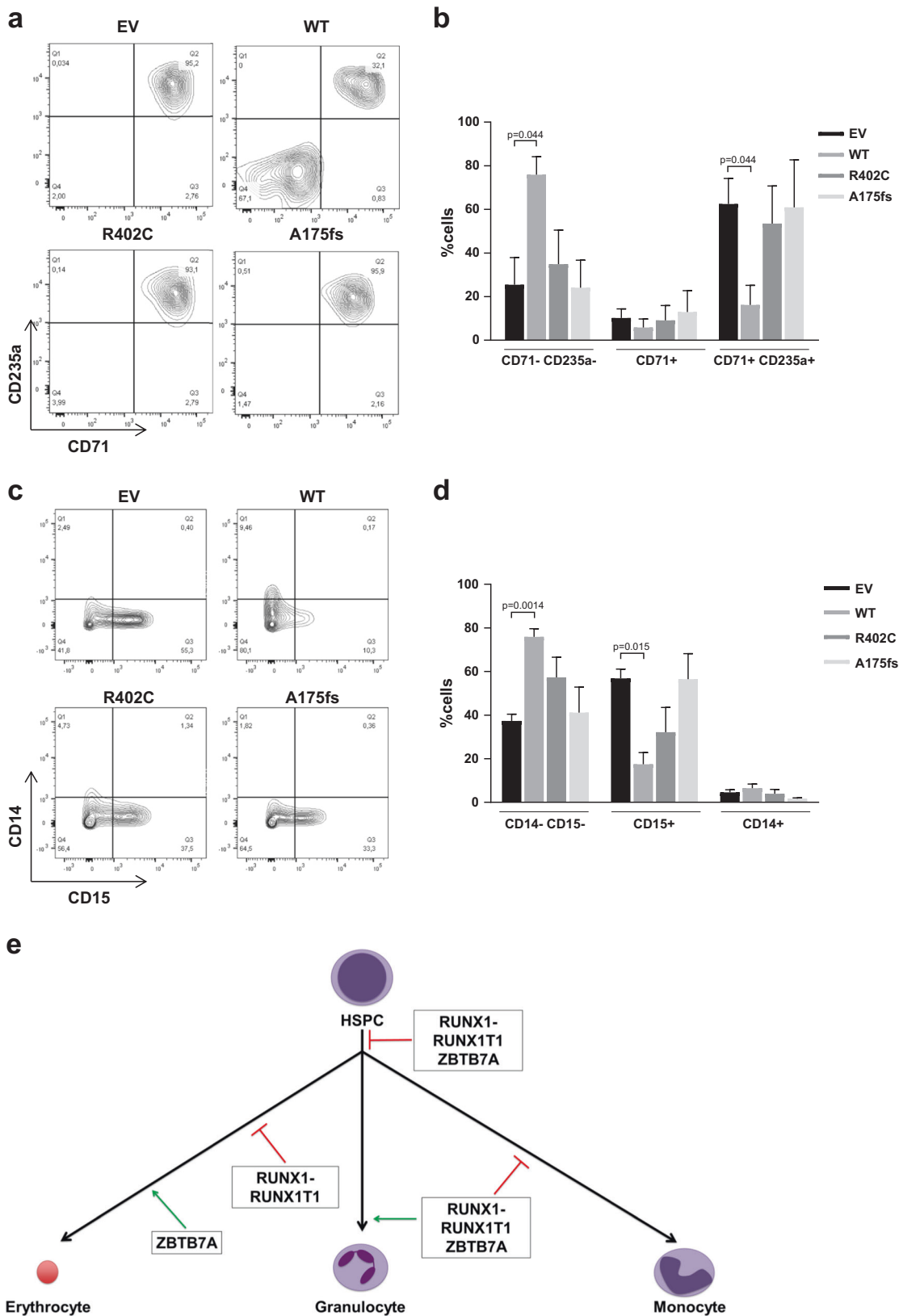


Fig. 2 ZBTB7A blocks the differentiation of HSPC. Flow cytometry measurements of human bone marrow CD34+ cells stably expressing ZBTB7A WT or mutants are shown. **a** Representative results of cells primed for differentiation into erythrocytes using StemSpan Erythroid Expansion Supplement for 7 days. **b** Summary of three independent experiments. **c** Representative results of cells primed for differentiation into monocytes and granulocytes using HemaTox Myeloid Kit for 7 days. **d** Summary of three independent experiments. **e** Schematic representation of the effects of ZBTB7A and RUNX1-RUNX1T1 expression on hematopoietic lineage commitment.

transport by solute carrier (SLC) proteins as the top significantly affected gene ontologies (Fig. 3a).

As ZBTB7A was previously described to be a negative regulator of glycolysis genes in colon cancer [17], we focused on the expression of genes implicated in glycolysis. This revealed an upregulation of the glucose transporters 1 (*SLC2A1*) and 3 (*SLC2A3*) in the knockout cells (Fig. 3b). Interestingly, two glycolytic enzymes not previously reported to be ZBTB7A targets were also found to be upregulated in KO cells: phosphoglycerate mutase isoforms 2 and 3 (*PGM2* and *PGM3*) responsible of converting 3-phosphoglycerate into 2-phosphoglycerate, and Enolase 2 (*ENO2*) responsible for converting 2-phospho-D-glycerate into phosphoenolpyruvate (Fig. 3b) (all comparisons $p < 0.05$). Other previously reported genes, such as *PKM* or *PKFP*, were not significantly deregulated in this setting (Supplementary Fig. 2b, c). The upregulated genes were confirmed as ZBTB7A targets (Supplementary Fig. 3) using publicly available ZBTB7A K562 ChIP-Seq data (ENCSR000BME, ENCODE database).

Based on these data, we selected two KO clones to test the functional impact of ZBTB7A loss on cellular metabolism. In metabolic flux analyses, ZBTB7A KO cells presented a slightly increased non-glycolytic acidification (Supplementary Fig. 4a, b). ZBTB7A KO cells did not show a statistically significant increase of glycolysis upon glucose administration (Fig. 3c, Supplementary Fig. 4c), but they presented a higher glycolytic capacity after inhibition of mitochondrial energy production compared with control (Fig. 3c–e). Interestingly, the increased energy demands of ZBTB7A KO cells could be compensated by the upregulation of mitochondrial respiration under glucose deprivation (Supplementary Fig. 4e). In addition, we observed that knockout cells were more sensitive to glycolysis inhibition with 2-deoxy-D-glucose (2DG) compared with control cells (mean IC₅₀ (mM): 8.03 in KO#1 and 5.05 in KO#2 vs 10.34 in control; p values = 0.124 and 0.0005, respectively) (Fig. 3f). This effect was also confirmed by long-term treatment, where control cells were hardly affected by glycolysis inhibition, while knockout cells grew significantly slower (Supplementary Fig. 4d). The differences observed between the two KO clones tested may arise due to off-target effects of the Cas9 treatment or due to the fact that these lines were generated from single cells, amplifying any preexisting differences in the cell of origin. However, both clones show the same trends, namely, increased glycolysis after mitochondrial shutdown and increased sensitivity to glycolysis inhibition. In addition, we evaluated ex vivo sensitivity to 2DG in six different AML patient-derived xenografts (PDX) models where we could observe variable degrees of sensitivity (Supplementary Fig. 5).

ZBTB7A prevents RUNX1-RUNX1T1-dependent clonal expansion

Since ZBTB7A mutations are associated with AML t(8;21), we assessed the interplay between ZBTB7A and the RUNX1–RUNX1T1 fusion. To this aim, we used the truncated version of RUNX1–RUNX1T1 (hereafter referred to as RUNX1–RUNX1T1tr) that causes clonal expansion of hCD34+ cells [13]. A scheme of the experimental setting is provided in Fig. 4a. As expected, single positive cells expressing RUNX1–RUNX1T1tr expanded, while single positive cells expressing ZBTB7A WT or mutants did not (representative experiment in Fig. 4b, replicates of this experiment in Supplementary Fig. 6). Interestingly, cells expressing both RUNX1–RUNX1T1tr and ZBTB7A WT did not clonally expand and were quickly outcompeted by RUNX1–RUNX1T1tr single positive cells. The clonal expansion was enabled by the ZBTB7A mutations R402C and A175fs. Upon coexpression of these mutants, double positive cells expanded and no significant disadvantage over the RUNX1–RUNX1T1tr single positive cells was observed.

ZBTB7A causes cell cycle arrest

In order to elucidate if the prevention of RUNX1–RUNX1T1tr-dependent clonal expansion by ZBTB7A arises either from downregulation of glycolysis, enhanced differentiation, or a combination of both effects, we expanded hCD34+ cells using RUNX1–RUNX1T1tr for 60 days and then transduced them with ZBTB7A WT and R402C. Cell-cycle analysis revealed that ZBTB7A WT expressing cells show a significant G0/G1 arrest in detriment of the S phase (Fig. 4c). In addition, we generated Kasumi-1 cells stably expressing ZBTB7A WT or mutants. We have previously shown that forced expression of ZBTB7A WT in Kasumi-1 causes a growth disadvantage [1]. Cell-cycle analysis revealed that ZBTB7A WT overexpressing cells show G0/G1 arrest in detriment of the S phase when compared with mutants and control (Fig. 4d). When glycolysis was inhibited by 2DG treatment, control cells showed a block of cell-cycle progression, reminiscent of the effect caused by ZBTB7A WT overexpression (Fig. 4d). At the same time, differentiation marker analysis (CD11b, CD14, and CD15) did not show any significant difference between the conditions tested (Supplementary Fig. 7).

Discussion

ZBTB7A mutations in the context of AML have not yet been extensively characterized. In the present study, we

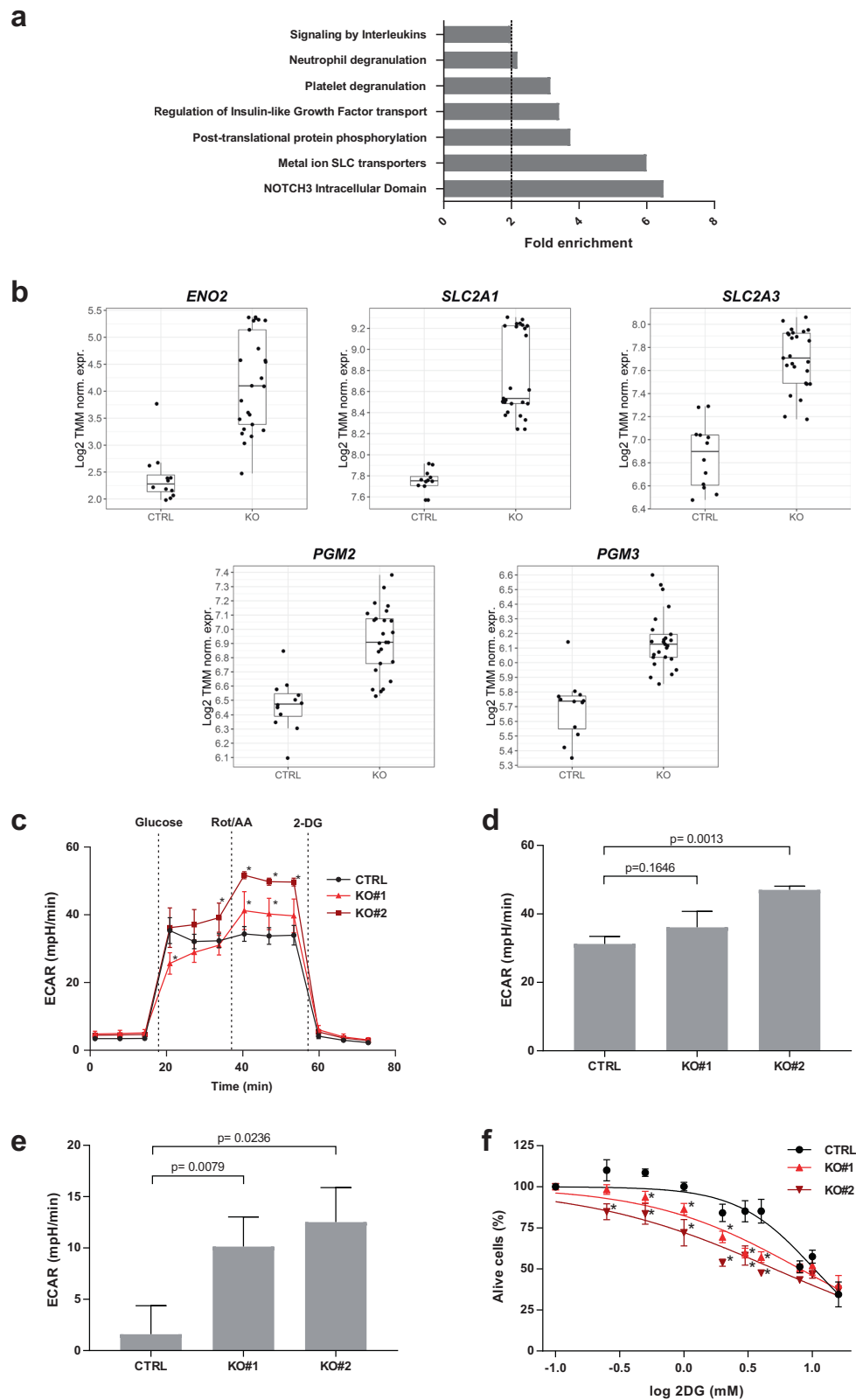


Fig. 3 Loss of *ZBTB7A* sensitizes to glycolysis inhibition. K562 *ZBTB7A* KO and control cells underwent transcriptional profiling, metabolic flux analysis, and 2DG treatment. **a** Gene set enrichment analysis from RNA-Seq data. **b** Expression of *ENO2* (Enolase), *SLC2A1*, and *SLC2A3* (glucose membrane transporters), *PGM2* and *PGM3* (phosphoglycerate mutases) measured by RNA-Seq. **c** ECAR following the addition of glucose, Rot/AA, and 2DG. **d** Glycolytic capacity calculated as the ECAR after electron transport chain inhibition. **e** Glycolytic reserve calculated as the difference between glycolysis after glucose infusion and glycolytic capacity (F) cell viability after 2DG treatment. **p* value < 0.05 compared with control cells.

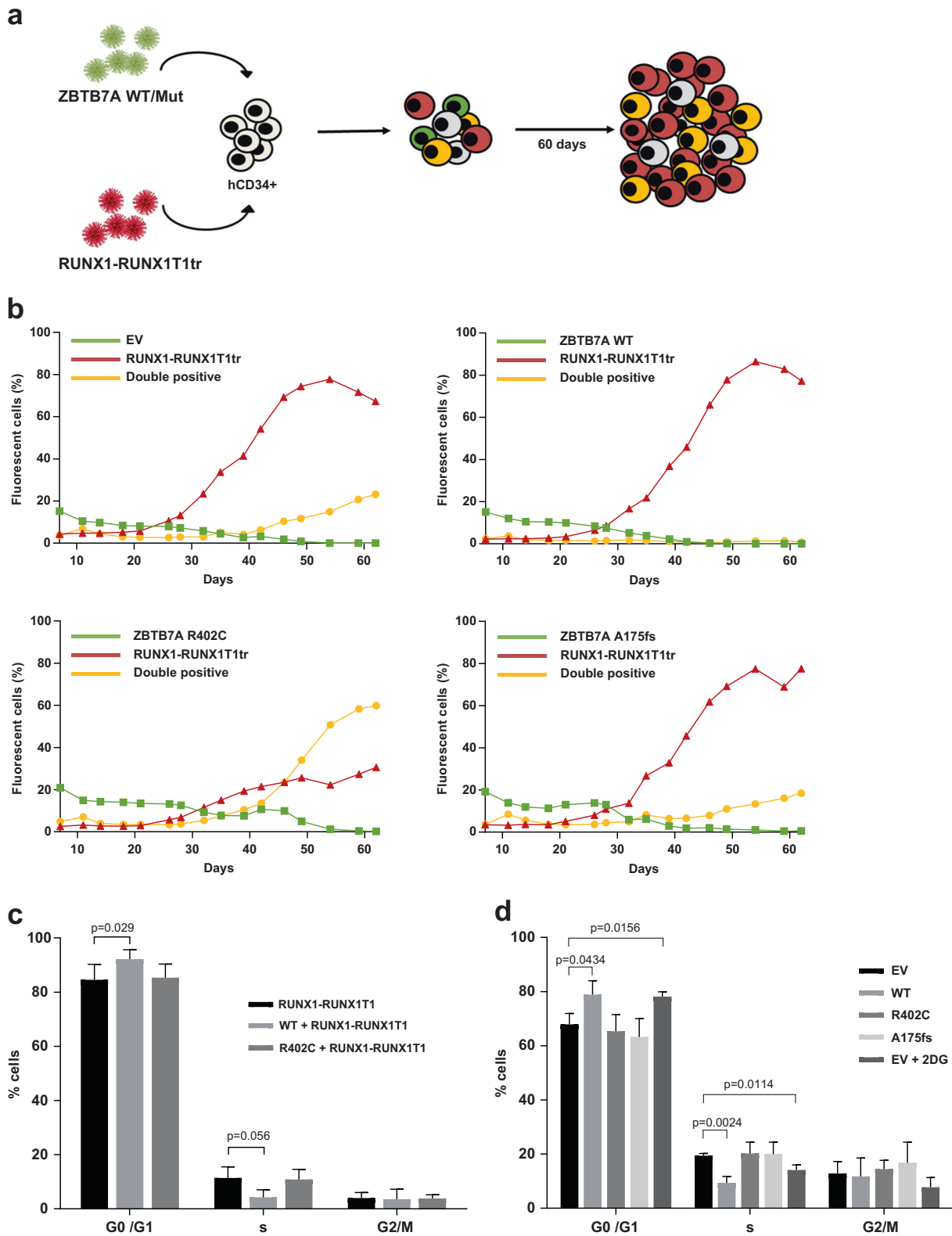


Fig. 4 ZBTB7A prevents RUNX1-RUNX1T1tr-dependent clonal expansion of hCD34⁺ cells. **a** Schematic representation of the experimental layout. hCD34⁺ cells were transduced with *ZBTB7A* WT or mutants (GFP) and *RUNX1-RUNX1T1tr* (tomato). **b** FACS measurements of a representative competitive growth assay. The read

out assessed was expansion or nonexpansion of GFP-tomato double positive cells. **c** Cell-cycle analysis of RUNX1-RUNX1T1 hCD34⁺ cells, transduced with the indicated constructs. **d** Cell-cycle analysis of GFP-positive Kasumi-1 cells stably expressing the indicated constructs.

demonstrated that ZBTB7A mutations have a loss-of-function phenotype with regard to differentiation and cell-cycle regulation (Figs. 1a, b, 2 and 4c, d). Moreover, ZBTB7A KO effects were only rescued by ectopic expression of the WT form but not by the mutants (Fig. 1c, f). We could though observe a slight residual activity of the point mutant R402C (Fig. 1a), as already described in other readouts [1]. Despite a previous report in the context of colon cancer suggesting that ZBTB7A zinc finger mutations act in a dominant negative manner [22], we could not find any evidence for this effect in our models, even when the expression of the R402C mutant was slightly higher than the control (Fig. 1e). The fact that the mutation A175fs results in an unstable truncated protein (Fig. 1e) also argues for a loss-of-function mechanism. In addition, we showed that the previously reported antiproliferative effect of ZBTB7A [1] is not exclusive to the t(8;21) background, as shown by loss of ZBTB7A WT expressing HL60 cells (Fig. 1d). This result is consistent with the assumption that ZBTB7A acts as a tumor suppressor and with our observation that higher ZBTB7A expression levels correlate with longer survival in cytogenetically normal AML patients [1]. Our results also corroborate a previously described role of ZBTB7A in erythroid differentiation (Figs. 1f, 2a, b) [10, 12] and suggest that ZBTB7A can block myeloid differentiation of HSPC (Fig. 2c, d).

The most puzzling fact about ZBTB7A mutations in AML is their exclusive presence in the context of core binding factor leukemia, mainly in t(8;21) AML [1–6], which suggests a specific collaboration between RUNX1–RUNX1T1 and loss of ZBTB7A function. Of note, it was previously reported that RUNX1–RUNX1T1 causes a block of the monocytic and erythrocytic lineages in favor of granulocytic differentiation in mouse and zebrafish [9, 23]. In addition, an accumulation of neutrophils in the bone marrow of mice was observed [24]. All these models failed to present any leukemic disease. Interestingly, our HL60 model indicates that ZBTB7A has a role in directing cells into the granulocytic compartment while blocking monocytic differentiation (Fig. 1a–c). A loss of ZBTB7A function may therefore increase the block of myeloid differentiation initiated by t(8;21) (Fig. 2e). These results are in contrast to other reports based on cell lines stating that RUNX1–RUNX1T1 is sufficient to completely block granulocytic differentiation [25], however, such effect likely depends on the cellular context. Furthermore, AML t(8;21) was described to depend on glycolysis for its survival, specifically depending on PFKP and SLC2A3 [16], both direct targets of ZBTB7A [17]. This is further supported by the fact that the t(8;21) translocation positive Kasumi-1 cell line is highly sensitive to glycolysis inhibition [26]. In this study, we show that loss of ZBTB7A increases the expression of *SLC* glucose transporter genes as well as

ENO2, *PGM2*, and *PGM3* (Fig. 3b), increasing glycolysis (Fig. 3c) and sensitizing to glycolysis inhibition (Fig. 3f). Interestingly, inhibition of mitochondrial respiration demasked a profoundly increased glycolytic reserve in ZBTB7A KO cells (Fig. 3e). This observation may encourage further studies regarding a possible advantage for ZBTB7A mutant cells in hypoxic environments. In vitro treatment of PDX cells revealed different degrees of sensitivity to 2DG (Supplementary Fig. 5), suggesting that response might be variable between patients and may depend on the genetic context. We also observed interference in RUNX1–RUNX1T1r-dependent outgrowth of hCD34+ cells by forced ZBTB7A expression (Fig. 4b, Supplementary Fig. 6). Expression of ZBTB7A WT in a t(8;21) rearranged background does not cause increased differentiation in comparison to mutants (Supplementary Fig. 7), however, it leads to a cell cycle arrest (Fig. 4c, d). This effect resembles the cell cycle arrest due to the inhibition of glycolysis through 2DG treatment (Fig. 4d). These observations indicate that ZBTB7A expression in t(8;21) leukemia may lead to a decreased glycolysis rate and cell cycle arrest, thus impairing leukemia development. While the translocation t(8;21) in AML was the first recurrent cytogenetic abnormality ever described in any cancer [27], a specific treatment for this entity is not yet available. This is in contrast to other leukemia-associated rearrangements, such as *PML-RARA* or *BCR-ABL1*, that are pharmacologically actionable [28, 29]. In the present study, we show that ZBTB7A can counteract RUNX1–RUNX1T1-dependent progenitor cell expansion through repression of glycolysis, opening up avenues for a targeted treatment of AML t(8;21) with metabolic inhibitors.

In summary, we have shown that ZBTB7A mutations contribute to a terminal block of myeloid differentiation as well as to deregulation of glycolysis. Further studies are required to elucidate the complex interplay between tumor metabolism and perturbed differentiation in myeloid malignancies.

Methods

Plasmids and cell culture

All cell lines were acquired from DSMZ (Braunschweig, Germany). HL60 and K562 were cultured in RPMI-1640 medium (Life Technologies, Darmstadt, Germany) with 10% fetal bovine serum (FBS) (Biochrom, Berlin, Germany) and 1% PenStrep (PAN-Biotech, Aidenbach, Germany). Kasumi-1 cells were cultured with RPMI-1640 medium, 1% PenStrep and 20% FBS.

Human bone marrow CD34+ cells, containing HSPCs, were purchased from Lonza (Cologne, Germany) and

cultured using IMDM (GE Healthcare Life Sciences, Pasching, Austria) complemented with 20% FBS 2% glutamine, 100 U PenStrep, 20 ng/ml FLT3-l, 20 ng/ml GM-CSF, hIL-3 10 ng/ml, hIL-6 20 ng/ml, hSCF 20 ng/ml, hTPO 20 ng/ml all from Peprotech (Hamburg, Germany).

PDX were described before [30]. Briefly, cells were isolated from NOD.Cg-Prkdc^{scid} Il2rg^{tm1Wjl}/SzJ (NSG) mice bone marrow and then cultured in StemPro-34 SFM Medium (StemCell Technologies, Grenoble, France) supplemented with 1% PenStrep, 1% L-Glutamine, 2% FBS and 10 ng/ml SCF, TPO and IL-3.

The pMSCV-IRES-GFP ZBTB7A WT, R402C, and A175fs were described before [1]. The pMSCV-RUNX1-RUNX1T1tr-IRES-tdTomato was described before [31]. pSpCas9(BB)-2A-GFP (px458) is available from Addgene (Plasmid #48138) and gRNA sequences targeting ZBTB7A (GACTCGAGGTACTCCTTGCGC or GCCGCCGCTGCCAGCTTCCCG) were cloned as described before [32].

CRISPR/Cas9 knockout

K562 and HL60 cells were electroporated with px458 containing a gRNA targeting ZBTB7A or an empty vector using Lonza 2b electroporation system following the manufacturer's recommendation. Single cells were sorted for GFP into a 96-well plate. Single cells were expanded and ZBTB7A status was assessed by Western blot and Sanger sequencing, respectively.

Differentiation assays

Cells were transduced and sorted for GFP. Granulocytic differentiation of HL60 cells was induced with 2 μ M ATRA treatment (Sigma-Aldrich, Taufkirchen, Germany) for 72 h followed by flow cytometry measurement of CD11b surface expression using a mouse PE-Cy7 anti-human CD11b antibody (clone: ICRF44, BD Biosciences, Temse, Belgium). Monocytic differentiation of HL60 cells was induced with 0.5 nM PMA (Abcam, Cambridge, UK) treatment for 48 h followed by flow cytometry measurement of CD14 surface expression using a mouse PE-Cy7 anti-human CD14 antibody (clone: M5E2, BD Biosciences). Erythroid differentiation of K562 was assessed by flow cytometry measurement of glycophorin A (CD235a) surface expression using a mouse PE anti-human glycophorin A antibody (clone: GA-R2, BD Biosciences) without induction of differentiation.

A total of 5000 Human CD34+ bone marrow cells were seeded either in StemSpan SFEM with StemSpan Erythroid Expansion Supplement or HemaTox Myeloid Kit (StemCell Technologies) in a 96-well plate. Cells were incubated for 7 days and differentiation was assessed by flow cytometry. Erythroid differentiation potential was assessed as stated before and with an additional mouse APC anti-human

CD71 antibody (clone: M-A712, BD Biosciences). Granulocytic differentiation was assessed by a mouse APC anti-human CD15 antibody (clone: SSEA-1, Biolegend, London, UK) and monocytic differentiation as stated above.

Metabolic flux analysis

In all, 8×10^4 cells were plated with Seahorse XF RPMI medium, pH 7.4 in a XF96 cell culture microplate (both Agilent, Waghuaesel-Wiesental, Germany) coated with Cell Tak (Corning, Berlin, Germany) according to the manufacturer's instructions. Oxygen consumption rate (OCR) and extracellular acidification rate (ECAR) were measured at 37 °C using a Seahorse XFe96 Analyzer (Agilent). Three measurements of OCR and ECAR were taken before and after each sequential injection of glucose at a final concentration of 1 mM, rotenone/antimycin A (Rot/AA) at a final concentration of 0.5 μ M and 2DG at a final concentration of 50 mM (all Agilent).

Drug sensitivity assays

In all, 10^4 cells were plated in a 96-well plate with increasing concentrations of 2DG or PMA in technical triplicates. Cells were incubated for 72 h and then viability was assessed using CellTiter-Blue Cell Viability Assay (Promega, Mannheim, Germany) following the recommended protocol.

Human CD34+ cells competitive growth

Human CD34+ bone marrow cells were double transduced with constructs harboring ZBTB7A WT, R402C, or A175fs (marked with GFP) together with RUNX1-RUNX1T1tr (marked with tomato). Expansion of single and double fluorescent marker-positive cells was then followed by flow cytometry over 60 days after transduction as described before [31].

Cell-cycle analysis

Kasumi-1 and hCD34 cells were transduced and 4×10^5 cells harvested and resuspended in 500 μ l PBS. DRAQ5 (Thermo Fisher Scientific, Darmstadt, Germany) was added at a final concentration of 5 μ M and incubated for 15 min. Cells were then analyzed by flow cytometry gating for GFP-positive cells and single events.

Statistical analysis

P values were calculated using two-tailed Student's *t* test for single comparison and analysis of variance followed by Dunnett's multiple comparisons test for multiple

comparisons in GraphPad Prism 7.03 (GraphPad Software, Inc., San Diego, CA, USA). Similarity of variance was evaluated using the Brown–Forsythe test. Graphs show mean and standard deviation of the mean of three independent experiments unless stated otherwise. Asterisk indicates significant differences (p value < 0.05). Sample exclusion was not carried out. FACS results were analyzed with FlowJo v10 (FlowJo LLC, Ashland, OR, USA).

Data availability

The RNA-Seq data from K562 ZBTB7A knockout cells supporting the findings of this study is available in the Gene Expression Omnibus repository, GEO accession: GSE140472.

Acknowledgements This study was supported by the German Research Foundation (DFG) within the Collaborative Research Centre (SFB) 1243 “Cancer Evolution” (Projects A05, A08, A14, and Z02). PAG and CW acknowledge support by the Wilhelm Sander-Stiftung (Förderantrag Nr. 2014.162.2). PAG received funds from the Munich Clinician Scientist Program (MCSP) Advanced Track. Open access funding provided by Projekt DEAL.

Author contributions ERM, WH, LCW, WE, CW, MC, ST, and PAG designed research. ERM, AW, LH, HB, and SK performed research. ERM, AW, and LH collected data. ERM, GL, PAG, and CW interpreted data. PK and JB provided bioinformatics support. ERM performed statistical analysis. ERM and PAG wrote the manuscript.

Compliance with ethical standards

Conflict of interest The authors declare that they have no conflict of interest.

Publisher’s note Springer Nature remains neutral with regard to jurisdictional claims in published maps and institutional affiliations.

Open Access This article is licensed under a Creative Commons Attribution 4.0 International License, which permits use, sharing, adaptation, distribution and reproduction in any medium or format, as long as you give appropriate credit to the original author(s) and the source, provide a link to the Creative Commons license, and indicate if changes were made. The images or other third party material in this article are included in the article’s Creative Commons license, unless indicated otherwise in a credit line to the material. If material is not included in the article’s Creative Commons license and your intended use is not permitted by statutory regulation or exceeds the permitted use, you will need to obtain permission directly from the copyright holder. To view a copy of this license, visit <http://creativecommons.org/licenses/by/4.0/>.

References

- Hartmann L, Dutta S, Opatz S, Vosberg S, Reiter K, Leubolt G, et al. ZBTB7A mutations in acute myeloid leukaemia with t(8;21) translocation. *Nat Commun*. 2016;7:11733.
- Lavallee VP, Lemieux S, Boucher G, Gendron P, Boivin I, Armstrong RN, et al. RNA-sequencing analysis of core binding factor AML identifies recurrent ZBTB7A mutations and defines RUNX1-CBFA2T3 fusion signature. *Blood*. 2016;127:2498–501.
- Faber ZJ, Chen X, Gedman AL, Boggs K, Cheng J, Ma J, et al. The genomic landscape of core-binding factor acute myeloid leukemias. *Nat Genet*. 2016;48:1551–6.
- Kawashima N, Akashi A, Nagata Y, Kihara R, Ishikawa Y, Asou N, et al. Clinical significance of ASXL2 and ZBTB7A mutations and C-terminally truncated RUNX1-RUNX1T1 expression in AML patients with t(8;21) enrolled in the JALSG AML201 study. *Ann Hematol*. 2019;98:83–91.
- Christen F, Hoyer K, Yoshida K, Hou HA, Waldhueter N, Heuser M, et al. Genomic landscape and clonal evolution of acute myeloid leukemia with t(8;21): an international study on 331 patients. *Blood*. 2019;133:1140–51.
- Opatz S, Bamopoulos SA, Metzeler KH, Herold T, Ksienzyk B, Braundl K, et al. The clinical mutome of core binding factor leukemia. *Leukemia*. 2020; <https://doi.org/10.1038/s41375-019-0697-0> [Online ahead of print].
- Rhoades KL, Hetherington CJ, Harakawa N, Yergeau DA, Zhou L, Liu LQ, et al. Analysis of the role of AML1-ETO in leukemogenesis, using an inducible transgenic mouse model. *Blood*. 2000;96:2108–15.
- Yuan Y, Zhou L, Miyamoto T, Iwasaki H, Harakawa N, Hetherington CJ, et al. AML1-ETO expression is directly involved in the development of acute myeloid leukemia in the presence of additional mutations. *Proc Natl Acad Sci USA*. 2001;98:10398–403.
- Schwieger M, Lohler J, Friel J, Scheller M, Horak I, Stocking C. AML1-ETO inhibits maturation of multiple lymphohematopoietic lineages and induces myeloblast transformation in synergy with ICSPB deficiency. *J Exp Med*. 2002;196:1227–40.
- Maeda T, Ito K, Merghoub T, Polisenio L, Hobbs RM, Wang G, et al. LRF is an essential downstream target of GATA1 in erythroid development and regulates BIM-dependent apoptosis. *Dev Cell*. 2009;17:527–40.
- Maeda T, Merghoub T, Hobbs RM, Dong L, Maeda M, Zakrzewski J, et al. Regulation of B versus T lymphoid lineage fate decision by the proto-oncogene LRF. *Science*. 2007;316:860–6.
- Lee SU, Maeda M, Ishikawa Y, Li SM, Wilson A, Jubb AM, et al. LRF-mediated Dll4 repression in erythroblasts is necessary for hematopoietic stem cell maintenance. *Blood*. 2013;121:918–29.
- Mulloy JC, Cammenga J, MacKenzie KL, Berguido FJ, Moore MA, Nimer SD. The AML1-ETO fusion protein promotes the expansion of human hematopoietic stem cells. *Blood*. 2002;99:15–23.
- Burel SA, Harakawa N, Zhou L, Pabst T, Tenen DG, Zhang DE. Dichotomy of AML1-ETO functions: growth arrest versus block of differentiation. *Mol Cell Biol*. 2001;21:5577–90.
- Yan JS, Li YD, Liu SH, Yin QQ, Liu XY, Xia L, et al. The t(8;21) fusion protein RUNX1-ETO downregulates PKM2 in acute myeloid leukemia cells. *Leuk Lymphoma*. 2017;58:1985–8.
- Isa A, Martinez-Soria N, McKenzie L, et al. Identification of glycolytic pathway as RUNX1/ETO-dependent for propagation and survival. *Klin Padiatr*. 2018;230:165.
- Liu XS, Haines JE, Mehanna EK, Genet MD, Ben-Sahra I, Asara JM, et al. ZBTB7A acts as a tumor suppressor through the transcriptional repression of glycolysis. *Genes Dev*. 2014;28:1917–28.
- Collins SJ. The HL-60 promyelocytic leukemia cell line: proliferation, differentiation, and cellular oncogene expression. *Blood*. 1987;70:1233–44.
- Martin SJ, Bradley JG, Cotter TG. HL-60 cells induced to differentiate towards neutrophils subsequently die via apoptosis. *Clin Exp Immunol*. 1990;79:448–53.
- Benz EJ Jr., Murnane MJ, Tonkonow BL, Berman BW, Mazur EM, Cavalleco C, et al. Embryonic-fetal erythroid characteristics

- of a human leukemic cell line. *Proc Natl Acad Sci USA*. 1980;77:3509–13.
21. Lunardi A, Guarnerio J, Wang G, Maeda T, Pandolfi PP. Role of LRF/Pokemon in lineage fate decisions. *Blood*. 2013;121:2845–53.
 22. Liu XS, Liu Z, Gerarduzzi C, Choi DE, Ganapathy S, Pandolfi PP, et al. Somatic human ZBTB7A zinc finger mutations promote cancer progression. *Oncogene*. 2016;35:3071–8.
 23. Yeh JR, Munson KM, Chao YL, Peterson QP, Macrae CA, Peterson RT. AML1-ETO reprograms hematopoietic cell fate by downregulating scl expression. *Development*. 2008;135:401–10.
 24. de Guzman CG, Warren AJ, Zhang Z, Gartland L, Erickson P, Drabkin H, et al. Hematopoietic stem cell expansion and distinct myeloid developmental abnormalities in a murine model of the AML1-ETO translocation. *Mol Cell Biol*. 2002;22:5506–17.
 25. Westendorf JJ, Yamamoto CM, Lenny N, Downing JR, Selsted ME, Hiebert SW. The t(8;21) fusion product, AML-1-ETO, associates with C/EBP-alpha, inhibits C/EBP-alpha-dependent transcription, and blocks granulocytic differentiation. *Mol Cell Biol*. 1998;18:322–33.
 26. Suganuma K, Miwa H, Imai N, Shikami M, Gotou M, Goto M, et al. Energy metabolism of leukemia cells: glycolysis versus oxidative phosphorylation. *Leuk Lymphoma*. 2010;51:2112–9.
 27. Rowley JD. Identification of a translocation with quinacrine fluorescence in a patient with acute leukemia. *Ann Genet*. 1973;16:109–12.
 28. Druker BJ, Talpaz M, Resta DJ, Peng B, Buchdunger E, Ford JM, et al. Efficacy and safety of a specific inhibitor of the BCR-ABL tyrosine kinase in chronic myeloid leukemia. *N Engl J Med*. 2001;344:1031–7.
 29. Huang ME, Ye YC, Chen SR, Chai JR, Lu JX, Zhou L, et al. Use of all-trans retinoic acid in the treatment of acute promyelocytic leukemia. *Blood*. 1988;72:567–72.
 30. Vick B, Rothenberg M, Sandhofer N, Carlet M, Finkenzeller C, Krupka C, et al. An advanced preclinical mouse model for acute myeloid leukemia using patients' cells of various genetic subgroups and in vivo bioluminescence imaging. *PLoS ONE*. 2015;10:e0120925.
 31. Wichmann C, Quagliano-Lo Coco I, Yildiz O, Chen-Wichmann L, Weber H, Syzonenko T, et al. Activating c-KIT mutations confer oncogenic cooperativity and rescue RUNX1/ETO-induced DNA damage and apoptosis in human primary CD34+ hematopoietic progenitors. *Leukemia*. 2015;29:279–89.
 32. Ran FA, Hsu PD, Wright J, Agarwala V, Scott DA, Zhang F. Genome engineering using the CRISPR-Cas9 system. *Nat Protoc*. 2013;8:2281–308.

SUPPLEMENTARY INFORMATION

ZBTB7A prevents RUNX1-RUNX1T1-dependent clonal expansion of human hematopoietic stem and progenitor cells.

Enric Redondo Monte¹⁻³, Anja Wilding¹⁻³, Georg Leubolt¹⁻³, Paul Kerbs¹⁻³, Johannes W. Bagnoli⁴, Luise Hartmann¹⁻³, Wolfgang Hiddemann¹⁻³, Linping Chen-Wichmann⁵, Stefan Krebs⁶, Helmut Blum⁶, Monica Cusan¹, Binje Vick⁷, Irmela Jeremias⁷, Wolfgang Enard⁴, Sebastian Theurich^{1,8}, Christian Wichmann⁵ and Philipp A. Greif¹⁻³.

- 1) Department Medicine III, University Hospital, LMU Munich, 81377 Munich, Germany
- 2) German Cancer Consortium (DKTK), partner site Munich, 81377 Munich, Germany
- 3) German Cancer Research Center (DKFZ), 69121 Heidelberg, Germany.
- 4) Anthropology & Human Genomics, Department of Biology II, LMU Munich, 82152 Martinsried, Germany
- 5) Department of Transfusion Medicine, Cell Therapeutics and Hemostasis, University Hospital, LMU Munich, 81377 Munich, Germany.
- 6) Gene Center - Laboratory for Functional Genome Analysis, LMU Munich, 81377 Munich, Germany
- 7) Research Unit Apoptosis in Hematopoietic Stem Cells, Helmholtz Center Munich, 81377 Munich, Germany
- 8) Cancer & Immunometabolism Research Group, Gene Center, LMU Munich, 81377 Munich, Germany

Correspondence: pgreif@med.lmu.de

Content:

Supplementary Methods

Supplementary References

Supplementary Figures 1-7

Supplementary Methods

Retroviral transduction

Cell lines and primary human CD34+ bone marrow cells were transduced as follows: Wells in a 24-well non-tissue-culture plate were coated with 400µL of Retronectin (50 µg/ml) (Takara, Saint Germain en Laye, France) overnight. The wells were blocked using 500µl of 2% bovine serum albumin (Sigma-Aldrich, Taufkirchen, Germany) in PBS (PAN-Biotech, Aidenbach, Germany) at room temperature (RT) for 30min. The blocking solution was then aspirated and the wells washed two times with PBS. 400µL of retrovirus containing medium were then added to each well and the plate centrifuged at 3500 r.p.m for 1h at 4°C. The virus loading was then repeated for 3 additional times. The supernatant was discarded and 500µL of media containing between 5×10^4 and 10^6 cells added to each well. The plate was incubated for 8h at 37°C and 5% CO₂.

Western blot

Cell lysates were run on a 10% SDS-PAGE gel and transferred to a PVDF membrane. Membranes were then blocked for 20 minutes at room temperature with 5% dried nonfat milk. Anti-Pokemon (ZBTB7A) antibody (clone: 13E9; eBioscience, Frankfurt am Main, Germany) (1:2000 dilution) and secondary anti-Armenian hamster IgG-HRP (clone: sc-2443; Santa Cruz Biotechnology, Dallas, TX, USA) (1:5000 dilution) were used to assess ZBTB7A protein levels. Mouse anti-GAPDH (clone: sc-32233; Santa Cruz Biotechnology) (1:10000 dilution) and mouse-IgGk BP-HRP (sc-516102; Santa Cruz Biotechnology) (1:10000 dilution) were used as a loading control.

Cell proliferation assay

Cells were seeded at a concentration between 5×10^4 and 10^5 cells per ml in a t-25 flask in technical triplicates. Cell number was measured every 24 or 48h using Vi-CELL XR cell counter and cell viability analyzer (Beckman Coulter, Munich, Germany).

Supplementary Methods

RNA-seq

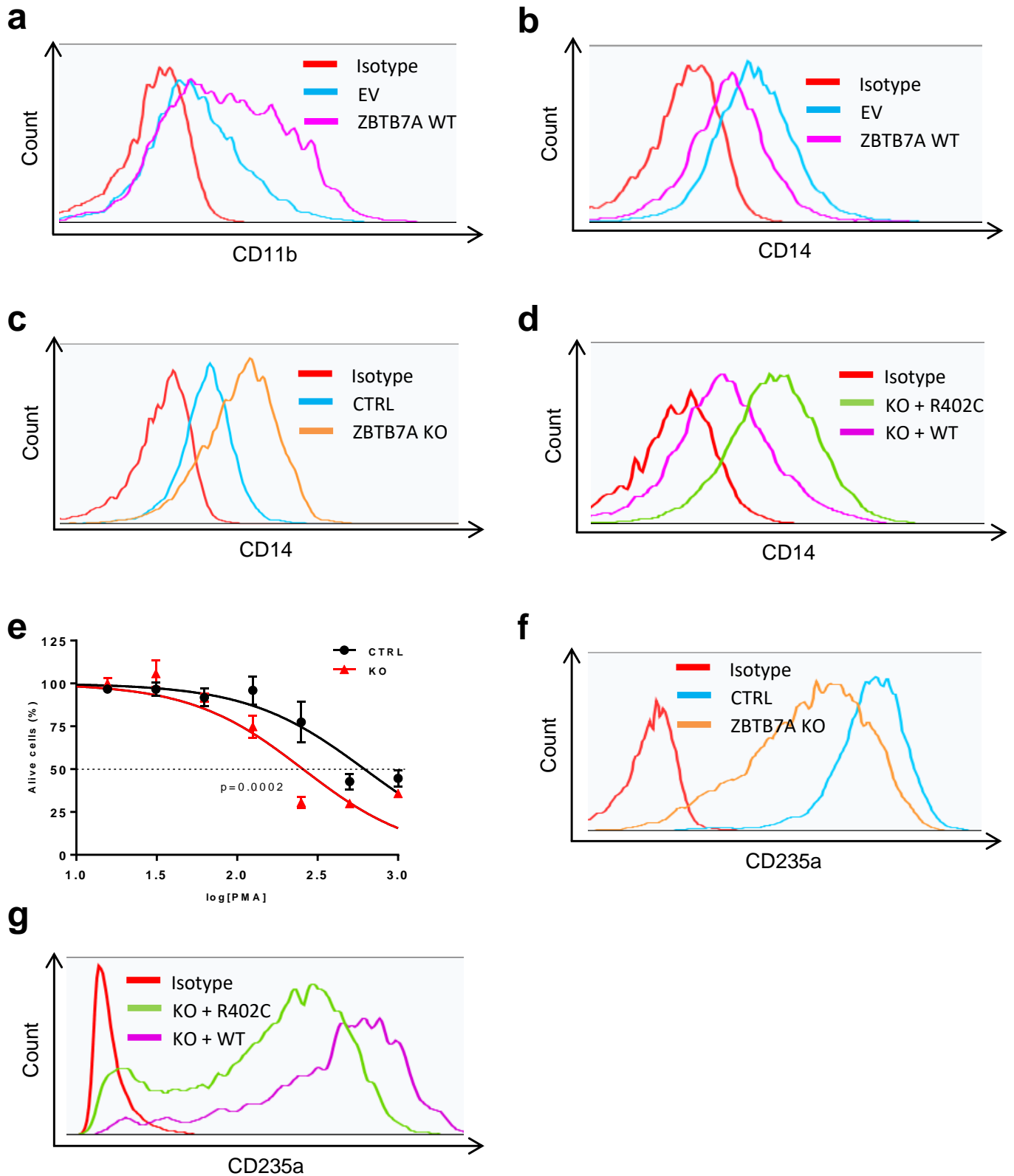
10⁴ cells of each individual sample were lysed in RLT Plus (Qiagen, Hilden, Germany) supplemented with 1% 2-Mercaptoethanol (Sigma-Aldrich) and stored at -80°C until processing. A modified SCRB-seq protocol (1) was used for library preparation. Briefly, proteins in the lysate were digested by Proteinase K (Thermo Fisher Scientific, Darmstadt, Germany), RNA was cleaned up using SPRI beads (GE, 22%PEG). In order to remove isolated DNA, samples were treated with DNase I for 15 minutes at RT. cDNA was generated by oligo-dT primers containing well specific (sample specific) barcodes and unique molecular identifiers (UMIs). Unincorporated barcode primers were digested using Exonuclease I (Thermo Fisher Scientific). cDNA was pre-amplified using KAPA HiFi HotStart polymerase (Roche, Basel, Switzerland) and pooled before Nextera libraries were constructed from 0.8 ng of preamplified cleaned up cDNA using Nextera XT Kit (Illumina, Eindhoven, Netherlands). 3' ends were enriched with a custom P5 primer (P5NEXTPT5, IDT) and libraries were size selected using a 2% E-Gel Agarose EX Gels (Life Technologies, Darmstadt, Germany), cut out in the range of 300–800 bp, and extracted using the MinElute Kit (Qiagen) according to manufacturer's recommendations.

All raw FASTQ data were processed with zUMIs (2) and mapped to the humanpeq genome (hg38) using the software STAR (3). Gene annotations were obtained from Ensembl (GRCh38.84). Differential expression was assessed using the Limma package (4). Gene set enrichment analysis, was performed using the GSEA software (5). Reactome Pathway was used as the gene set database for the GSEA analysis (6) only pathways with a false discovery rate smaller than 0.05 were considered.

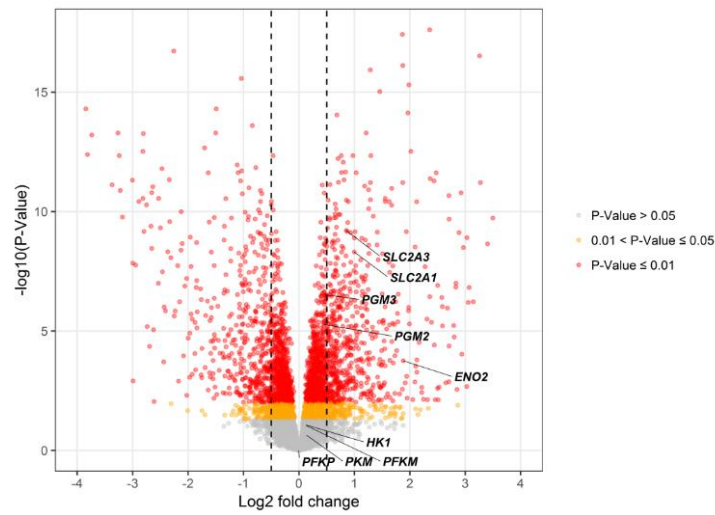
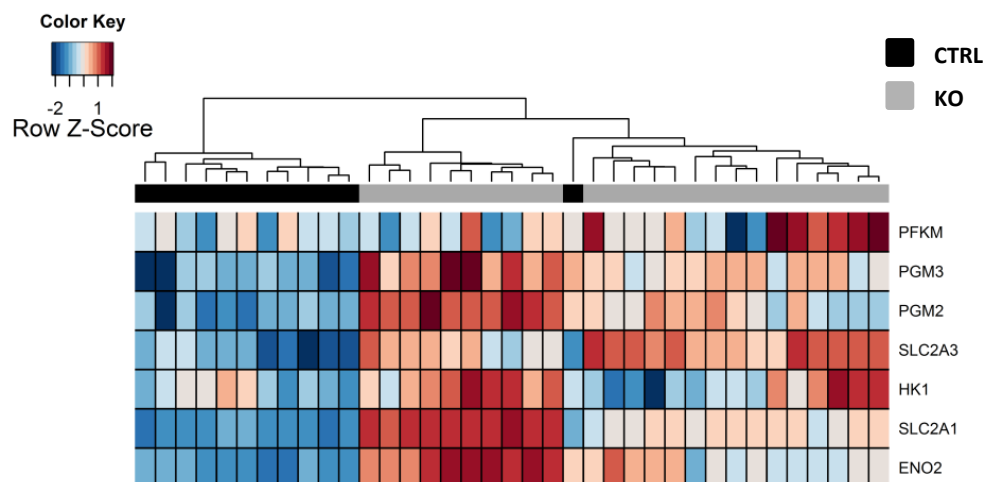
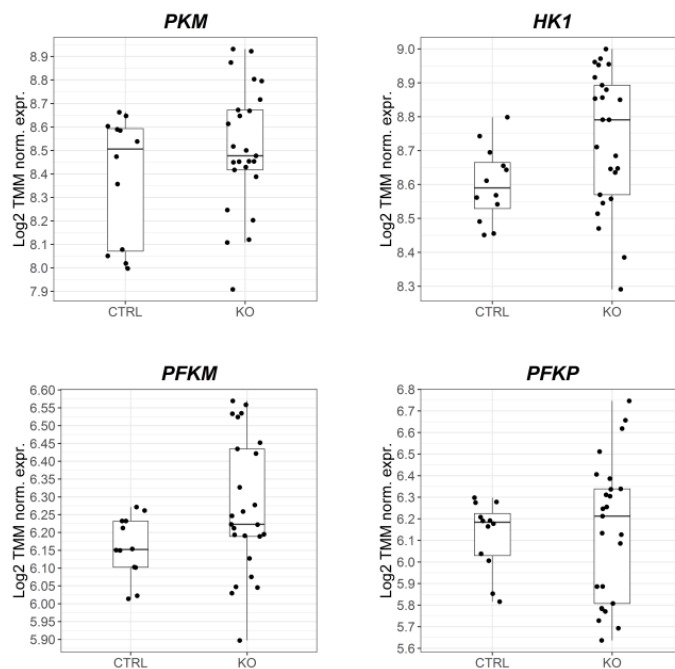
Supplementary References

1. Soumillon M, Cacchiarelli D, Semrau S, van Oudenaarden A, Mikkelsen TS. Characterization of directed differentiation by high-throughput single-cell RNA-Seq. *bioRxiv*. 2014:003236.
2. Parekh S, Ziegenhain C, Vieth B, Enard W, Hellmann I. zUMIs - A fast and flexible pipeline to process RNA sequencing data with UMIs. *Gigascience*. 2018;7(6).
3. Dobin A, Davis CA, Schlesinger F, Drenkow J, Zaleski C, Jha S, et al. STAR: ultrafast universal RNA-seq aligner. *Bioinformatics*. 2013;29(1):15-21.
4. Ritchie ME, Phipson B, Wu D, Hu Y, Law CW, Shi W, et al. limma powers differential expression analyses for RNA-sequencing and microarray studies. *Nucleic Acids Res*. 2015;43(7):e47.
5. Subramanian A, Tamayo P, Mootha VK, Mukherjee S, Ebert BL, Gillette MA, et al. Gene set enrichment analysis: a knowledge-based approach for interpreting genome-wide expression profiles. *Proc Natl Acad Sci U S A*. 2005;102(43):15545-50.
6. Fabregat A, Sidiropoulos K, Viteri G, Forner O, Marin-Garcia P, Arnau V, et al. Reactome pathway analysis: a high-performance in-memory approach. *BMC Bioinformatics*. 2017;18(1):142.

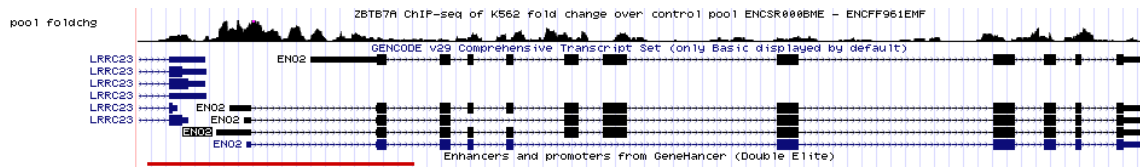
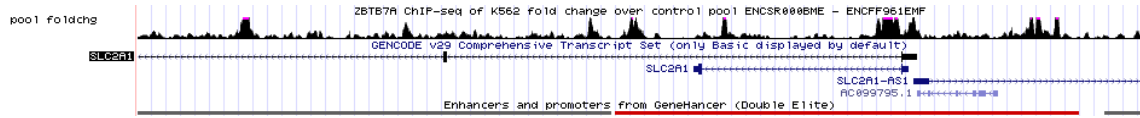
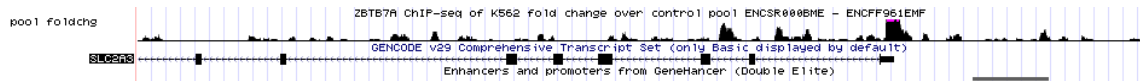
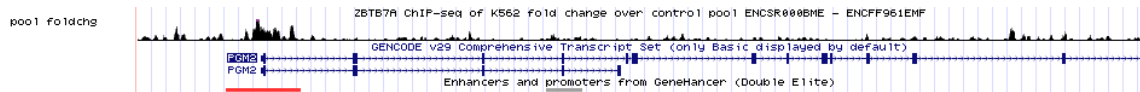
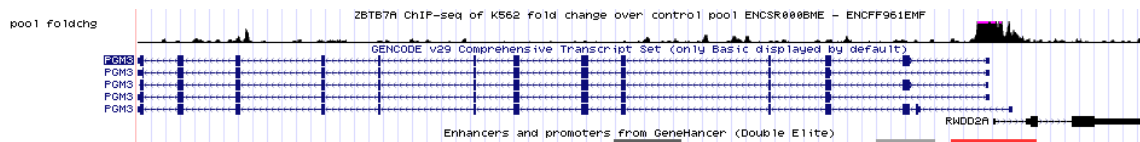
Supplementary Figures



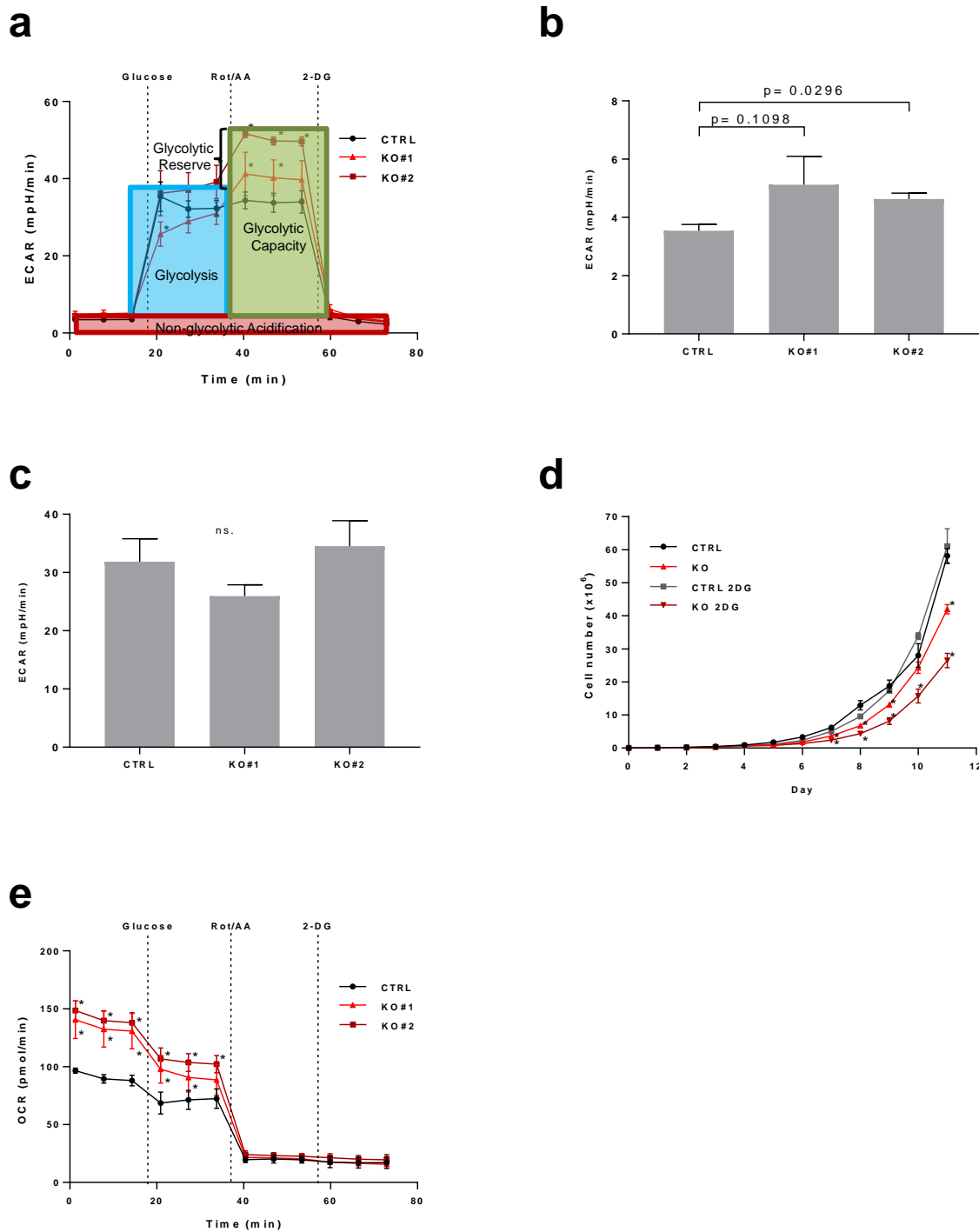
Supplementary Figure 1. ZBTB7A regulates lineage commitment in HL60 and K562 (a) CD11b membrane expression in HL60 after ATRA treatment. (b) CD14 membrane expression in HL60 after PMA treatment. (c) and (d) CD14 membrane expression in HL60 without any treatment. (e) HL60 viability after PMA treatment. (f) and (g) CD235a membrane expression in K562 without any treatment.

a**b****c**

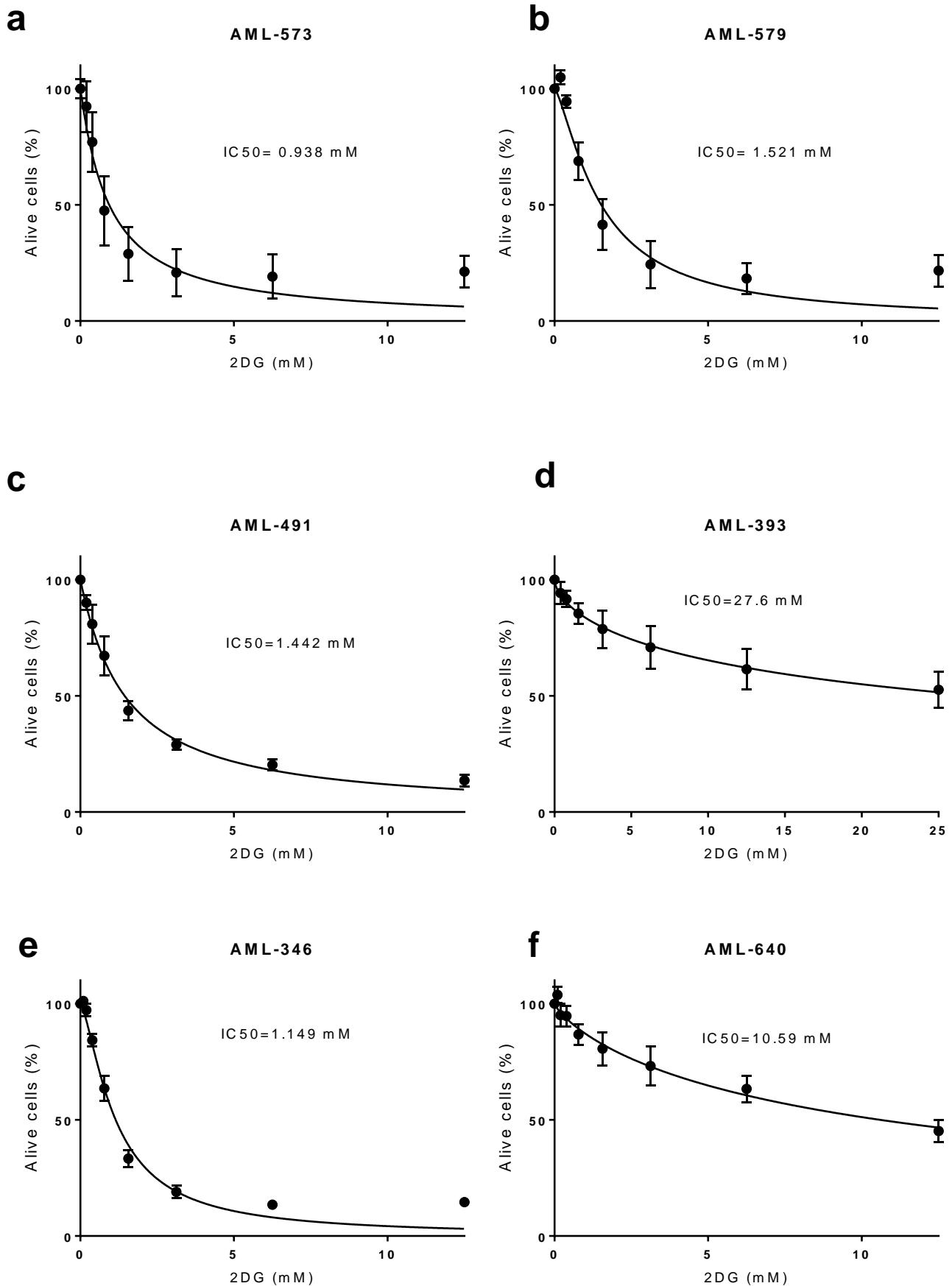
Supplementary Figure 2. ZBTB7A regulates the expression of glycolytic genes in K562 (a) Volcano plot representing deregulated gene expression in ZBTB7A KO vs control. (b) Heat map of gene expression from a selected group of genes related to glycolysis. (c) *PKM*, *HK1*, *PFKM* and *PFKP* normalized expression measured by RNA-Seq.

a**b****c****d****e**

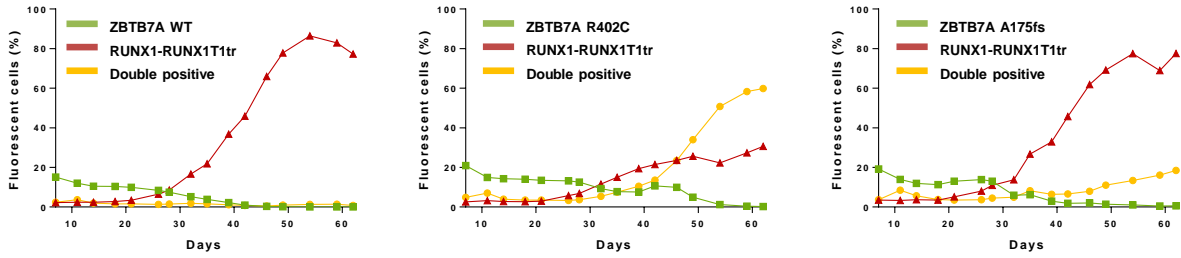
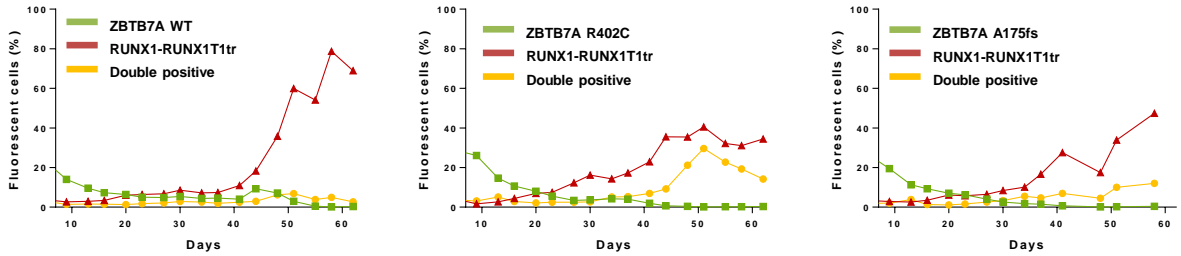
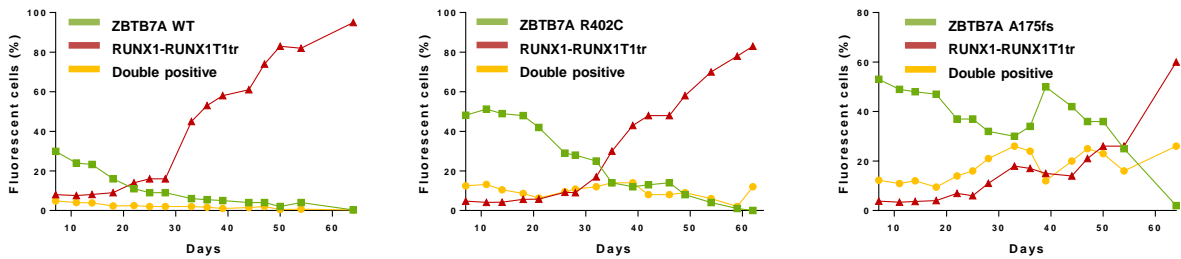
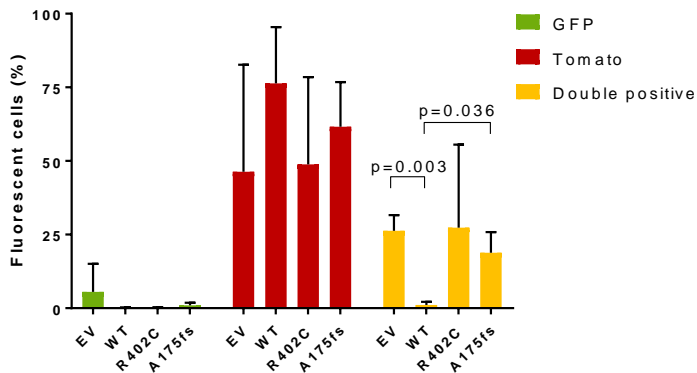
Supplementary Figure 3. ZBTB7A binding of target genes. ZBTB7A ChIP-Seq (ENCSR000BME) including enhancer and promoters from GeneHancer representing the fold change over control pool for *ENO2* (a), *SLC2A1* (b), *SLC2A3* (c), *PGM2*, (d) *PGM3*.



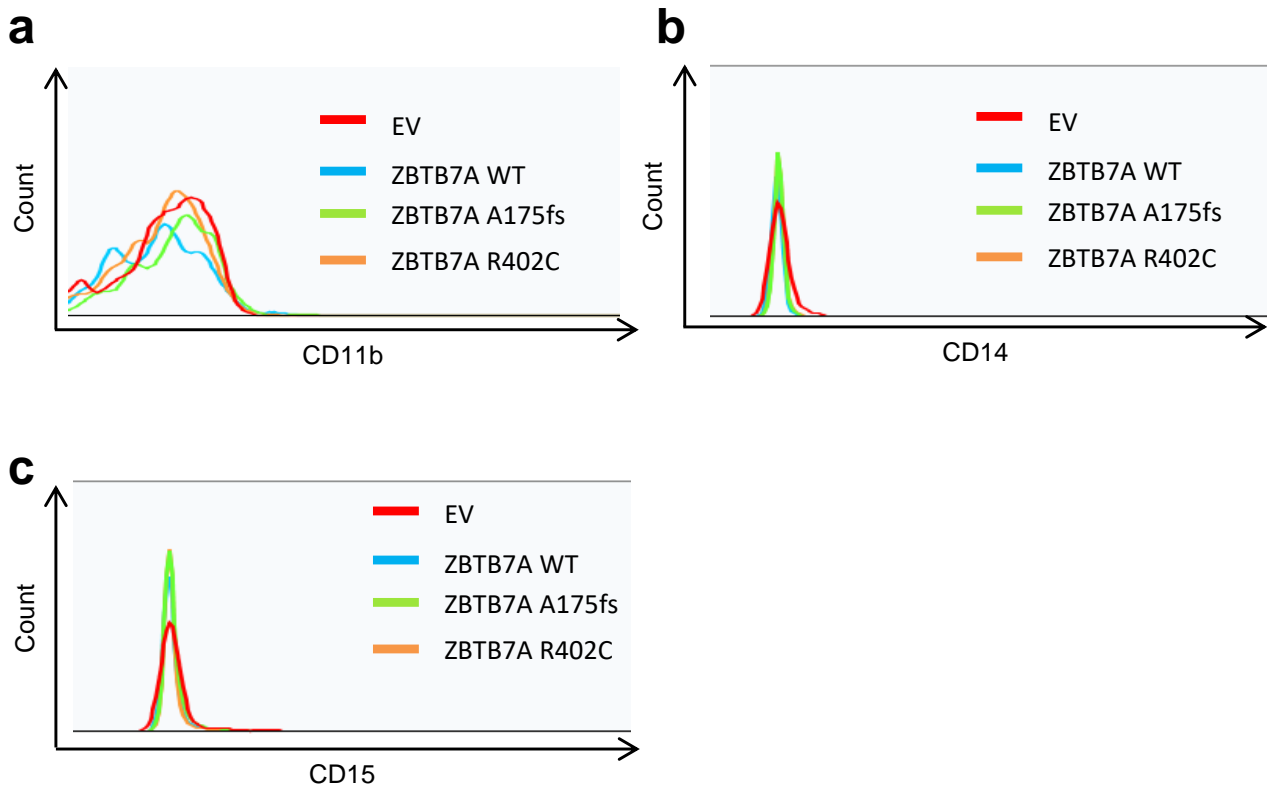
Supplementary Figure 4. ZBTB7A regulates glycolysis in K562 (a) Representation of the parameters calculated from the ECAR. (b) Non-glycolytic acidification. (c) Glycolysis. (d) Cell counts over a period of ten days under 2DG treatment [2mM]. (e) Oxygen consumption in the same set of experiments over a period of 80min. Mean \pm s.d. are given for three independent experiments. * p -value <0.05 compared to control cells.



Supplementary Figure 5. 2DG inhibits the growth of patient derived xenograft cells *in vitro*. (a) Sensitivity for AML-573 (WT1, DNMT3A, IDH2 mutated and FLT3 ITD). (b) AML-579 (DNMT3A, IDH1, NPM1 mutated and FLT3 ITD). (c) AML-491 (DNMT3A, RUNX1, ETV6, PTPN11, BCOR, KRAS, NRAS mutated). (d) AML-393 (MLL-AF10 rearranged, BCOR and KRAS mutated) (e) AML-346 (interstitial 5q deletion / interstitial 13q deletion) (f) AML-640 (IDH1 and NPM1 mutated, FLT3-ITD t(11;15)(p1?1;q?22)).

a**b****c****d**

Supplementary Figure 6. ZBTB7A prevents RUNX1-RUNX1T1tr dependent clonal expansion of hCD34+ cells. (a-c) Three independent experiments, the read out assessed was expansion or non-expansion of GFP-tomato double positive cells. (d) Summary of three independent experiments at final day of readout.



Supplementary Figure 7. Kasumi-1 cells do not differentiate upon ZBTB7A expression. (a) Representative flow cytometry plot showing the CD11b surface expression after transduction. (b) Representative plot showing CD14 expression. (c) Representative plot showing CD15 expression.

